Aptamers for targeted activation of T cell-mediated immunity

Dissertation

zur

Erlangung des Doktorgrades (Dr. rer. nat.)

der

Mathematisch-Naturwissenschaftlichen Fakultät

der

Rheinischen Friedrich-Wilhelms-Universität Bonn

vorgelegt von

Silvana Katharina Haßel, geb. Albers

aus

Bielefeld

Bonn 2016

Angefertigt mit Genehmigung der Mathematisch-Naturwissenschaftlichen Fakultät der
Rheinischen Friedrich-Wilhelms-Universität Bonn

Für Dominique, in Liebe und Dankbarkeit

Index

1 Abstract

An attractive way of preventing or curing infections and diseases is to mobilize patient's own defense mechanisms, the immune system. Treatments following this approach are commonly known as immunotherapies. The development of protective long-term immunity requires activation of the effectors of the adaptive immune system, in particular T cells, by cells involved in innate immunity.

Dendritic cells (DCs) represent the interface between the non-specific innate immunity and the highly specific adaptive immunity. Upon recognition of antigenic structures, DCs deliver all signals necessary for adequate T cell priming. Hence, immunization with DC-based vaccines became of utmost importance in immunotherapy. One remarkable approach is to conjugate antigens to carrier molecules that specifically target DCs.

In the study at hand, it was investigated if aptamers represent a promising novel class of DC-targeting carriers for immunotherapeutic applications. Aptamers are nucleic acids ligands with a defined shape that bind with high affinity and specificity to their particular targets.

Herein, DC-binding aptamers were selected by two different strategies. First, aptamer CTL#5 was identified by addressing recombinant proteins originated from the murine mannose receptor (MR) in a protein-SELEX approach. The MR is an endocytic receptor crucial in recognizing, uptake and processing of antigens by DCs. Second, aptamers D#5 and D#7 were selected by directly using murine bone marrow-derived DCs as complex targets in a cell-SELEX process.

It was demonstrated that the selected aptamers exhibit all properties to function as suitable carriers. They bind specifically to DCs, are internalized and localized within adequate antigen processing compartments and are low immunogenic.

Most importantly, the present study revealed that the selected aptamers are potent mediators of targeted activation of specific T cells. By using an ovalbumin (OVA) model system it was demonstrated that aptamer-based delivery of antigenic OVA peptides to DCs resulted in a strong activation of OVA-specific CD4 or CD8 T cells.

In summary, the present thesis demonstrates the potential applicability of aptamers as DC-targeting carriers and paves the way for the development of aptamer-based DC vaccines for *in vivo* applications.

2 Zusammenfassung

Das körpereigene Immunsystem von Patienten kann therapeutisch angeregt werden zur Prävention und Heilung von Erkrankungen und Infektionen. Anwendungen dieser Art sind allgemein bekannt als Immunotherapien. Ziel ist hierbei die Ausbildung einer schützenden Langzeit-Immunität, die durch spezialisierte Effektorzellen des erworbenen Immunsystems vermittelt wird. Diese sogenannten T-Zellen müssen hierfür durch Zellen des angeborenen Immunsystems aktiviert werden.

Dendritische Zellen (DZ) repräsentieren die Interphase zwischen dem relativ unspezifischen angeborenen Immunsystems und dem hoch-spezifischen erworbenen Immunsystems. Diese Zellen erkennen antigene Strukturen und unterlaufen dabei einen Reifungsprozess. Reife DZ generieren alle nötigen Signale, um T-Zellen optimal zu aktivieren. Es besteht daher ein großes Interesse an DZ-basierten Immunotherapien. Hervorzuheben ist hierbei die Vakzinierung mit Antigenen, die durch Trägermoleküle spezifisch zu DZ transportiert werden.

Im Rahmen dieser Arbeit wurde untersucht, ob Aptamere eine neue Klasse an DZ-spezifischen Trägermolekülen darstellen. Aptamere sind Nukleinsäure-Liganden, die aufgrund ihrer Konformation affin und spezifisch an ihre Zielstruktur binden.

Zwei unterschiedliche Strategien wurden verfolgt, um die hier beschriebenen DZ-bindenden Aptamere zu selektieren. Einerseits wurde Aptamer CTL#5 mit einer Protein-SELEX Methode identifiziert. Rekombinante Proteine, die vom Mannose Rezeptor (MR) stammen, wurden hierbei als Zielstruktur verwendet. Der MR ist ein endozytischer Rezeptor und ist entscheidend für die Erkennung, Aufnahme und Prozessierung von Antigenen durch DZ. Die Aptamere D#5 und D#7 wurden andererseits durch die sogenannte Zell-SELEX Methode identifiziert, hierfür wurden DZ isoliert aus dem Knochenmark von Mäusen als komplexe Zielstrukturen eingesetzt.

Es konnte gezeigt werden, dass die Aptamere alle notwendigen Eigenschaften als Trägermoleküle besitzen. Sie binden spezifisch an DZ, werden internalisiert und gelangen in adäquate Zellkompartimente, die wichtig für die Prozessierung von Antigenen sind. Zudem sind die Aptamere nur schwach immunogen.

Abschließend wurde in dieser Arbeit demonstriert, dass die Aptamere zur zielgerichteten Aktivierung von T-Zellen verwendet werden können. Durch Verwendung eines Ovalbumin (OVA) Modellsystems konnte gezeigt werden, dass der Aptamer-vermittelte Transport von antigenen OVA-Peptiden eine starke Aktivierung von OVA-spezifischen CD4 oder CD8 T-Zellen auslöst.

Zusammenfassung

Die Ergebnisse der vorliegenden Arbeit zeigen deutlich die Verwendbarkeit von Aptameren als DZ-spezifische Trägermoleküle und ebnen den Weg für die Entwicklung einer Aptamer-basierten Vakzinierung von DZ *in vivo*.

3   Introduction

A patient's own immune system can be used to clear the body from infections, diseases or cancer. Treatments following this approach are commonly known as immunotherapies.

Already in the late 18th century the surgeon William B. Coley observed that cancer disappeared in patients suffering severe bacterial infections. Therefore, he injected a mix of attenuated S*treptococcus pyogenes* and *Serratia marcescens* into tumors of patients and it is described that some patients experienced tumor reduction[1].
Since then, much work has been carried out to identify the mechanisms of the immune system and how these are applicable for therapeutic treatments.

3.1 The immune system

The mammalian immune system is a complex network of organs, cells and proteins. It protects the host from invading pathogens like microorganisms and pollutants.

In general, the mammalian immune system is divided into innate and adaptive immunity[2]. Initial defense mechanisms are mediated by the innate immunity. Various components like physical barriers, innate immune cells, antimicrobial proteins, complement and cytokines are involved in the rapid and relatively non-specific response towards broad classes of pathogenic structures.
A key feature of the innate immunity is the discrimination between self and non-self molecules. Monocytes, granulocytes, macrophages, dendritic cells (DCs) and natural killer cells, for example, recognize highly conserved pathogen-associated molecular patterns (PAMPs) by a range of pattern recognition receptors (PRRs)[3]. As a consequence, these cells degrade ingested pathogens and secrete cytokines and chemokines to promote inflammation. In turn, inflammation triggers the recruitment of more immune cells and anti-microbial molecules such as complement to the site of infection[4]. Innate immune responses occur within the first 96 hours of infections and lead to the elimination of pathogens. The establishment of infection is thereby hampered or retarded.

If the innate immunity is evaded or overwhelmed, an adaptive immune response is required[2]. Adaptive immune responses take days rather than hours to develop and

result in protective immunological memory formation. Consequently, upon exposure to the same antigen, an amplified immune response is induced.

Specialized lymphocytes, namely B and T cells, are the effector cells of adaptive immunity. They are activated by cells involved in innate immunity and realize highly antigen-specific immunity. One discriminates between humoral and T cell-mediated immunity. Activated B cells differentiate into antibody-producing plasma cells and execute humoral immunity, whereby T cell-mediated immunity is initiated by activated T cells. Activation of T cells is the critical event of most adaptive immune responses[2].

3.2 T cell-mediated immunity

The transition between innate and adaptive immune responses is mediated by specialized immune cells. These cells, including dendritic cells, macrophages and B cells, are termed professional antigen-presenting cells (APCs). The interaction of APCs with T cells in peripheral lymphoid tissues, i.e. lymph nodes, spleen and mucosal-associated lymphoid tissues, initiates T cell-mediated immunity[2].

During cell development, every T cell is equipped with a specific T cell receptor (TCR) that recognizes a single antigenic structure bound to major histocompatibility complex (MHC) molecules present on the surface of an activated APC. Remarkably, every mammalian organism expresses millions of different TCR gene variants. On the plasma membrane TCR pairs with CD4 or CD8 co-receptors[2].

Naïve T cells continuously circulate through peripheral lymphoid tissues to encounter their appropriate peptide-MHC complex presented on an activated APC. Consequently, T cells undergo clonal expansion and differentiation into highly antigen-specific CD4 or CD8 effector T cells. Activated CD8 T cells acquire cytotoxic capability, whereas CD4 T cells polarize into either activator or suppressor cells[5] (**Figure 3.2.1AB**).

Cytotoxic CD8 T cells mediate apoptosis of target cells expressing the respective antigen-MHC complex; in doing so, they either interact with death receptors such as Fas or directly release cytotoxic granules like perforin and granzymes.

Activating CD4 T helper 1 (Th1) or Th2 cells promote the differentiation of B cells into antibody-producing plasma cells or enhance the development of cytotoxic CD8 T cells, while suppressing regulatory CD4 T cells negatively regulate the activation of T cells[5].
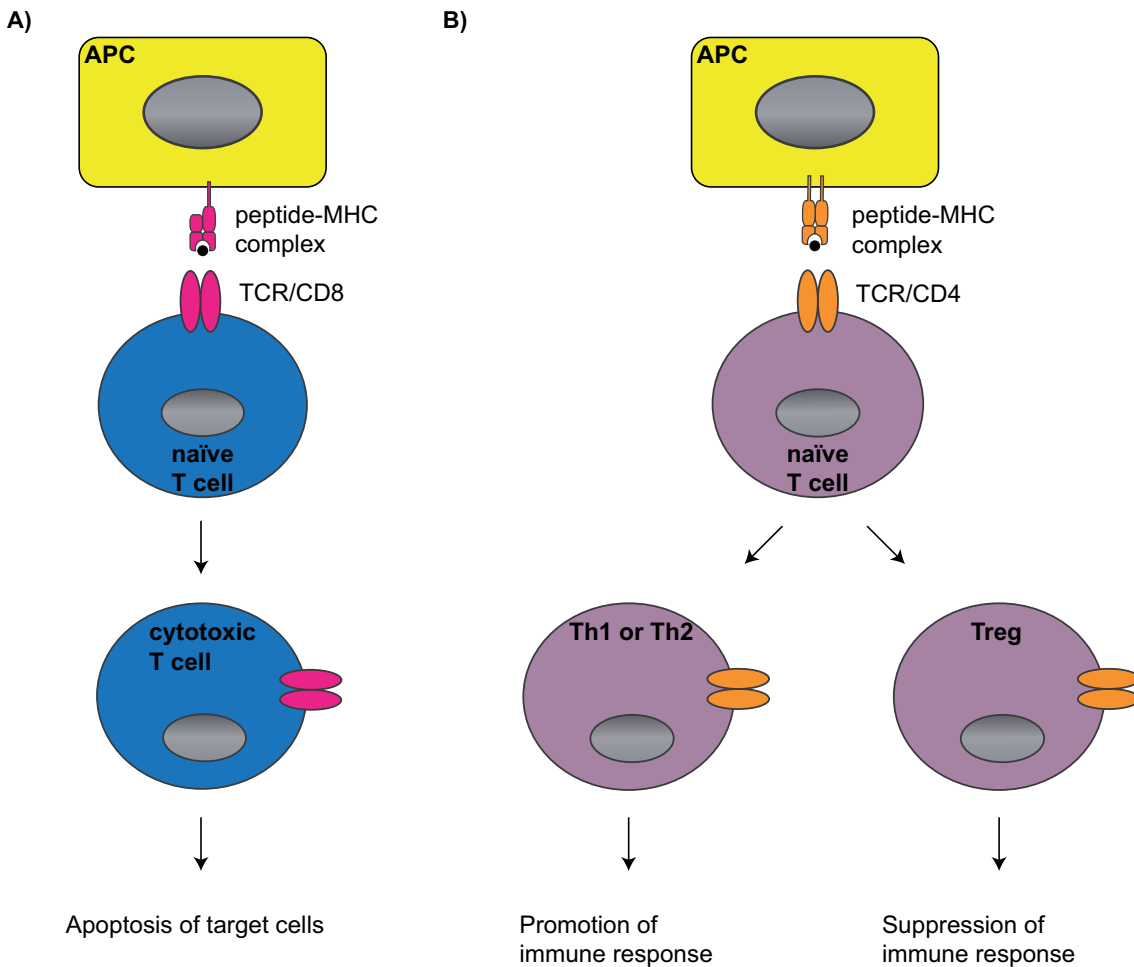
Figure 3.2.1: Schematic representation of the differentiation of T cells
Upon recognition of the respective peptide-MHC complex on an activated APC, naïve CD8 **(A)**
or CD4 **(B)** T cells undergo differentiation. CD8 T cells acquire cytotoxic capacity and induce
apoptosis of target cells, whereas CD4 T cells differentiate into either activating T helper 1 (Th1)
or Th2 or suppressing regulatory T cells (Treg).

3.2.1 T cell priming

Three signals are necessary for adequate T cell priming. First, the convenient peptide-
MHC complex is recognized by TCR/CD4 or TCR/CD8 molecules. Second, interaction
of co-stimulatory molecules, e.g. CD28:CD80/CD86 or 4-1BB:4-1BBL, initiate signaling
cascades which trigger activation, differentiation and survival of T cells[6,7]. Third,
inflammatory cytokines like IL-12 and IFN-α/β polarize the differentiation of T cells into
effector cells[8]. Furthermore, activated T cells upregulate the expression of IL-2
receptors (IL-2R) and IL-2, which in turn promote their proliferation and differentiation.
Long-term effector function of T cells requires prolonged signaling of all three activation
signals[9].

Incomplete activated T cells become tolerant. Consequently, T cells undergo clonal
anergy or deletion[10]. T cell anergy describes the induced unresponsive state of T cells;

in other words, these cells fail to develop effector functions and additionally become refractory to activation by the respective antigen even if adequate activation signals are present. Apart from that, some incomplete activated T cells undergo clonal deletion through activation-induced cell death initiated by e.g. Fas/Fas ligand-mediated apoptosis[11]. After a brief period of activation and cell division, these T cells experience apoptosis. Both mechanisms, anergy and deletion, are thought to maintain the peripheral self-tolerance of mammals[10].

After an infection is effectively repelled, some effector T cells undergo apoptosis and are rapidly cleared by cells of the innate immunity. However, a small population of effector cells persists as so-called memory T cells. These cells mediate long-lasting immunological protection for a certain antigen. Upon re-infection, memory T cells induce immediate and amplified immune responses[12].

As previously stated, T cell-mediated immunity is initiated by the interaction of APCs with T cells. The underlying reason is that the three signals necessary for adequate T cell priming are only provided by activated APCs[2] (**Figure 3.2.2**). APCs are distributed all over the body and are thereby able to recognize pathogens invading through different routes. Antigens are captured, processed into T cell epitopes and subsequently loaded on MHC molecules to facilitate antigen presentation to T cells. The cells migrate to peripheral lymphoid tissues to enable the recognition of the peptide-MHC complex by rare T cell clones expressing the TCR specific for that particular peptide (signal 1). High levels of co-stimulatory molecules such as CD80/CD86 are only expressed on the surface of activated APCs and interact with a binding molecule, e.g. CD28, on the T cell side (signal 2)[6,13]. Signal 3 is delivered through secretion of inflammatory cytokines, e.g. IL-12, by the APC[8]. After the T cell received all three signals, it migrates to the side of infection and executes its effector function.
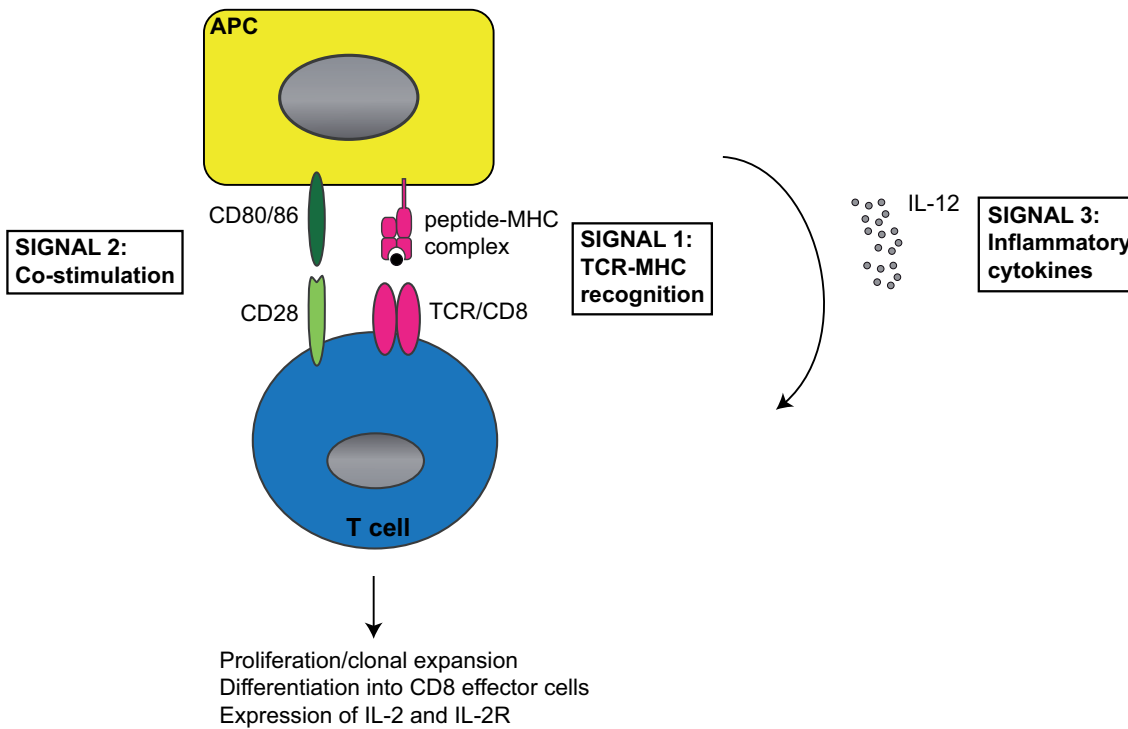
Figure 3.2.2: Schematic representation of the priming of T cells
Efficient T cell priming requires three signals delivered by an APC. First, the respective antigen bound to MHC molecules is presented by the APC and recognized by the TCR and, in this example, a CD8 co-receptor. Second, co-stimulatory molecules like CD80/CD86 and CD28 are expressed and interact. Third, the APC secretes inflammatory cytokines such as IL-12. The priming of T cells results in proliferation and clonal expansion, differentiation into effector cells and expression of IL-2 and IL-2R.

3.3 Dendritic cells

It is generally accepted that dendritic cells (DCs) are the most potent T cell activators among the APCs[14,15]. DCs link the unspecific innate immunity to the antigen-specific adaptive immunity by priming T cells.

DCs originate from both myeloid and lymphoid progenitors within the bone marrow. Under non-inflammatory steady-state conditions immature DCs reside in most tissues and continuously sample a wide array of pathogens[13]. Consequent to inflammatory stimuli, DCs mature into professional APCs and thus acquire capability to initiate T cell-mediated immunity.

Maturation of DCs is induced by activation of PRRs such as Toll-like receptors (TLRs) or tumor necrosis factor (TNF) receptors like CD40[16]. For instance, microbial agents like lipopolysaccharides (LPS) are recognized by TLR4, which in turn triggers downstream signaling for DC maturation[17]. As a result, DCs undergo radical functional and morphological changes; they up-regulate adhesion and co-stimulatory molecules and increase their antigen-presenting capacity[16]. Mature DCs migrate subsequently to

peripheral lymphoid tissues to present peptide-MHC complexes to T cells (**Figure 3.3.1A**).

In the absence of inflammatory stimuli, DCs become tolerogenic upon pathogen recognition. Tolerogenic DCs are deficient in adequate signaling for T cell activation or they only deliver co-inhibitory signals[18]. Consequently, T cells become tolerant or polarize into regulatory T cells (**Figure 3.3.1B**).

A)

B)
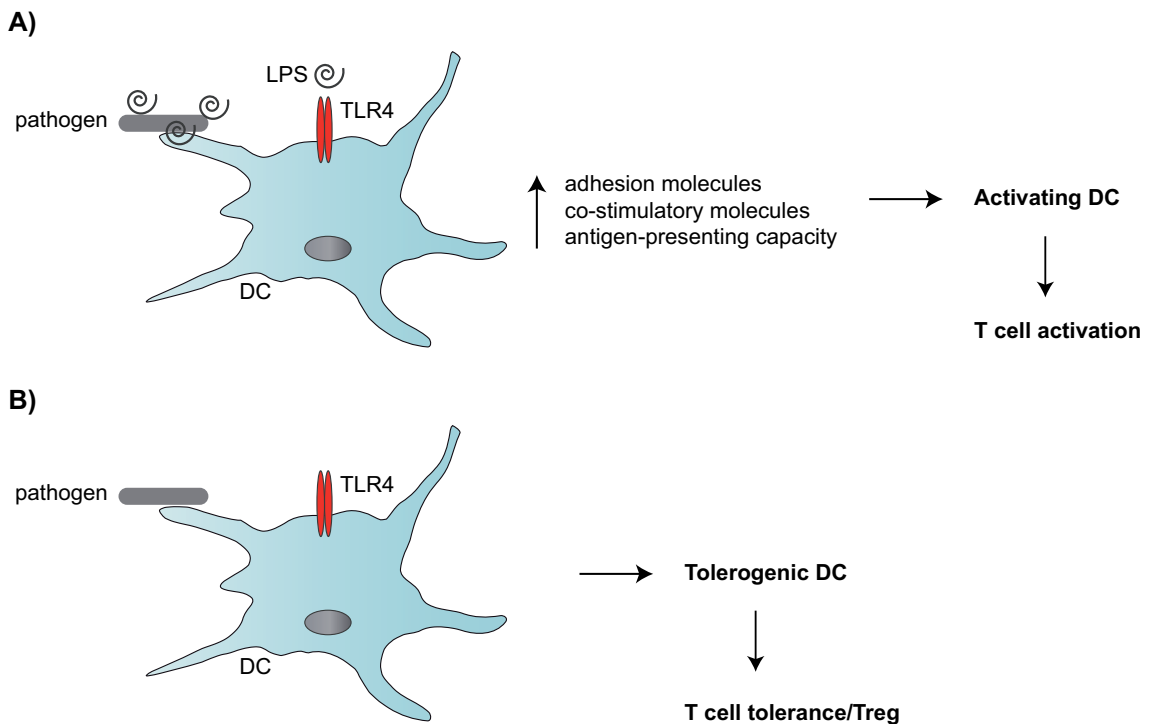
Figure 3.3.1: Schematic representation of the maturation of DCs
Immature DCs recognize a wide array of pathogens. Dependent on the presence **(A)** or absence **(B)** of inflammatory stimuli such as lipopolysaccharides (LPS), DCs polarize into activating or tolerogenic DCs. The TLR4 ligand LPS triggers the expression of adhesion and co-stimulatory molecules and enhance the antigen-presenting capacity. Activating DCs activate T cells, whereas tolerogenic DCs induce T cell tolerance or the differentiation of T cells into regulatory T cells (Treg).

3.3.1 Antigen presentation

Depending on the entry route of pathogens into DCs, they are degraded into antigenic peptides in distinct cellular compartments and are loaded on either MHC class I (MHC I) or class II (MHC II) molecules[19,20]. MHC molecules are glycoproteins encoded by genes known to be the most polymorphic in higher mammals[21]. Every individual possesses multiple MHC molecules with highly variable peptide binding properties. Basically, MHC molecules consist of two different polypeptide chains[2]. An MHC I molecule is composed of a membrane-spanning α chain which is non-covalently associated with a polypeptide termed β_2-microglobulin (**Figure 3.3.2A**). The α chain is

further subdivided into the α_1, α_2 and α_3 domains and two of them, α_1 and α_2, form the peptide binding groove, whereas α_3 is connected to the cell membrane[2,22].

MHC II molecules consist of two non-covalently associated transmembrane polypeptides, namely α and β chains (**Figure 3.3.2B**). Each chain has two domains and one domain of every chain, α_1 and β_1, are part of the peptide binding groove[2,23]. The α_2 and β_2 domains span the membrane. The α chains of the MHC molecules are different polypeptides.
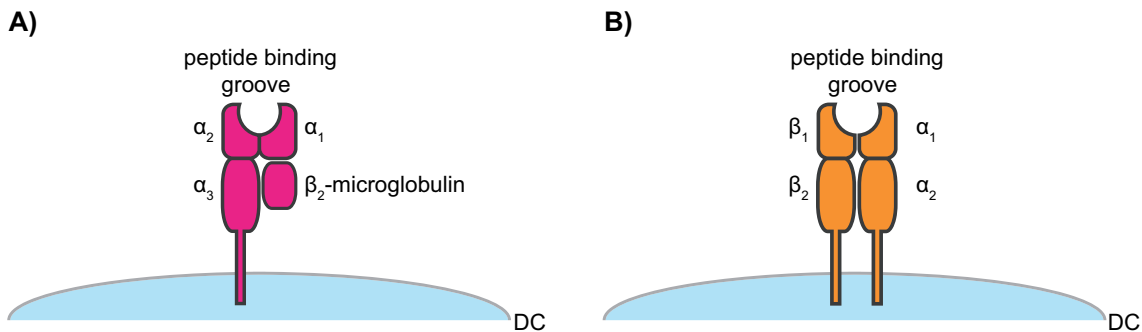
Figure 3.3.2: Schematic representation of the MHC molecules
MHC class I **(A)** or class II **(B)** molecules are composed of two non-covalently associated polypeptide chains. The MHC I molecule consists of an α chain and a β_2-microglobulin and its peptide binding groove is formed by the α_1 and α_2 domains of the α chain. The α_3 domain spans the membrane. The MHC II molecule is composed of an α and a β chain. The α_1 and β_1 domains fold into the peptide binding groove, whereas α_2 and β_2 are connected to the cell membrane.

Peptide-MHC complexes are presented on the surface of maturated DCs to activate either CD8 or CD4 T cells[13].

3.3.1.1 MHC I-mediated antigen presentation to CD8 T cells

In classical MHC I-mediated antigen presentation, intracellular antigens are immobilized on MHC I molecules and recognized by CD8 T cells. MHC I molecules are expressed on all nucleated cells[2].

Processing of intracellular antigens originating from viruses or parasites, for example, starts within the cytosol. Here, a multicatalytic protease complex, the immunoproteasome, degrades antigens in an ubiquitin-dependent manner[24]. The peptides are subsequently shuttled into the endoplasmic reticulum (ER) and finally trimmed by endoplasmic reticulum aminopeptidase associated with antigen processing (ERAAP). The folding and complete assembly of the two chains of MHC I molecules and the antigenic peptides occurs within the ER. MHC I molecules preferentially bind peptides being 8-9 amino acids in length and having hydrophobic or basic residues at

the C-terminus[2,25]. Finally, the peptide-MHC I complex is transported to the cell membrane (**Figure 3.3.3**).

In addition to the classical MHC I pathway, DCs are able to load exogenous antigens on MHC I molecules by a mechanism termed cross-presentation[16]. During cross-presentation, extracellular antigens are recognized by endocytic receptors like the mannose receptor (MR) and internalized via clathrin-mediated endocytosis. The antigens are entrapped in slowly maturing early endosomes and are subsequently translocated into the cytosol for degradation by the immunoproteasome[19,24,26] (**Figure 3.3.3**).
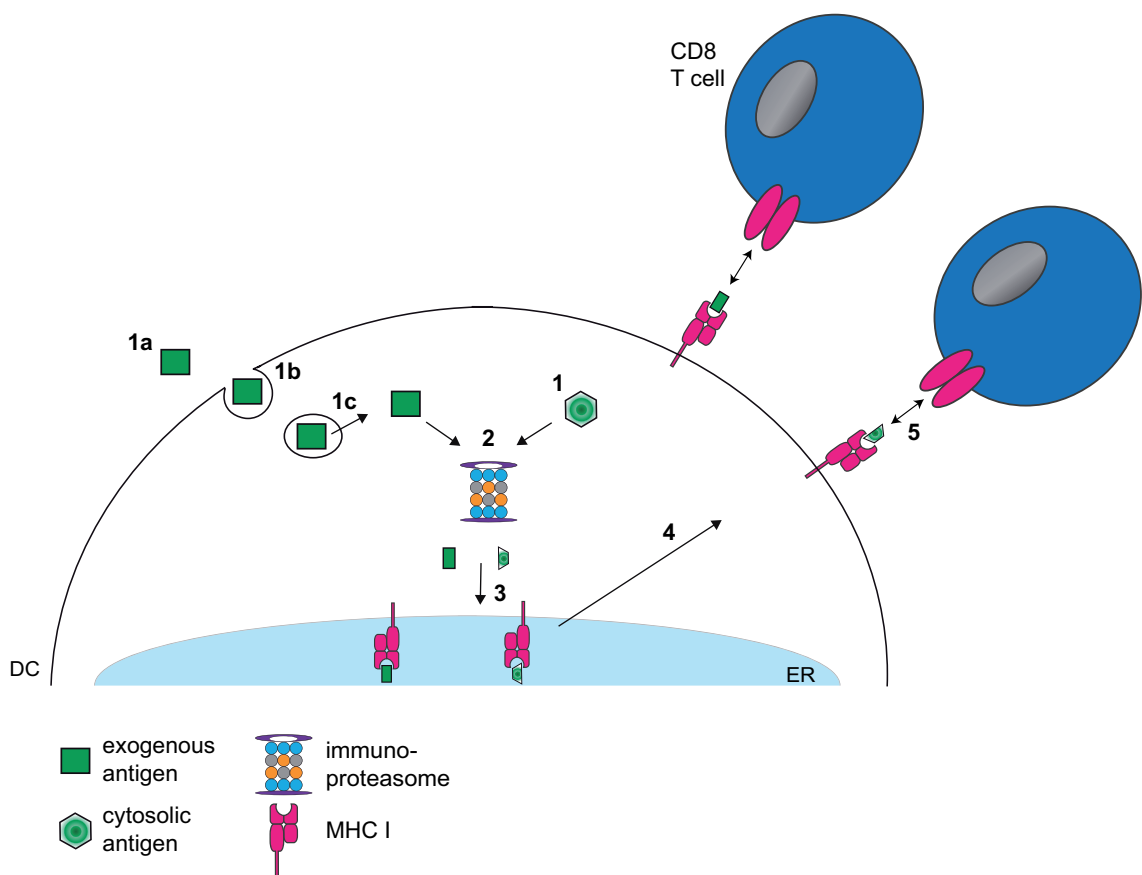
Figure 3.3.3: Schematic representation of the MHC I pathway
In the classical MHC I pathway a cytosolic antigen (1) is degraded by the immunoproteasome (2) and loaded on MHC I molecules in the endoplasmic reticulum (ER) (3). Peptide-MHC I complexes are transported to the cell membrane (4) for the presentation to a CD8 T cell expressing the appropriate TCR (5).The alternative MHC I pathway is cross-presentation. An exogenous antigen (1a) is endocytosed (1b) and translocated out of the early endosome (1c) to encounter the immunoproteasome.

3.3.1.2 MHC II-mediated antigen presentation to CD4 T cells

The classical MHC II pathway facilitates the presentation of exogenous antigens to CD4 T cells. MHC class II expression is restricted to professional APCs[2].

MHC II-restricted antigens are endocytosed by macropinocytosis, phagocytic or endocytic receptors, and are degraded in late endosomes or lysosomes[27]. These late endolysosomal antigen-processing compartments are enriched in acid proteases like cathepsin S and L, and disulphide reductases[2,27]. The two chains of MHC II molecules are assembled in the ER, the peptide binding groove is thereby blocked by a protein so-called the invariant chain, and the whole complex is enclosed and released within multivesicular bodies (MVBs)[2]. Subsequently, MVBs fuse with peptide-containing vesicles, the invariant chain is degraded and supplemented by the antigenic peptide. MHC II molecules bind peptides being at least 18 amino acids in length[28]. In the end, the peptide-MHC II complex is inserted into the plasma membrane[2,27] (**Figure 3.3.4**).

The classical MHC II pathway can be bypassed by a process named autophagy. Cytosolic macromolecules and organelles that are entrapped within autophagosomes are delivered to late endolysosomal antigen-processing compartments for degradation[27,29] (**Figure 3.3.4**).
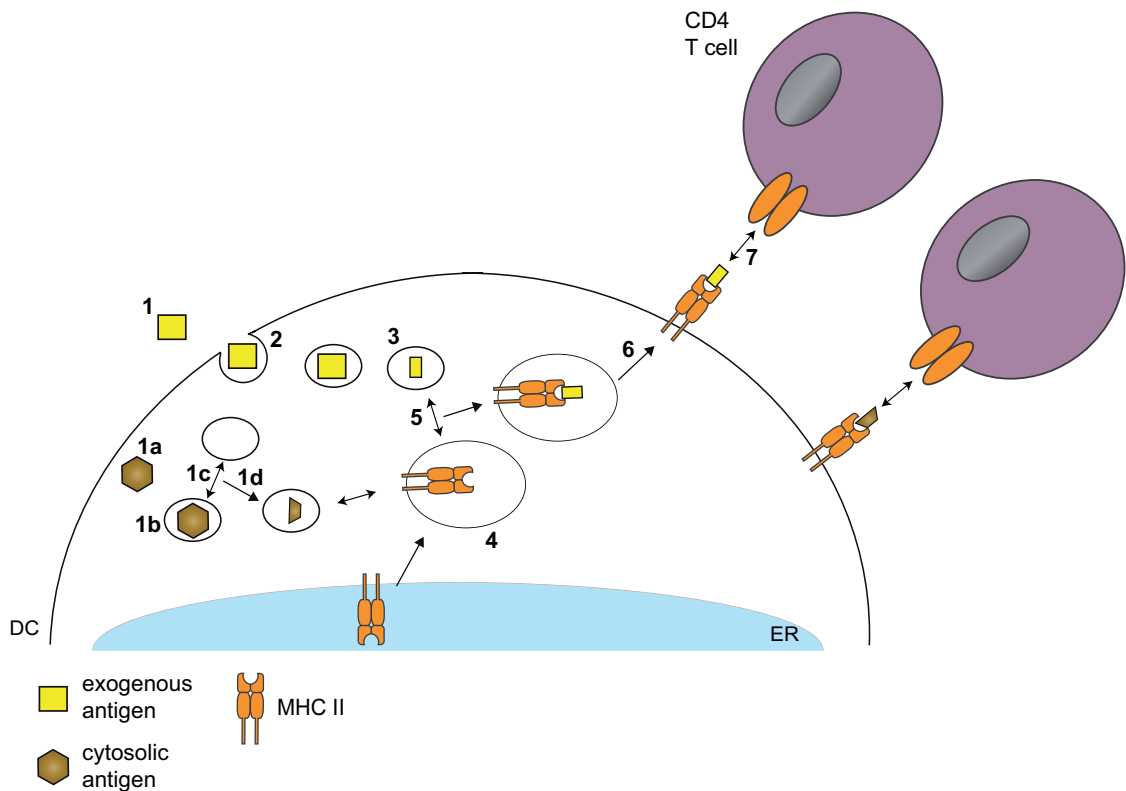
Figure 3.3.4: Schematic representation of the MHC II pathway
In the classical MHC II pathway an exogenous antigen (1) is internalized (2) and processed into peptides inside late endosomes or lysosomes (3). MHC II molecules are formed in the endoplasmic reticulum (ER) and released within multivesicular bodies (MVBs) (4). MVBs subsequently fuse with the peptide-containing vesicle, where the peptide is loaded on the MHC II molecule (5). The peptide-MHC complex is translocated to the membrane (6) and presented to CD4 T cells (7). The alternative MHC II pathway is autophagy. A cytosolic antigen (1a) is entrapped by an autophagosome (1b) which fuses with late endosomes or lysosomes (1c). In accordance with the classical pathway, the antigen is degraded (1d) and the peptide-containing vesicle fuse with MVBs.

3.3.2 Internalization mechanisms

DCs feature various mechanisms to internalize pathogens; they practice phagocytosis, macropinocytosis and receptor-mediated clathrin-dependent endocytosis[13,27].

Macropinoctytosis or phagocytosis mediate the non-specific uptake of large quantities of extracellular fluids or macromolecules; solutes or large particles are thereby engulfed by plasma membrane protrusions and subsequently transported into endolysosomal compartments[27,30]. However, phagocytosis can also be mediated by phagocytic receptors such as Fc receptors or scavenger receptor A[16,27].

Moreover, DCs express a variety of endocytic receptors to facilitate specific clathrin-dependent endocytosis of pathogens[13]. Prominent examples are receptors of the C-type lectin family like the mannose receptor (MR) or dendritic and epithelial cells 205 kDa (DEC-205)[31,32] (**Figure 3.3.5AB**). C-type lectin receptors are non-canonical PRR that capture specific ligand structures, but fail to induce adequate signaling for DC

maturation[33]. Basically, C-type lectins were identified to bind carbohydrates in a Ca^{2+}-dependent manner using highly conserved C-type lectin like domains (CTLDs)[34]. For example, the MR is described to recognize glycan residues of various microorganisms such as *Candida albicans* and *Mycobacterium tuberculosis*[35]. However, other C-type lectin receptors such as DEC-205 were reported to express non-classical CTLDs lacking the ability to bind carbohydrates[31]. The natural ligand for DEC-205 has not been defined yet[36].

Interestingly, the recognition and uptake of pathogens by C-type lectin receptors determine the subsequent processing and antigen presentation[19,37]. For example, ligands internalized by the MR are entrapped in slowly maturing early endosomes for cross-presentation on MHC I molecules[19,38], whereas ligands taken up by DEC-205 are transported towards late endolysosomal antigen-processing compartments for presentation on MHC II molecules[37,39].
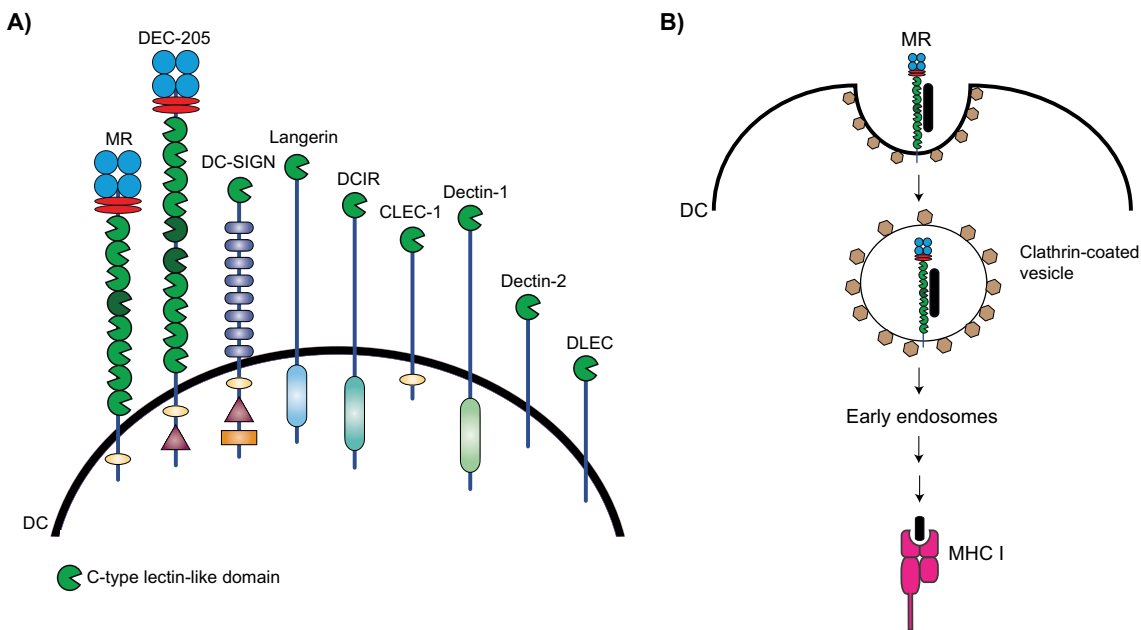
Figure 3.3.5: Schematic representation of C-type lectin receptors expressed on DCs and the MR-mediated clathrin-dependent endocytosis of pathogens
Several receptors composed of at least one C-type lectin-like domain are expressed on DCs **(A)** (modified from Figdor *et al.*[31]). Upon ligand (black bar) binding to endocytic receptors, in this example the C-type lectin receptor mannose receptor (MR), the receptor-ligand complex is internalized by clathrin-dependent endocytosis into DCs **(B)**. A clathrin-coated vesicle is formed and fuse subsequently with early endosomes for enabling cross-presentation on MHC I molecules. MR=mannose receptor; DEC-205=dendritic and epithelial cells, 205 kDa; DC-SIGN=DC specific ICAM-3 grabbing non-integrin; DLEC=DC lectin; DCIR=DC immunoreceptor; CLEC-1=C-type lectin receptor-1; Dectin=DC-associated C-type lectins

3.4 DCs as targets for immunotherapy

The superior capacity of DCs in modifying downstream T cell responses has made them suitable targets in the development of vaccines for immunotherapeutic

applications. DC-based vaccines are currently under investigation for the prevention and treatment of infections, cancer, allograft rejections or autoimmune diseases[40-44]. To this end, DCs are either stimulated to become activating or tolerogenic (**Figure 3.3.1AB**). Immunologists follow different strategies to generate these immunocompetent DCs. DCs are either pulsed *ex vivo* with antigens or targeted *in situ* by different carriers coupled to antigens.

Autologous DCs are loaded *ex vivo* with antigens and reinfused into the patient. Depending on the kind of co-delivered stimuli, DCs develop an activating or tolerogenic phenotype.

To date, one DC-based vaccine, which is based on pulsed DCs, has been approved by the Food and Drug Administration (FDA). Sipuleucel-T, sold under the trade name Provenge®, is used in prostate cancer therapy[45]. For this purpose, autologous APCs are isolated and activated *ex vivo* with the recombinant protein PA2024 consisting of prostatic acid phosphatase (PAP) fused to granulocyte macrophage colony-stimulating factor (GM-CSF). GM-CSF is a hematopoietic growth factor that initiates activation and maturation of DCs[13]. Consequently, DCs up-regulate adhesion and co-stimulatory molecules and increase their antigen-presenting capacity. PAP is a prostate-derived enzyme which is often up-regulated in prostate cancers[46]. Although the precise mechanism of action of sipuleucel-T is not defined yet, it was demonstrated that the PA2024 fusion protein is internalized, processed and presented by DCs[47,48]. Upon re-infusion, a T cell-mediated anti-tumor immune response is initiated[48]. Because of the high treatment costs of $ 104,534 (around € 93,000) for the three prescribed infusions[49], the marketing authorization of sipuleucel-T in the European Union was withdrawn by the European Commission in 2015[50].

Ex vivo generation of tolerant DCs has also been tested for the treatment of several autoimmune diseases. For example, DCs isolated from patients suffering multiple sclerosis were incubated with a tolerogenicity-inducing vitamin D_3 metabolite in addition to myelin peptides as specific self-antigen[51]. As a result, DCs developed a tolerogenic phenotype and mediated anergy of myelin-reactive T cells.

Much work on the potential of *ex vivo* pulsed DCs has been carried out[40,42,43,52], however there are still some critical issues. For example, it is proven to be difficult to sufficiently recapitulate DC maturation *ex vivo*[52] and *ex vivo* induced tolerogenicity of DCs was observed to be rapidly inverted into an activating phenotype after reinfusion into the patient[53]. Moreover, treatments with *ex vivo* pulsed DCs can result in the development of severe autoimmune diseases[54-56].

Therefore, enabling DC-based vaccination in their natural environment *in vivo* is a major goal in the field of DC-based immunotherapy. For this purpose, carrier molecules were applied to deliver antigens specifically to DCs. Often, monoclonal antibodies targeting DC surface molecules such as C-type lectin receptors, are used and two are currently investigated in clinical trials[44,57] (**Table 3-1**). For example, vaccination with the mannose receptor antibody CDX-1307 is currently tested in phase II clinical trial for the treatment of muscle-invasive bladder cancer[58]. CDX-1307 consists of a human anti-MR monoclonal antibody fused to the human chorionic gonadotropin beta-chain, a tumor antigen frequently expressed by epithelial tumors[59]. When co-administered with the hematopoietic growth factor GM-CSF and TLR agonists, CDX-1307 induces activation of APCs and subsequent activation of a T cell-mediated anti-tumor immune response[58,60].

Table 3-1 DC-targeting with C-type lectin receptor-binding antibodies

Phase	Targeting strategy	Indication	Reference
I/II	MR Ab CDX-1307 fused with recombinant human chorionic gonadotropin beta-chain tumor antigen with/without GM-CSF and TLR 3 or 7/8 agonists	Advanced epithelial malignancies/Muscle-invasive bladder cancer	Morse et al. 2011[60], Morse et al. 2011[58]
I/II	DEC-205 Ab CDX-1401 fused with NY-ESO-1 tumor antigen with TLR3 or 7/8 agonists	Advanced malignancies/Ovarian, Fallopian Tube, Primary peritoneal cancer	Riedmann 2012[61], Dhodapkar et al. 2014[62]

Examples of antibodies used in pre-clinical studies:

-	DEC-205 Ab fused with HIV gap 24	HIV	Cheong et al. 2010[63], Idoyaga et al. 2011[64], Flynn et al. 2011[65]
-	DEC-205 Ab fused with mycobacterial ESX antigen	Tuberculosis	Dong et al. 2013[66]
-	DC-SIGN Ab fused to gp100/pmel17 tumor antigen	Melanoma	Tacken et al. 2008[67]
-	MR Ab fused with gp100/pmel17 tumor antigen	Melanoma	Ramakrishna et al. 2004[68]
-	Dectin-1 Ab fused to MART-1 tumor antigen	Melanoma	Ni et al. 2010[69]

Ab=antibody

Other molecules used for antigen delivery are nanoparticles[70], synthetic long peptides[71,72], receptor ligands[73], viruses[65], toxins[74] and liposomes[75].

Even though more than 100 DC-targeting studies were published so far[44], efficient and specific delivery of antigens remains a challenge. The reasons are multifarious. Carriers like antibodies, viruses or toxins, for example, exhibit intrinsic immunostimulatory potential and, thus, increase the risk of adverse side effects[41,76]. Furthermore, the design and development of some carrier molecules are pricey, time-consuming and associated with technical challenges[41,77,78]. For example, the generation and screening of monoclonal antibodies is time-consuming and expensive[77,78] and liposomal vesicles have critical stability issues[41]. Moreover, the shelf-life of antibodies or proteins is limited and cell-based products like antibodies are difficult to process into clinical grade reagents with invariable quality[41]. Last, liposomes and nanoparticles lack specificity for DCs and they are internalized by highly phagocytically active macrophages rather than by DCs[79].

Obviously, there is a need for eligible carriers and a promising alternative are nucleic acids ligands, known as aptamers.

3.5 Aptamers

In general, aptamers are nucleic acids, which bind target molecules with high specificity and affinity[80]. They adopt unique conformations like stems, loops, hairpins or quadruplexes that enable the specific interaction with their targets[81,82]. Aptamer-target interactions are mediated through pi-stacking of aromatic rings, electrostatic and van der Waals forces, or by hydrogen bond formation[81] (**Figure 3.5.1AB**).

A)

B)
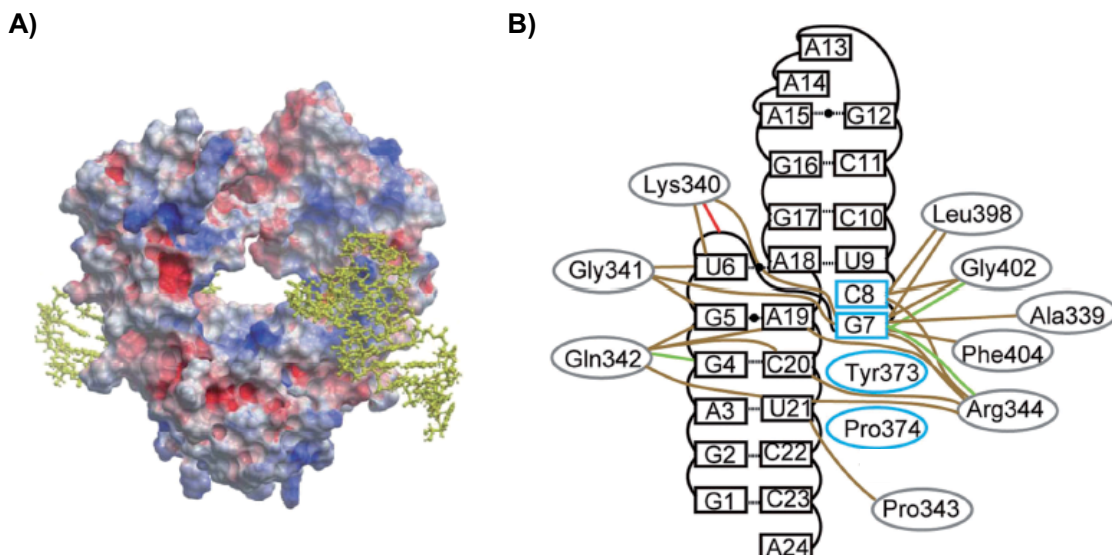
Figure 3.5.1: Interactions between aptamers and their targets
Aptamers bind to their target molecules via different intermolecular interactions. In this example, the structure of an aptamer (green) bound to the Fc fragment of human IgG_1 ($hIgG_1$ Fc; colored according to the electrostatic surface potential) is shown **(A)**. The interactions between the nucleotides of the aptamer and the amino acids of $hIgG_1$ Fc are ion pairing (red), hydrogen bond formation (green), van der Waals forces (brown) and pi-stacking (blue) **(B)** (modified from Nomura *et al.*[83]).

3.5.1 Identification of aptamers

In 2015, the first identified aptamers celebrated their 25th anniversary. Tuerk & Gold and Ellington & Szostak both published the identification of the first nucleic acids-based ligands by a novel technique termed systematic evolution of ligands by exponential enrichment (SELEX)[83,84]. Briefly, target-binding nucleic acid sequences are enriched in an oligonucleotide library by iterative cycles of incubation, separation and amplification (**Figure 3.5.2**). The starting point of a SELEX process is the incubation of the target of interest with the naïve oligonucleotide library. This oligonucleotide library is composed of a random region embedded between fixed primer binding sites. Next, background or target non-binding sequences are removed and the binders eluted from the target. To achieve that, the respective target is either immobilized on a matrix or the non-binders are removed by centrifugation, electrophoresis or flow cytometry[85-88]. Elution is carried out either by denaturing conditions or, for instance, by using competitive molecules[89,90]. The eluted sequences are amplified by polymerase chain reaction (PCR) and subsequently single-stranded nucleic acids are generated. Single chained RNA is easily obtained by *in vitro* transcription methods, whereas multiple methods are employed to separate double-stranded DNA. For example, biotin or phosphate moieties are introduced during PCR and used to separate the strands by biotin-

streptavidin interaction or enzymatic cleavage, respectively[91,92]. Finally, the resulting library of nucleic acid sequences is used in the next selection cycle.
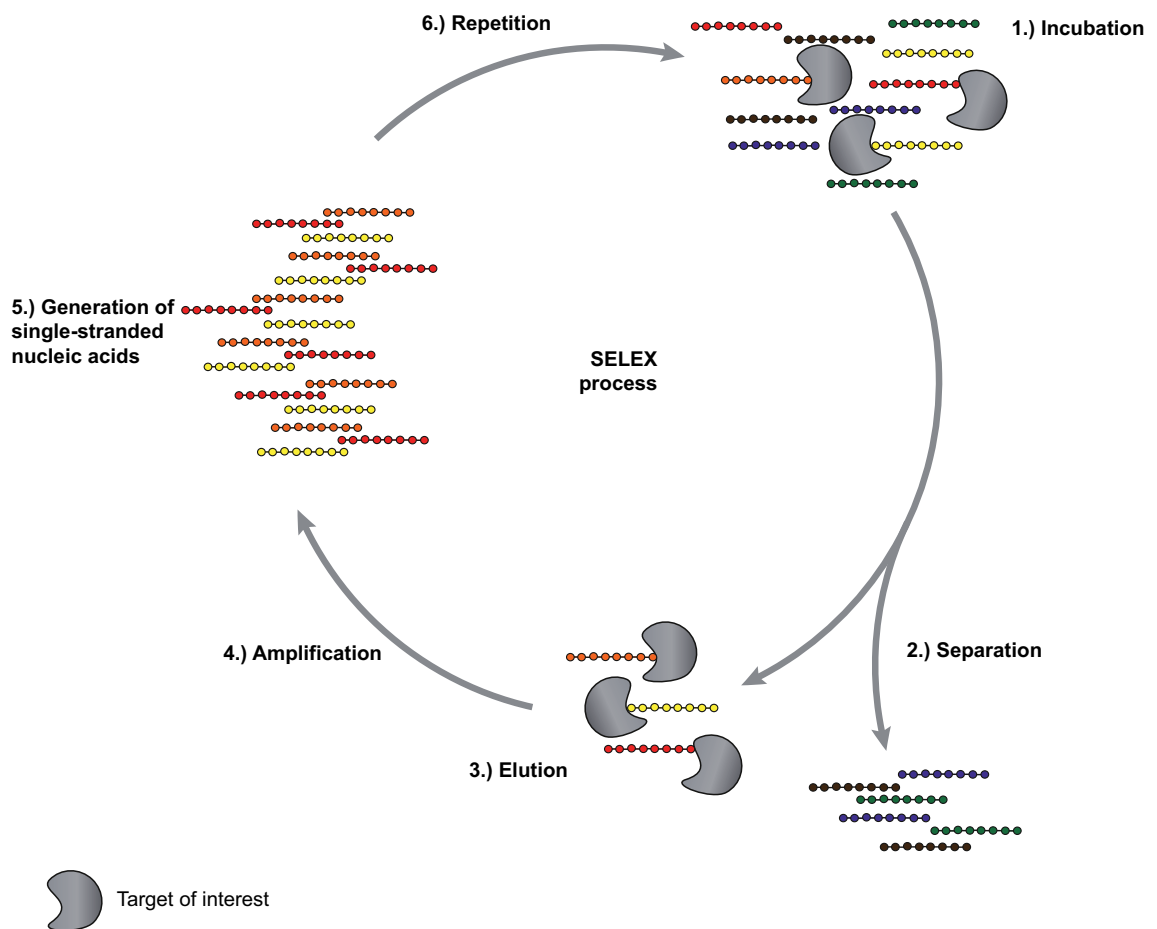
Figure 3.5.2: Schematic representation of the SELEX process
Systematic evolution of ligands by exponential enrichment (SELEX) is carried out to identify high affinity aptamers. The SELEX process is initiated by incubating the target of interest with the naïve oligonucleotide library (1). The bound sequences are separated from the unbound (2), eluted from the target (3), amplified (4) and implemented as single-stranded oligonucleotides (5) in the next selection cycle (6).

To identify individual aptamers, the enriched nucleic acid libraries are inserted into bacterial vectors, transformed into bacteria and sequenced or they are analyzed by next-generation sequencing[82,93]. For further analysis, selected aptamers are obtained by solid phase synthesis.

3.5.2 Cell-binding aptamers

Aptamers can be developed for a plethora of target structures, ranging from small molecules to complex organisms[91,94-100]. Nowadays, aptamers represent essential tools for fundamental research and bioanalytical diagnostics[101-103], and a growing number of aptamers are extensively investigated in pre-clinical studies[77,104]. Moreover, a few

aptamers are currently in clinical trials[104,105] (**Figure 3.5.3**). In 2004 the first, and up to now only, aptamer-based drug was approved by the FDA. Aptamer NX1838, sold under the trade name Macugen®, is used for the therapy of age-related macular degeneration[106].

Aptamer	Molecular target	Sponsor	Medical indications	Current status
ARC1779	Activated von Willebrand Factor (vWF)	Archemix Corporation	Purpura; Thrombotic Thrombocytopenic; Von Willebrand Disease Type-2b	Phase 2 completed
ARC1905	Complement factor C5	Ophthotech Corporation	Age-Related Macular Degeneration	Phase 1 completed
ARC19499	Tissue Factor Pathway Inhibitor (TFPI)	Baxter Healthcare Corporation	Hemophilia	Phase 1 terminated
AS1411	Nucleolin	Antisoma Research	Leukemia, Myeloid	Phase 2 completed
			Metastatic Renal Cell Carcinoma	Phase 2 status is unknown
E10030	Platelet-derived growth factor (PDGF)	Ophthotech Corporation	Age-Related Macular Degeneration	Phase 3 recruiting participants
NOX-E36	Monocyte Chemoattractant Protein-1 (MCP-1)	NOXXON Pharma AG	Type 2 Diabetes Mellitus; Albuminuria	Phase 2 completed
NOX-A12	Stromal Cell-Derived Factor-1	NOXXON Pharma AG	Multiple Myeloma; Chronic Lymphocytic Leukemia	Phase 2 recruiting participants
NOX-H94	Hepcidin	NOXXON Pharma AG	Anemia of Chronic Disease	Phase 2 completed
NU172	Thrombin (Factor IIa)	ARCA Biopharma	Heart Disease	Phase 2 status is unknown
REG1	Coagulation factor IX	Regado Biosciences	Coronary Artery Disease	Phase 3 recruiting participants

Figure 3.5.3: Overview on aptamers that are currently tested in clinical trials
Aptamers successfully tested in pre-clinical trials are now investigated in clinical trials for the treatments of different cancer types or diseases (adapted from Sun *et al.*[104])

In recent years, there has been considerable interest in using aptamers recognizing mammalian cells[96,100,107]. Cell-specific aptamers are identified by using purified cell surface proteins in a protein-SELEX approach or living cells in a cell-SELEX process[100]. Mammalian cells express several accessible target structures on their surface. In cell-SELEX, membrane proteins maintain their native conformation and the consistent accessibility of the epitopes is warranted. Target molecules which are difficult to isolate from the cell surface can be addressed by this selection strategy[100]. In addition, aptamers can be identified by a sole *in vivo* selection process[108,109]. For example, aptamers targeting colon cancer cells were identified by injecting a modified RNA library into tumor-bearing mice for several selection cycles[108].

Cell-specific aptamers have several advantageous properties. Because of their nucleic acid composition, they can be easily modified to increase their chemical diversity and biological properties. Some modifications like unnatural base pairs or modified nucleobases are applied during aptamer selection[110,111], whereas others like disulfide or amino groups can be incorporated post-selectively[80].
A second property is that they represent promising delivery vehicles. They are often internalized by the respective cell[96,99,112,113] and a variety of cargo molecules can be attached covalently or by hybridization[96,114,115]. Indeed, several cargo molecules such

as proteins or small molecules conjugated to cell-specific aptamers were effectively delivered and endocytosed[112,116-118] (**Figure 3.5.4**). The ribosomal toxin gelonin, for example, was selectively delivered to pancreas carcinoma cells upon conjugation to an aptamer[112].
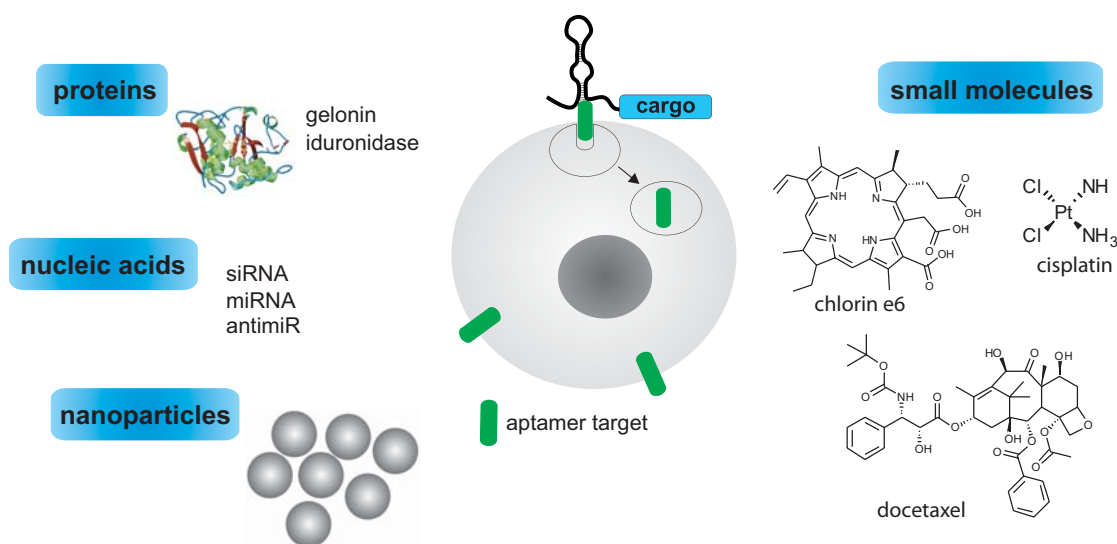
Figure 3.5.4: Overview on cargo molecules delivered by cell-specific aptamers
Cell-specific aptamers can be conjugated to multiple cargo molecules for selective delivery approaches (modified from Mayer *et al.*[96]).

Moreover, studies in mammals elucidated low to no immunogenicity and toxicity of aptamers *in vivo*[78,119]. The main reason for this is that the identified aptamers are obtained by cell-free solid phase synthesis, therefore they are free of contaminations derived from other species[77,78]. The chemical synthesis warrant reproducibility, thus, leading to a reduced batch to batch variability[82].

However, chemical modifications are often required to increase the stability of aptamers for *in vivo* applications. Because of their small size and composition, aptamers are prone to be degraded by nucleases or rapidly removed by renal clearance[96]. Addition of high-molecular weight compounds, for example, could slow down the clearance of aptamers. For instance, attached polyethylene glycol moieties increased the *in vivo* circulation half-life of a breast cancer targeting aptamer from 16 to 22 hours[120].

Considering the characteristics and possible applications, cell-specific aptamers are a promising alternative class of cell-targeting molecules that might overcome the limitations of other molecules used for immunotherapy so far.

3.5.3 Aptamers for immunotherapeutic applications

In recent years there has been a considerable interest in identifying aptamer-based immunomodulatory ligands. Aptamers have been proven to function as inhibitors, agonists, opsonizing agents or antigen delivery tools for vaccination strategies[77,115].

One strategy of immunomodulation is to block immunosuppressive pathways and thereby circumvent tumor evasion mechanisms. Programmed cell death (PD-1) and cytotoxic T-lymphocyte-associated protein 4 (CTLA-4) are examples of receptors which negatively regulate T cell effector functions[121]. Remarkably, both receptors were successfully addressed and blocked by aptamers[122,123]. Moreover, these aptamers potentiated anti-cancer immunity in murine tumor models.

Another strategy of immunotherapy is to enhance T cell activation by applying receptor agonists. Besides recognition of antigen-MHC complex by TCR and triggering of cell differentiation by inflammatory cytokines, co-stimulatory signals are necessary for adequate priming of naïve T cells. 4-1BB is the major co-stimulatory receptor expressed on activated CD8 T cells[7]. In 2008, McNamara *et al.*[124] selected aptamers which function as natural ligands of 4-1BB and thereby boost T cell activation and survival.

A further attempt of immunomodulation is to opsonize cancer cells, in other words, to recruit T cells directly to the tumor site. On that account, 4-1BB aptamers were conjugated with prostate cancer-binding prostate-specific membrane antigen (PSMA) aptamers and thereby T cell co-stimulation straight at the tumor site was facilitated[125].

Although cell-specific aptamers are proven to be suitable carriers (**Section 3.5.2** and **Figure 3.5.4**), only few researchers addressed their ability to bind or to deliver antigens to DCs for vaccination strategies. When the study at hand was initiated, only the investigations conducted by Berezovski *et al.*[126] and Hui *et al.*[127] were published. Berezovski and co-workers enriched DNA libraries targeting either immature or mature murine bone marrow-derived DCs (BM-DCs) for the identification of cell state-specific biomarkers[126]. However, binding or functionality of individual aptamers was not examined. In the study of Hui *et al.*[127], they identified BM-DC-binding aptamers by using a recombinant protein of the C-type lectin receptor DC-SIGN in a SELEX approach. Nevertheless, the inhibitory function of the aptamers on the adhesion of DCs to endothelial cells was investigated rather than their capability as delivery tools.

In 2014 the first, and to date sole, aptamer-based antigen delivery was reported by Wengerter *et al.*[115]. Here, DC-targeting aptamers were selected against the C-type lectin receptor DEC-205 using a combinatorial approach of protein- and cell-SELEX. These aptamers were subsequently conjugated with ovalbumin (OVA) and reported to facilitate cross-presentation by DCs following CD8 T cell activation. In addition, multivalent aptamer-OVA conjugates were observed to induce CD8 cytotoxicity against OVA-expressing melanoma cells *in vivo*. Still, open questions remain. First and foremost, no investigations concerning CD4 T cell activation were done, although the used antigen OVA exhibits both MHC I- and MHC II-restricted epitopes[128,129]. Second, there is no general agreement on DEC-205 mediated MHC I-restricted CD8 T cell activation. In other studies, it was demonstrated that targeting of DEC-205 boost MHC II-restricted CD4 T cell activation rather than CD8 T cell stimulation[37,39]. Third, OVA was demonstrated to be internalized, processed and cross-presented by DCs in its natural unconjugated form[19,38]. It is then questionable if the aptamers improve the effect of OVA on DCs and T cells.

Obviously, it is worth to further investigate the potential of aptamer-based DC vaccines.

3.6 Aims of the thesis

One approach of DC-based immunotherapy is to deliver antigens specifically to DCs for efficient T cell activation. Even though several molecules like antibodies, viruses or nanoparticles are currently under investigations, antigen delivery to DCs remains a challenge[41,44].

The aim of this thesis was to investigate the potential applicability of aptamers as a novel class of DC-targeting carriers for immunotherapeutic applications. In particular, we were interested in answering the following questions.

What is the best SELEX strategy to identify DC-binding aptamers? Two strategies can be followed to identify DC-binding aptamers. On the one hand, purified membrane proteins can be implemented in a protein-SELEX approach, and on the other hand, DCs can be directly used in a cell-SELEX process.

Does the choice of SELEX strategy influence the properties of the aptamers? In protein-SELEX, specific membrane proteins can be chosen, because of their ability to facilitate presentation on MHC I or MHC II molecules. For example, the C-type lectin receptor MR is described to direct its ligands towards cross-presentation[19,38]. Thus, aptamers specific for MR may be internalized into cellular compartments adequate for presentation on MHC I molecules. In cell-SELEX, the specific target structure is

unknown. Nevertheless, aptamers could be identified for targets that enable presentation to T cells and that are not easy to isolate from the membrane.

Are the aptamers exhibiting all properties of suitable carrier molecules? Potential DC-based antigen delivery tools have to meet several criteria. They need to bind specifically to DCs, internalize within adequate antigen processing compartments and be non-immunogenic.

Can the aptamers be conjugated to antigenic peptides without loss of binding ability? Selective delivery of antigens to DCs is only warranted if the aptamers keep their binding ability upon conjugation.

Do the aptamers deliver antigens to DCs and does this delivery result in specific T cell activation? Effective targeting of antigens to DCs results in activation of T cell-mediated immunity. To investigate whether the selected aptamers are functional in antigen delivery, an OVA model system was chosen. Both targeted CD4 and CD8 T cell activation were analyzed.

4 Results

This chapter describes the investigations on the potential applicability of aptamers as DC-targeting carriers for targeted activation of T cell-mediated immunity.

The first part of the chapter outlines the identification of aptamers recognizing dendritic cells (DCs) (**Section 4.1**). In the second part, the properties of aptamers in terms of cell binding, specificity, internalization and immunogenicity are investigated (**Section 4.2**). The chapter concludes with the analysis on the potential of aptamers to deliver antigens for specific T cell activation (**Section 4.3**).

4.1 Identification of BM-DC targeting aptamers

DC-binding aptamers can be identified by using purified cell surface proteins or living cells as target structures in SELEX approaches[100]. DCs express a variety of endocytic receptors and prominent examples among them are the C-type lectin receptors[31,32]. The C-type lectin receptor MR is described to direct antigens towards cross-presentation for CD8 T cell activation[19,38]. Thus, the MR was chosen as an attractive target to identify aptamers that are internalized and localized in DCs in a similar way as MR ligands. To identify aptamers recognizing the MR, the recombinant proteins Fc-CTL and Fc-FN were deployed in a protein-SELEX approach (**Section 4.1.1**). These proteins were designed and described by Linehan *et al.*[130] and Martinez-Pomares *et al.*[131] and were used to analyze the ligand binding specificity of the MR protein domains. Fc-CTL consists of the C-type lectin-like domains 4-7 (CTLD 4-7) of the MR fused to the human IgG_1 Fc portion, whereas Fc-FN is composed of the MR domains cysteine-rich domain, fibronectin type II domain and CTLD 1-3, fused to the Fc part (**Figure 4.1.1A**).

Murine bone marrow-derived dendritic cells (BM-DCs) are a widely used cellular model[132]. In general, DCs develop from bone marrow-derived progenitors and are distributed as a rare cell population in most of mammalian tissues[13]. By treating murine bone marrow-derived progenitors with the hematopoietic growth factor GM-CSF for 7 days, a high yield (up to 1-3 x 10^8) of BM-DCs can be generated[133]. BM-DCs were often used to investigate the capacity of DCs to modify downstream T cell responses[19,71,134] and are therefore a suitable target in cell-SELEX for the identification of DC-binding aptamers (**Figure 4.1.1B** and **Section 4.1.2**).
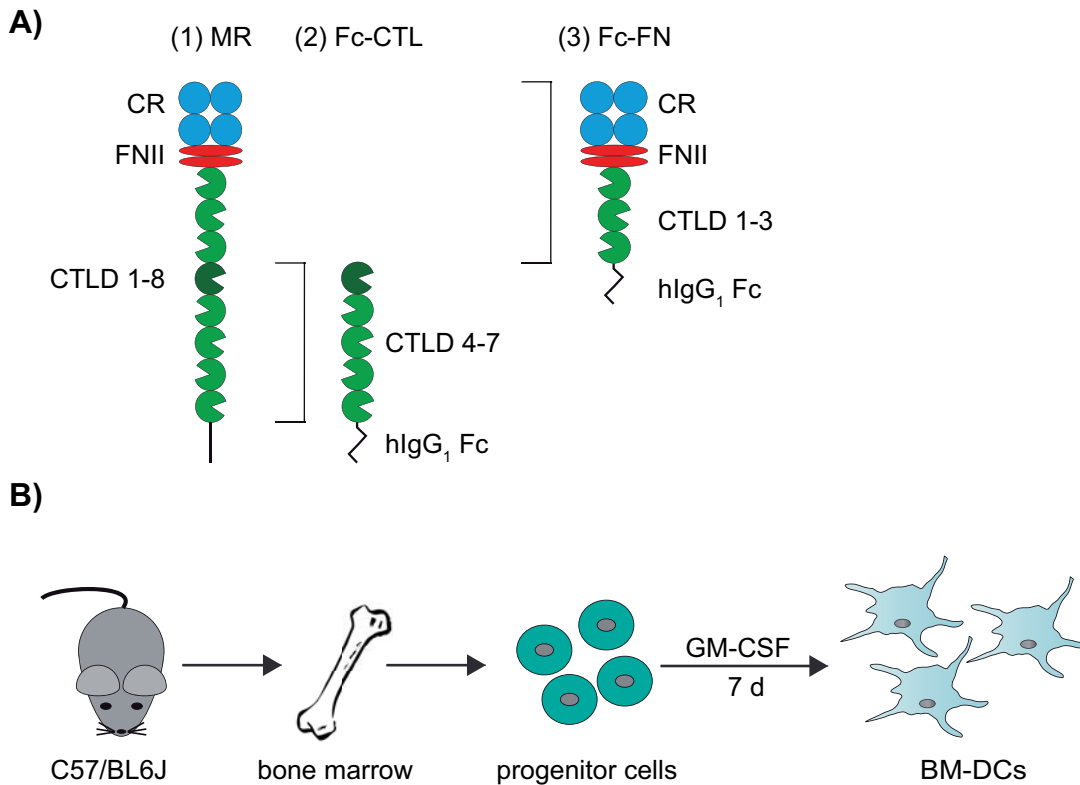
Figure 4.1.1: Schematic representation of the targets used in SELEX approaches to identify BM-DC-binding aptamers

Recombinant mannose receptor (MR) proteins or murine bone marrow-derived DCs (BM-DCs) were used to identify aptamers. The recombinant proteins Fc-CTL (2) or Fc-FN (3) consist of the human IgG$_1$ Fc portion and protein domains of the murine MR (1) **(A)**. The murine MR (1) consists of a cysteine-rich (CR), a fibronectin type II (FNII), eight C-type lectin-like domains (CTLD 1-8) and a transmembrane domain (modified after Martinez-Pomares et al.[131]). BM-DCs were isolated from the C57/BL6J mouse strain and cell progenitors derived from bone marrow of hind limbs were differentiated for 7 d with GM-CSF **(B)**. CR=cystein-rich, FNII=fibronectin type II, CTLD=C-type lectin-like domain; MR=mannose receptor, GM-CSF=granulocyte macrophage colony-stimulating factor

4.1.1 Enrichment of DNA libraries targeting Fc-CTL and Fc-FN

The recombinant Fc-CTL and Fc-FN proteins were kindly provided by Prof. Sven Burgdorf from the LIMES Institute, University of Bonn. Briefly, the proteins were expressed in HEK293 cells and purified by immobilization on protein G columns.

Previously to the SELEX process, the proteins were immobilized on protein G-coated magnetic beads. The SELEX processes were initiated by incubation of the immobilized Fc-CTL or Fc-FN with a naïve DNA library in selection buffer (PBS, 1 mM MgCl$_2$, 1 mM CaCl$_2$, 0.01 mg/ml BSA) for 30 minutes at 37 °C. From the second selection cycle, counter selection steps were introduced, i.e. DNA was pre-incubated with Fc-FN in SELEX targeting Fc-CTL and *vice versa*. After 11 selection cycles, the DNA libraries were analyzed by radioactive filter retention assay. To this end, the obtained DNA was labeled with ^{32}P at the 5'-end, incubated with increasing concentrations of the proteins

in selection buffer, the mixture was then passed through a nitrocellulose membrane, washed and the retained ^{32}P-DNA on the proteins was quantified by autoradiography.

The percentage of ^{32}P-labeled DNA bound to Fc-CTL strongly increased from the 1st to the 6th and 11th selection cycle (**Figure 4.1.2A**). Additionally, the quantity of bound DNA increased in a concentration-dependent manner.

In contrast, the increase of the percentage of Fc-FN-bound ^{32}P-DNA was observed to be much weaker (**Figure 4.1.2B**). The amount of bound DNA of the 6th and 11th selection cycle increased only around 2-2.5-fold in comparison to the first selection cycle.
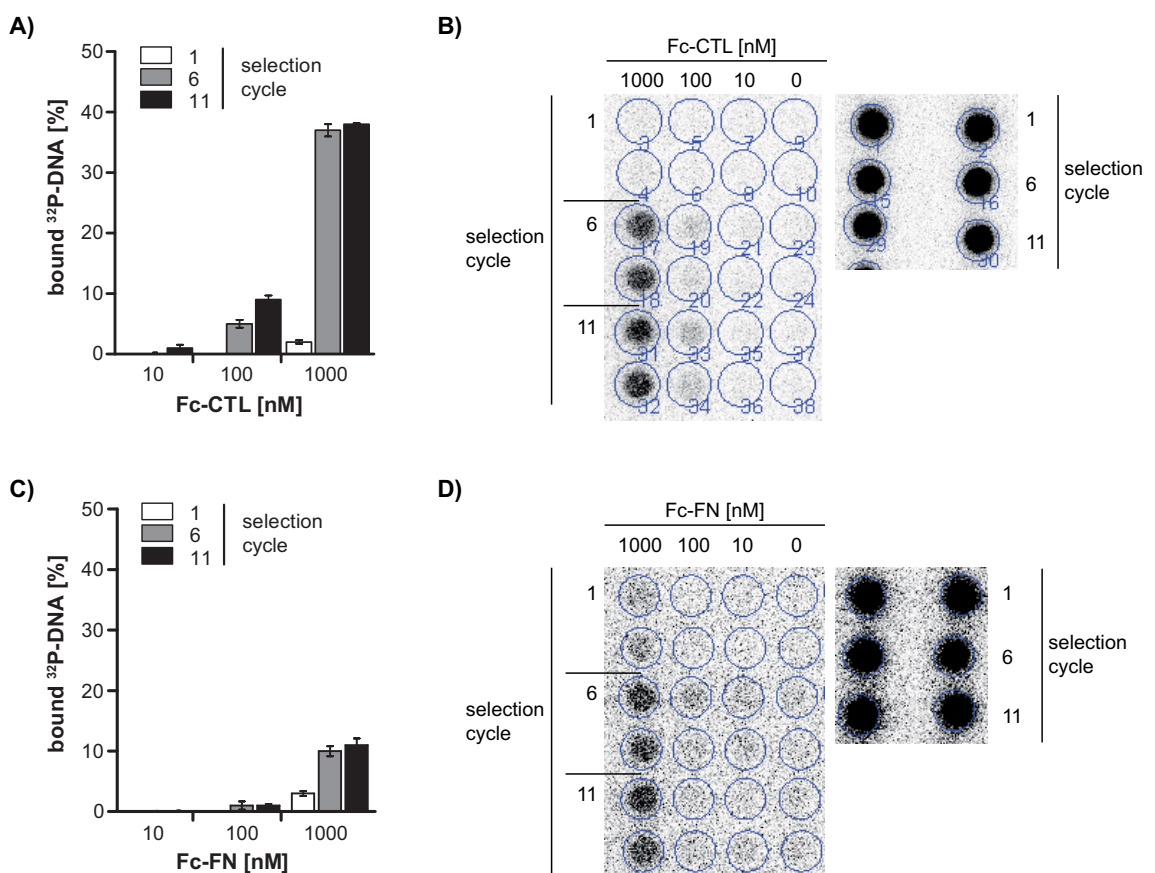
Figure 4.1.2: Aptamer selection targeting Fc-CTL or Fc-FN results in enrichment of DNA
1 pmol of ^{32}P-DNA was incubated with increasing concentrations of Fc-CTL **(A+B)** or Fc-FN proteins **(C+D)** and the mixtures were passed through a nitrocellulose membrane. The amount of ^{32}P-DNA retained on Fc-CTL or Fc-FN was determined by autoradiography (n=2, mean ±. SD). Representative dot blots are shown in **(B)** and **(D)**. Radioactivity appears as black spots. On the left, ^{32}P-DNA retained on the proteins is shown and on the right, 0.8 µl of ^{32}P-DNA is spotted to allow the quantification of the percentage of bound DNA.

Even though SELEX is a notionally simple method, it does not always result in the enrichment of aptamers with desired properties. There is a risk of an accumulation of

non-selective background binders[82]. Therefore, the enriched libraries of the sixth selection cycle were taken for the analysis of target selectivity.

4.1.1.1 Selectivity of Fc-CTL and Fc-FN binding DNA libraries

The selectivity of the enriched DNA libraries for recombinant Fc-CTL or Fc-FN protein was tested by radioactive filter retention assay. To this end, the obtained DNA libraries of the 1st and 6th cycle of both selections were 5'-labeled with ^{32}P and incubated with Fc-CTL, Fc-FN, hIgG$_1$ Fc, protein G, activated protein C (aPC), thrombin, extracellular signal-regulated kinase 2 (Erk2) or the Sec7 domain of cytohesin-1 (Cyt1 Sec7) in selection buffer for 30 minutes at 37 °C.

During SELEX, Fc-CTL and Fc-FN were immobilized on protein G magnetic beads through their hIgG$_1$ Fc tag. To exclude the binding of the enriched libraries to the protein tag or the immobilization matrix, hIgG$_1$ Fc and protein G were included in the radioactive filter retention assays. In addition, the binding to the proteins thrombin, aPC, Erk2 and Cyt1 Sec7 which differ in their protein structures and were successfully addressed in previous aptamer selections[91,94,98,135,136], were also examined.

The DNA libraries derived from the 6th selection cycle targeting Fc-CTL (**Figure 4.1.3A**) or Fc-FN (**Figure 4.1.3B**) bound to both Fc-CTL and Fc-FN proteins. This result was not expected, because Fc-FN was used in the counter selection step in Fc-CTL-SELEX and *vice versa*. However, binding to both proteins is partly mediated by addressing the hIgG$_1$ Fc tag (**Figure 4.1.3AB**). Plus, Fc-CTL as well as Fc-FN contains C-type lectin-like domains (**Figure 4.1.1A**). Although the eight CTLDs of MR differ in their function and ligand specificity, they share conserved amino acid residues to form the typical CTLD fold[35,137-140].

Apart from that, no or a low amount of ^{32}P-DNA retained on aPC, thrombin, Erk2 or Cyt1 Sec7 was observed. Plus, no binding to the immobilization matrix protein G was detected. It can be concluded that the enriched DNA specifically bound to the protein domains used in SELEX.

A)

B)
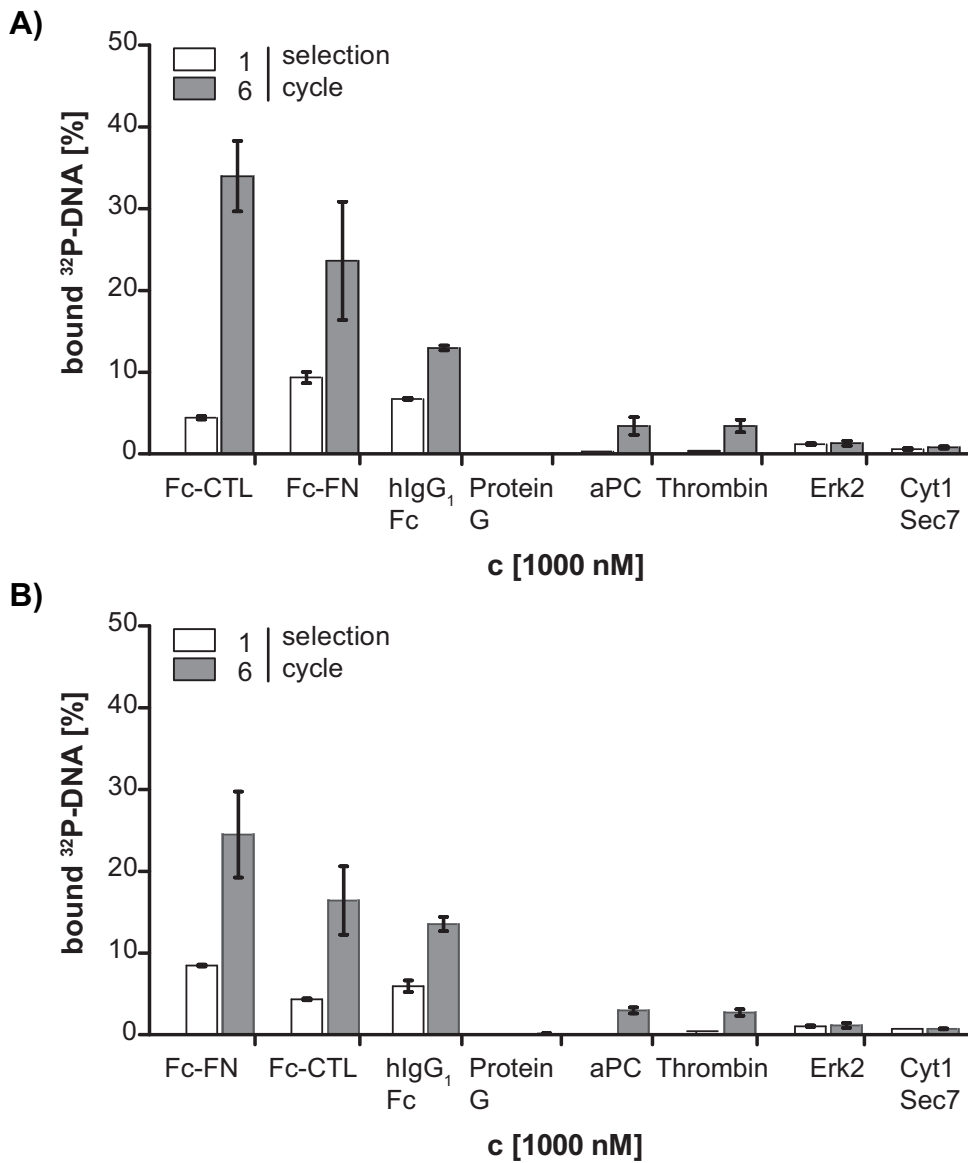
Figure 4.1.3: DNA libraries targeting Fc-CTL or Fc-FN discriminate between recombinant proteins
DNA libraries of the 1st and 6th selection cycle of Fc-CTL **(A)** and Fc-FN **(B)** targeting SELEX were incubated with 1000 nM of proteins and analyzed by radioactive filter retention assay. The protein-^{32}P-DNA mixture was therefore passed through a nitrocellulose membrane and the retained DNA was measured by autoradiography (n=2, mean ± SD).

To investigate whether the enriched DNA libraries consisted of specific aptamers, further experiments based on single sequence level were done.

4.1.1.2 Identification of aptamer sequences obtained from protein-SELEX

To identify individual aptamer sequences, DNA libraries from the 6th selection cycle were amplified by PCR, ligated into pCR2.1-TOPO vectors, transformed in the chemically competent TOP10 *E. coli* strain and subsequently sequenced. For Fc-CTL,

19 DNA sequences were obtained (**Figure 4.1.4** and **Table S 9-2**) and 14 DNA sequences were found within the Fc-FN selected DNA library (**Table S 9-1**).

At this point, the selection against Fc-FN was not further investigated. First of all, the libraries of the 6th and 11th selection cycles bound weakly to Fc-FN (**Figure 4.1.2B**). Second, on the single sequence level no similarities within the DNA sequences were found (**Table S 9-1**). Taking all this into account, no enrichment of high-affinity and specific DNA aptamers against Fc-FN was achieved.

On contrary, Fc-CTL-targeting DNA libraries bound strongly to Fc-CTL (**Figure 4.1.2A** and **Figure 4.1.3A**). Furthermore, two families sharing DNA motifs were identified among the 19 found DNA sequences. DNA sequences named CTL#5, 7, 9, 10 and 13 formed family 1, whereas CTL#6, 16 and 21 were grouped as family 2 (**Figure 4.1.4**). The remaining DNA sequences were unique (**Table S 9-2**).

```
Family 1

CTL#5   TGCAATCTAGCTGACAATGGGGGGGGAAGAATGTGGGTGGGTG
CTL#7   CGCAATCTAGCTGACAATGGGGGGGGAAGAATGTGGGTGGGTG
CTL#9   ------------CGAGATGGGGGGGGAAGGATGTGGGTGGGTGATCTTCGTTGGGT
CTL#10  ------------CGTTGTGGGGGGGGAAGGATGTGGGTGGGTCTGTTTCAGGAGCA
CTL#13  ---------------CGTGGGGGGGGTTGATGAGCATTGGGTGGGAGTTCAGGGTTTGG

Family 2

CTL#6   ----------CCGTGGGTGGGTGGGAATTGGGAGGATGCGGAATTAACTCAGG
CTL#16  CGTACTGATGCGTGGGTGGGTGGGTACTTTCTTGATTTGGGA
CTL#21  ---------CTGTGGGTGGGGGGGGATTTGGGAGGATGCAGGGTAGGTTGTCC
```

Figure 4.1.4: DNA sequences share motifs
DNA sequences obtained by cloning and sequencing of DNA library targeting Fc-CTL were grouped according to their sequence similarities.

Next, the binding properties of individual sequences were investigated by radioactive filter retention assay.

4.1.1.3 Binding of Fc-CTL selected DNA sequences

Representative DNA sequences of each motif family (**Figure 4.1.4**), namely CTL#5, CTL#9, CTL#6 and CTL#16, and unique sequences CTL#1, #2, #3, #14 and #18 (**Table S 9-2**) were chosen for further analysis. Therefore, their binding ability to Fc-CTL, Fc-FN and the IgG$_1$ Fc protein tag was monitored by radioactive filter retention assay (**Figure 4.1.5**). DNA was end labeled with ^{32}P and mixed with the corresponding proteins at a concentration of 500 nM. The mixtures were incubated in selection buffer

for 30 minutes at 37 °C and applied on a nitrocellulose membrane. Finally, the amount of bound DNA was detected by autoradiography.

Equally to the 6th selection cycle library (**Figure 4.1.3A**), some sequences targeted both proteins, Fc-CTL and Fc-FN (**Figure 4.1.5**). Exceptions were CTL#5 and CTL#9 which showed more than two-fold higher binding to Fc-CTL in comparison to Fc-FN, and a low binding to the protein tag.
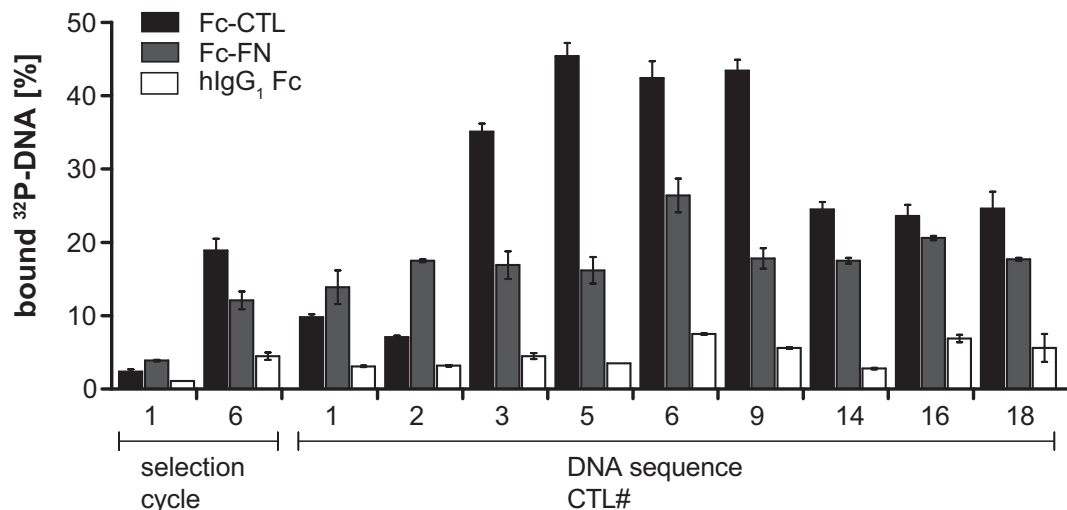
Figure 4.1.5: Binding behavior of DNA sequences to Fc-CTL, Fc-FN and hIgG$_1$ Fc
1 pmol of ^{32}P-DNA was incubated with 500 nM of proteins, the mixture was passed through a nitrocellulose membrane and the retained ^{32}P-DNA was measured by autoradiography (n=2, mean ± SD).

CTL#5 and CTL#9 belong to sequence family 1 whereby the shared motif is located differently within these sequences (**Figure 4.1.4**). As CTL#5 showed a higher degree of discrimination between Fc-CTL and Fc-FN, it is most likely that its sequence composition favors tertiary structure formation critical for specific Fc-CTL binding. For that reason, CTL#5 was picked for further analysis.

4.1.2 Enrichment of DNA libraries in cell-SELEX

The second approach to identify DC-binding aptamers was the use of living murine BM-DCs as targets in a cell-SELEX process (**Figure 4.1.1B**). BM-DCs express a variety of molecules on their surface that are involved in modulating downstream T cell responses[13]. These molecules represent accessible targets for aptamer selection.

Previously to every selection cycle, murine bone marrow-derived progenitor cells were isolated from the hind limbs and differentiated for 7 days into BM-DCs with the hematopoietic factor GM-CSF. The cell-SELEX process was initiated by incubating living BM-DCs with a naïve DNA or 2'F-RNA library in cell-SELEX selection buffer (DPBS, 1 mM MgCl$_2$, 0.01 mg/ml BSA) at 37 °C for 30 minutes. To increase the

selection pressure during SELEX, the incubation time was decreased to 10 minutes in the 9th selection cycle. After 10 and 12 selection cycles, ^{32}P-labeled DNA or 2'F-RNA libraries were examined by radioactive binding assay. For this purpose, ^{32}P-DNA or ^{32}P-2'F-RNA was incubated with BM-DCs in cell-SELEX selection buffer and the amount of bound ^{32}P-labeled nucleic acids was measured by liquid scintillation (**Figure 4.1.6**). A 2'-deoxy-2'-fluoro-ribonucleic acid (2'F-RNA)-based library was used because 2'F-RNA is described to be less immunogenic in comparison to unmodified RNA[142]. In addition, by substituting the 2'-hydroxyl group by a fluoro group, the stability of RNA to chemical or enzymatic hydrolysis is enhanced[141].
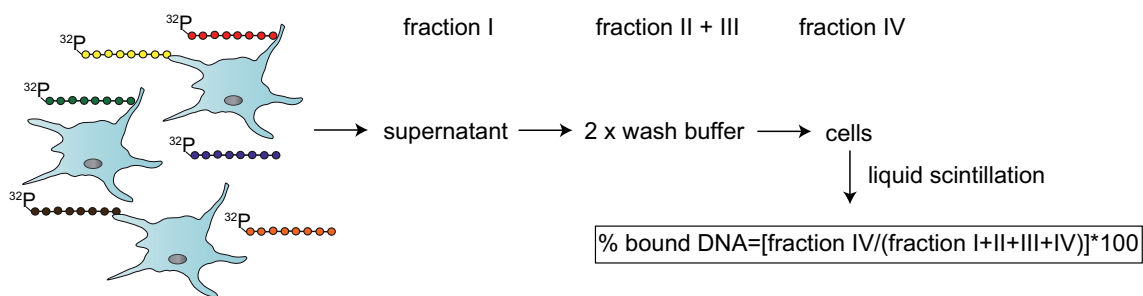
Figure 4.1.6: Schematic representation of the radioactive binding assay
0.5×10^5 BM-DCs were incubated with 1 pmol of ^{32}P-DNA or ^{32}P-2'F-RNA for 10 minutes at 37 °C. Afterwards, the cell supernatant was collected as fraction I. The cells were washed twice and both wash fractions were transferred into new tubes (fraction II + III). The cells were detached and collected as fraction IV. Finally, the radioactivity of the fractions was measured by liquid scintillation and the percentage of bound DNA calculated by using the depicted formula.

As a result, around 4-fold higher binding of the DNA library of the 10th selection cycle in comparison to the 1st cycle was determined (**Figure 4.1.7A**), indicating enrichment of DNA binders targeting BM-DCs. In contrast, no enrichment of 2'F-RNA was observed (**Figure 4.1.7B**). Therefore, the obtained 2'F-RNA library was not further investigated.
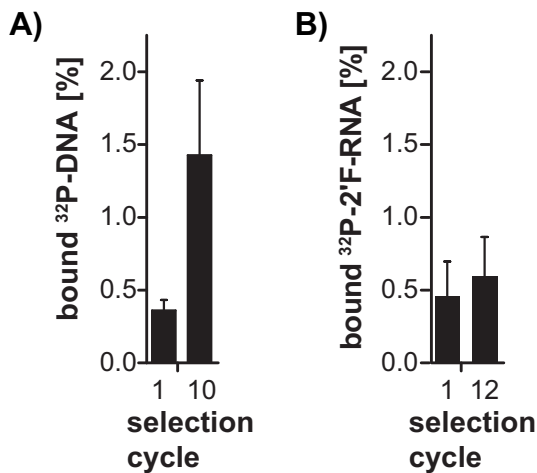
Figure 4.1.7: SELEX targeting BM-DCs results only in enrichment of DNA
^{32}P-DNA **(A)** or ^{32}P-2'F-RNA **(B)** were incubated with 0.5 x 10^5 BM-DCs and the retained radioactivity on the cells was determined by liquid scintillation (n=6 **(A)**/n=2 **(B)**, mean ± SD).

To find high-affine and specific DNA aptamers, further experiments were done on single sequence base.

4.1.2.1 Identification of aptamer sequences obtained from cell-SELEX

Cloning and sequencing of the 10th selection cycle of cell-SELEX resulted in 31 DNA sequences. Eight sequences were grouped into two motif-sharing sequence families (**Figure 4.1.8**). The remaining sequences were unique (**Table S9-3**).

```
Family 1

D#4   -GTGGGCGGGTTTATATTCGGTGGTGGTGGGGGTGGTTCTGTT
D#7   CGTGGGTGGGTTTATATTCGGTGGTGGTGGGGGTGGTACTGTT
D#23  CGTGGGCGGGTTTATATTTGGTGGTGGTGGGGGTGGTACTGTT
D#28  CGTGGGTGGGTTTATATTCGGTGGTGGTGGGGGTGGTACTGTT

Family 2

D#2   GCATGTTTGGGTGGGATATTGGCGTGTTTGGGTTGGGACTGCT
D#3   GCATGTTTGGGTGGGATATTGGCGTGTTTGGGTTGGGACTGCT
D#5   -CGCATTTGGGTGGGATTGTTATTTGGGTCGGGATTGGCAGTT
D#8   -CGCATTTGGGTGGGATTGTTATTTGGGTCGGGATTGGCAGTT
```

Figure 4.1.8: DNA sequences share sequence similarities
According to their composition, some DNA sequences obtained from cell-SELEX were grouped into sequence family 1 and 2.

Next, the cloned sequences were analyzed by radioactive binding assay.

4.1.2.2 Binding of selected DNA sequences to BM-DCs

The binding ability of the individual sequences was analyzed by radioactive binding assay (**Figure 4.1.6**). For that purpose, ^{32}P-DNA was incubated with BM-DCs in cell-SELEX selection buffer for 10 minutes at 37 °C. The amount of ^{32}P-DNA retained on BM-DCs was determined and the ratio of binding calculated as the amount of bound DNA of the sample divided by the 1st selection cycle. A ratio of binding higher than 1 indicates binding to BM-DCs.

As a result, the binding ability of DNA sequences D#2, #5, #7, #11, #16, #22, #23 and #27 was comparable to the 10th selection cycle library, thus, they were categorized as BM-DC binding sequences (**Figure 4.1.9**). Notably, sequences from both motif-sharing sequence families (**Figure 4.1.8**) are classified as BM-DC binders.
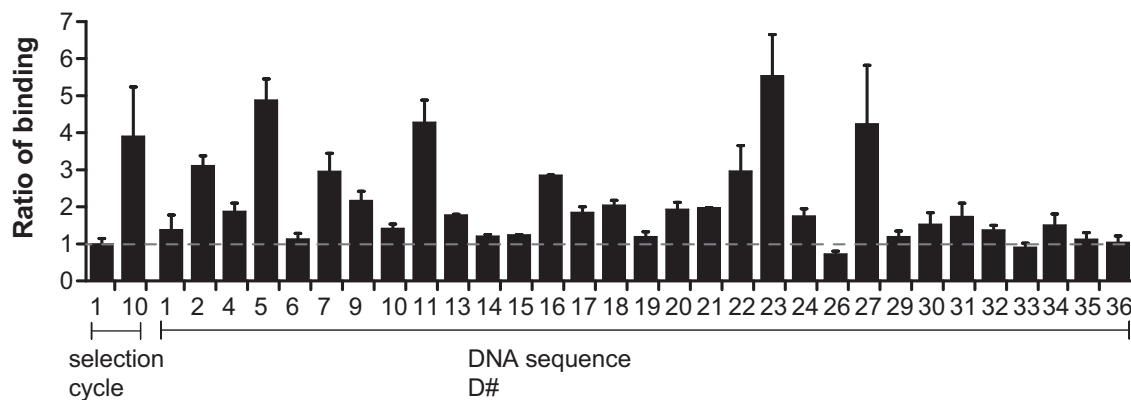
Figure 4.1.9: DNA sequences derived from cell-SELEX show different binding capabilities
0.5 x 10^5 BM-DCs were incubated with 1 pmol of ^{32}P-labeled DNA. Subsequently, the amount of cell-bound DNA was determined by liquid scintillation. The percentages of bound ^{32}P-DNA of samples were divided by the 1st selection cycle to give the ratio of binding. The experiments were performed at least twice (mean ± SD).

The outcome of cell-SELEX was additionally verified by next-generation sequencing (NGS).

4.1.2.3 Analysis of cell-SELEX by NGS

To further investigate the enrichment of BM-DC-binders, the naïve DNA library and the libraries of the 1st, 2nd, 3rd, 4th, 7th and 10th selection cycles of cell-SELEX were introduced in NGS analysis[143]. This high-throughput sequencing technology enables the identification of millions of DNA sequences[93]. The raw data was analyzed by algorithms developed by AptaIT GmbH (München)[144].

Around 100 % of sequences in selection cycle 1 were unique. Starting from the 3rd round, the number of unique sequences decreased to around 50 % in the 10th selection

cycle (**Figure 4.1.10A**). Certain DNA sequences become more frequent, indicating that the complexity of the libraries decreased with increasing selection cycle.

Moreover, a change of nucleotide distribution in the random region was observed. The naïve SELEX starting DNA library contained equal amounts of nucleotides, around 25 % each of adenine, cytosine, guanine and thymine (**Figure 4.1.10B**). In contrast, the composition of the library of the 10th selection cycle was changed; adenine strongly decreased whereby the amount of thymine at certain sequence positions increased (**Figure 4.1.10C**). These results suggest that certain sequence arrangements were favorably accumulated within cell-SELEX.

Correlated to the nucleic acid sequences composition, the sequence reads were grouped in patterns (**Figure 4.1.10D** and **Table S 9-4**). These patterns were numbered according to their read frequencies, where pattern 1 had the highest frequency of around 4 % in the 10th selection cycle.

A)

B) starting library

C) selection cycle 10

D)
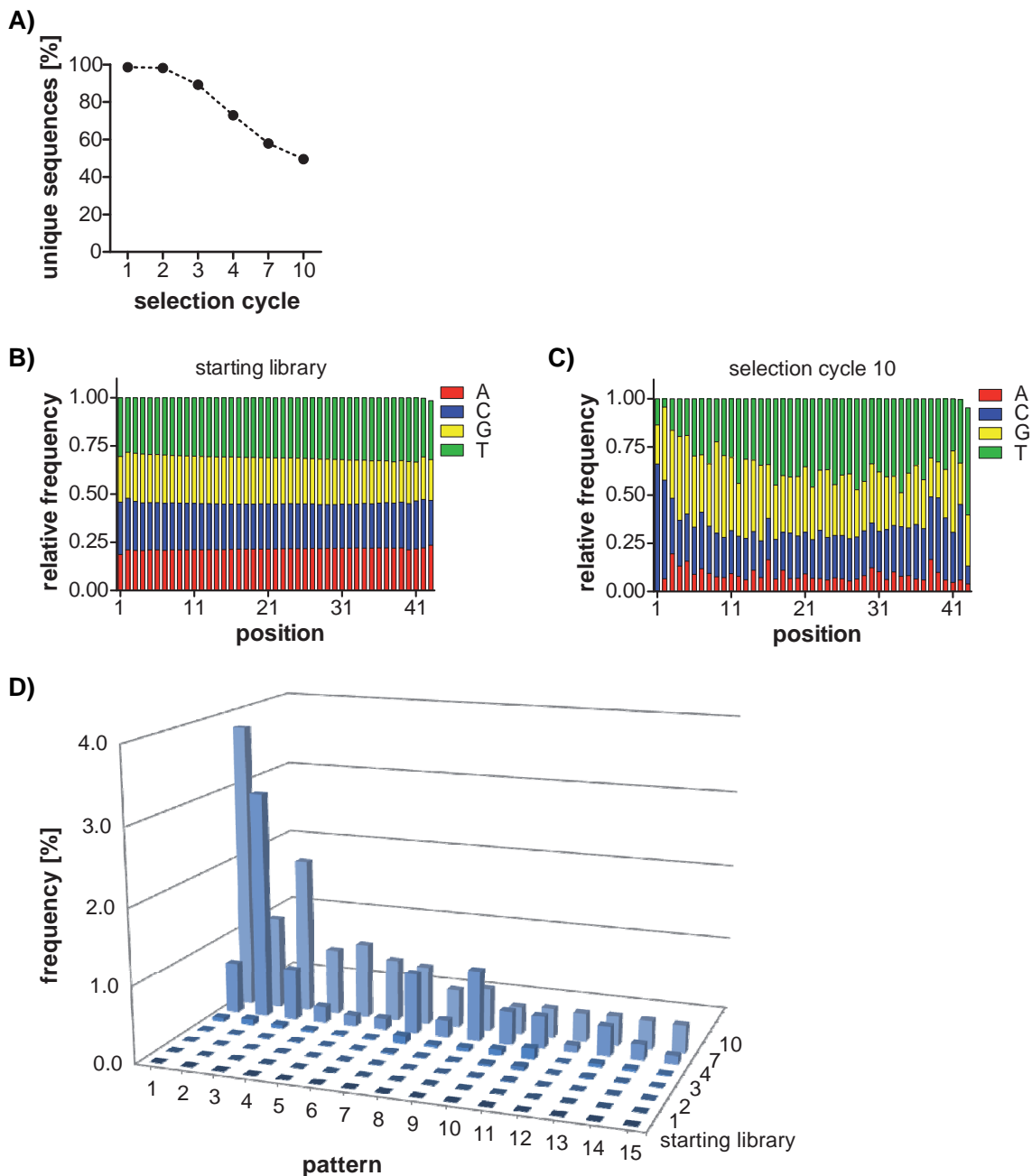
Figure 4.1.10: NGS analysis verified enrichment of DNA sequences in cell-SELEX

DNA of the naïve starting library and different selection cycles obtained from SELEX targeting BM-DCs were introduced in high throughput NGS analysis. The alterations of unique sequence numbers **(A)** and nucleotide distributions **(B+C)** were investigated by algorithms developed by AptaIT GmbH (München). Plus, dependent on the degree of similarities, DNA sequences were grouped into patterns **(D)**. The patterns were numbered according to their frequencies. Here, the 15 most abundant patterns are shown (refer to Table S 9-4).

Next, DNA sequences obtained by classical cloning and sequencing procedure were traced within the NGS reads (**Table S9-3**). Remarkably, sequences grouped to motif-sharing families (**Figure 4.1.8**) were present in pattern 1 and 2. Taking that into account in addition to the results of the radioactive binding assay (**Figure 4.1.9**), D#5 (family 1) and D#7 (family 2) were chosen for further investigations.

4.2 Characterization of BM-DC targeting aptamers

Aptamer-based antigen delivery tools have to meet the following requirements: target binding and specificity, cell internalization and non-immunogenicity. In the previous **Section 4.1** the selection of BM-DC targeting DNA sequences were described, resulting in the identification of aptamers CTL#5, D#5 and D#7. To test whether these aptamers fulfill the above mentioned requirements, flow cytometry binding assay, confocal microscopy analysis and TNF-α HTRF assay were used to evaluate their performance.

4.2.1 Binding and specificity of BM-DC-binding aptamers

4.2.1.1 Binding of aptamers to BM-DCs

The binding of aptamers was analyzed by flow cytometry binding assay. Increasing concentrations of 5'-ATTO 647N-labeled aptamers CTL#5, D#5 and D#7 were incubated with 4 x 10^5 BM-DCs, the amount of bound DNA was detected by flow cytometry and the mean fluorescence intensities (MFI) were determined (**Figure 4.2.1BC**). A scrambled sequence based on CTL#5 was used as non-specific control sequence (ctrl). Here, the binding capacities of the aptamers were analyzed in DC cell medium for 10 minutes at 37 °C.

All aptamers showed an increased binding capacity to murine BM-DCs compared to the control sequence, which is also concentration-dependent (**Figure 4.2.1**). Mean fluorescence intensities (MFI) increased with increasing concentrations of aptamers. Remarkably, CTL#5 derived from Fc-CTL protein-SELEX (**Section 4.1.1**) was also able to bind BM-DCs.

D#7, obtained from cell-SELEX, was shown to have the highest MFI, followed by D#5 and CTL#5. Surprisingly, the MFI of the labeled control sequence also rose with increasing concentrations, albeit to a lesser extend (**Figure 4.2.1A**). This fact is probably caused by the ability of BM-DCs to continuously internalize surrounding fluids by macropinocytosis[30].

As observed in **Figure 4.2.1**, binding curves fail to access saturation even at high concentrations. One reason could be the continuous endocytosis of aptamers.

A)

B)

	Sample		MFI
■ (purple)	CTL#5	500 nM_2	181
■ (cyan)	CTL#5	500 nM	162
■ (orange)	CTL#5	50 nM_2	30.8
■ (green)	CTL#5	50 nM	31.9
■ (blue)	unstained cells_2		1.47
■ (red)	unstained cells		1.48

C)

	Sample		MFI
■ (purple)	ctrl	500 nM_2	96.7
■ (cyan)	ctrl	500 nM	111
■ (orange)	ctrl	50 nM_2	22.6
■ (green)	ctrl	50 nM	21.9
■ (blue)	unstained cells_2		1.47
■ (red)	unstained cells		1.48
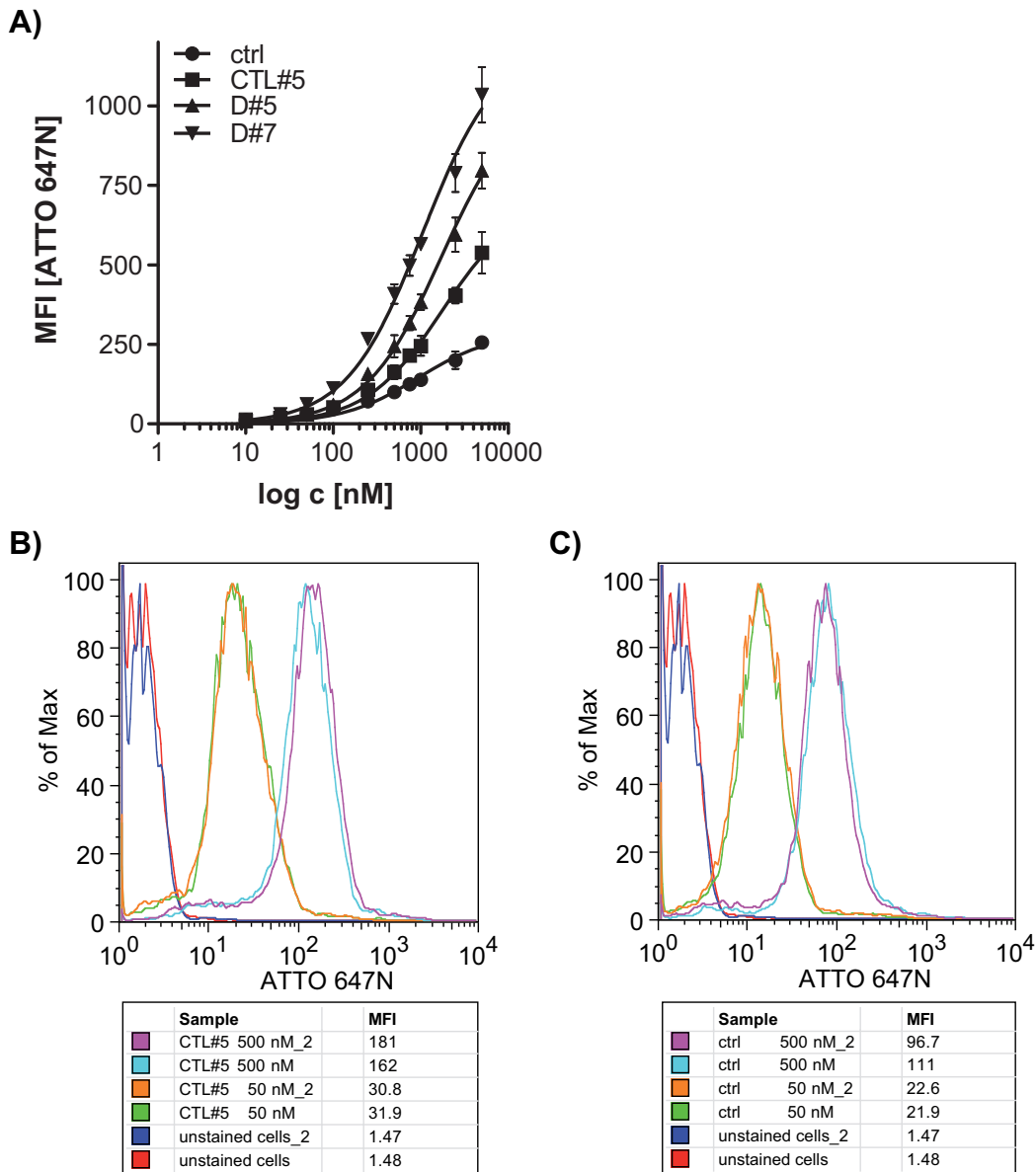
Figure 4.2.1: Aptamers bind in a concentration-dependent manner to BM-DCs
4×10^5 BM-DCs were incubated with increasing concentrations of ATTO 647N-labeled aptamers and analyzed by flow cytometry **(A)**. The mean fluorescence intensities (MFI) of ATTO 647N were determined (n=2, mean ± SD). Representative flow cytometry histograms of 50 and 500 nM CTL#5 and ctrl and the corresponding MFI are depicted in **(B)** and **(C)**. ctrl=control sequence

Next, the specificity of the aptamers binding to BM-DCs was analyzed.

4.2.1.2 Specificity of aptamers to BM-DCs

As the aptamers were intended to be used to mediate the activation of adaptive immunity, binding of effector cells, B and T cells, had to be excluded.

For that purpose, murine splenocytes were isolated and stained for T and B cell surface marker CD8, CD4 and B220, respectively. CD8 is mainly expressed by MHC I-restricted T cells, CD4 is primarily expressed by MHC II-restricted T cell subsets and

B220 can be found in general on cells of the B cell lineage[2]. 2 x 10^5 BM-DCs or splenocytes were incubated with 500 nM of 5'-ATTO 647N-labeled aptamers for 30 minutes at 37 °C, the amount of cell-bound ATTO 647N-labeled aptamers was measured by flow cytometry and normalized to the control sequence.

Results are given in **Figure 4.2.2**. Aptamers bound specifically to BM-DCs whereas no binding to T cells was observed and less than 10 % of B cells were recognized by aptamers.
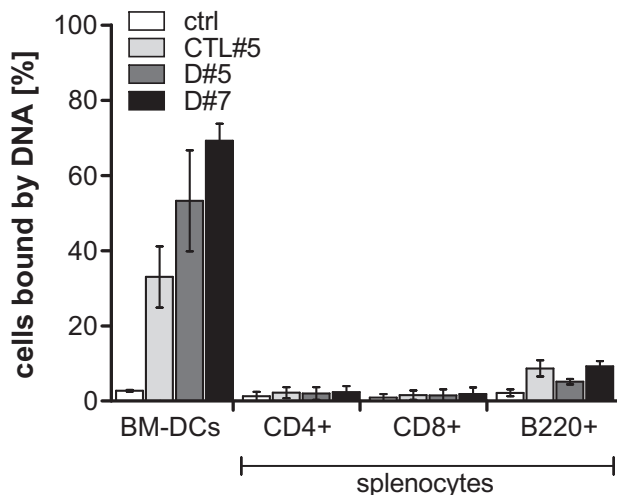
Figure 4.2.2: Aptamers bind specifically to BM-DCs
500 nM ATTO 647N-labeled aptamers were incubated with 2 x 10^5 BM-DCs or splenocytes and analyzed by flow cytometry. Cells bound by DNA were normalized to the control DNA (ctrl), the experiments were performed at least twice (mean ± SD). Splenocytes were co-stained with CD4, CD8 or B220 (CD45RA) antibodies.

B cells are grouped together with DCs and macrophages as professional APCs according to their ability to activate T cell responses. Additionally, professional APCs share some common cell surface structures for antigen recognition, e.g. Fc receptors for IgG[27]. This may mean that the aptamer target structures are expressed by B cells as well. However, the results suggest that the target expression is less prominent on B cells in contrast to BM-DCs.

4.2.2 CTL#5 specificity towards MR

The recombinant protein Fc-CTL was used to select CTL#5. As shown in **Figure 4.1.1A**, Fc-CTL is composed of CTLD 4-7 derived from murine MR and human IgG$_1$ Fc region. In 2002, Figdor *et al.*[31] reviewed several receptors of the C-type lectin family expressed on DCs (**Figure 4.2.3**). Even though the receptors differ in their ligand specificity, their C-type lectin-like domains share conserved residues responsible for the typical formation of a hydrophobic fold[35,137]. To evaluate if only the CTLDs of MR

were bound by CTL#5, confocal microscopy and flow cytometry binding assay were used.
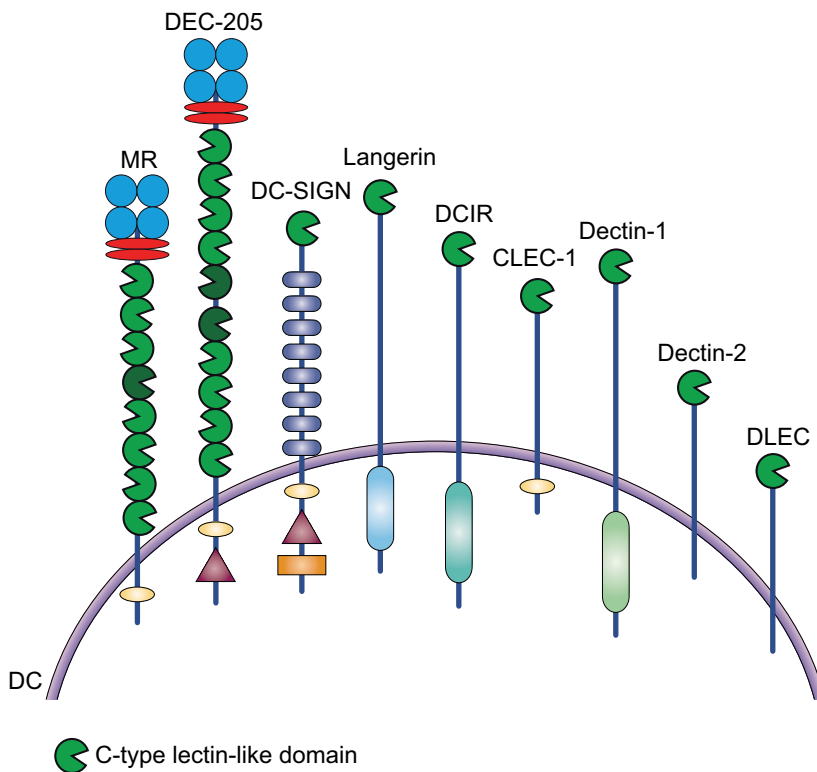
Figure 4.2.3: Schematic representation of CTLD-containing receptors expressed on DCs
Several receptors composed of at least one C-type lectin-like domain are expressed on DCs (modified from Figdor *et al.*[31]). MR=mannose receptor; DEC-205=dendritic and epithelial cells, 205 kDa; DC-SIGN=DC specific ICAM-3 grabbing non-integrin; DLEC=DC lectin; DCIR=DC immunoreceptor; CLEC-1=C-type lectin receptor-1; Dectin=DC-associated C-type lectins

First, co-localization of CTL#5 with MR was investigated. In 2006, Burgdorf *et al.*[38] elucidated that the uptake of OVA by BM-DCs is dependent on MR expression. Hence, co-localization studies of CTL#5 with MR were carried out in comparison with the co-localization of OVA with MR.

2×10^5 BM-DCs were double stained with MR antibody-Alexa Fluor 488 conjugate and 250 ng/ml OVA-Alexa Fluor 647 or 250 nM CTL#5-ATTO 647N in DC cell medium for 30 minutes at 37 °C. The co-localization was analyzed by confocal microscopy and quantified with Pearson's correlation coefficient (PCC). PCC correlates fluorescence intensities; 1 means perfect relation, while 0 means no relation of the fluorescence intensities. High values of PCC indicate that the stained molecules are in close proximity. According to Zinchuk *et al.*[145] PCC values were translated in weak to strong correlation.

In line with Burgdorf *et al.*[99] and Rauen *et al.*[34], co-localization of OVA and MR was observed. In accordance to Zinchuk *et al.*[145], the correlation of both CTL#5 and OVA

with MR is classified as strong (**Figure 4.2.4AB**). These results support the idea that similar to OVA, CTL#5 targets MR.

To attest that CTL#5 only binds to MR, binding to wildtype and MR knockout (MR$^{-/-}$) BM-DCs was compared in flow cytometry (**Figure 4.2.4C**). To this end, 4×10^5 BM-DCs were incubated with increasing concentrations of CTL#5 or the control sequence (ctrl) for 30 minutes at 37 °C in DC cell medium. Surprisingly, binding behavior of CTL#5 was similar for both cell types, as the knockout of MR did not change the amount of cells bound by the aptamer. It can thus be conceivably assumed that CTL#5 targeting is not MR-specific.
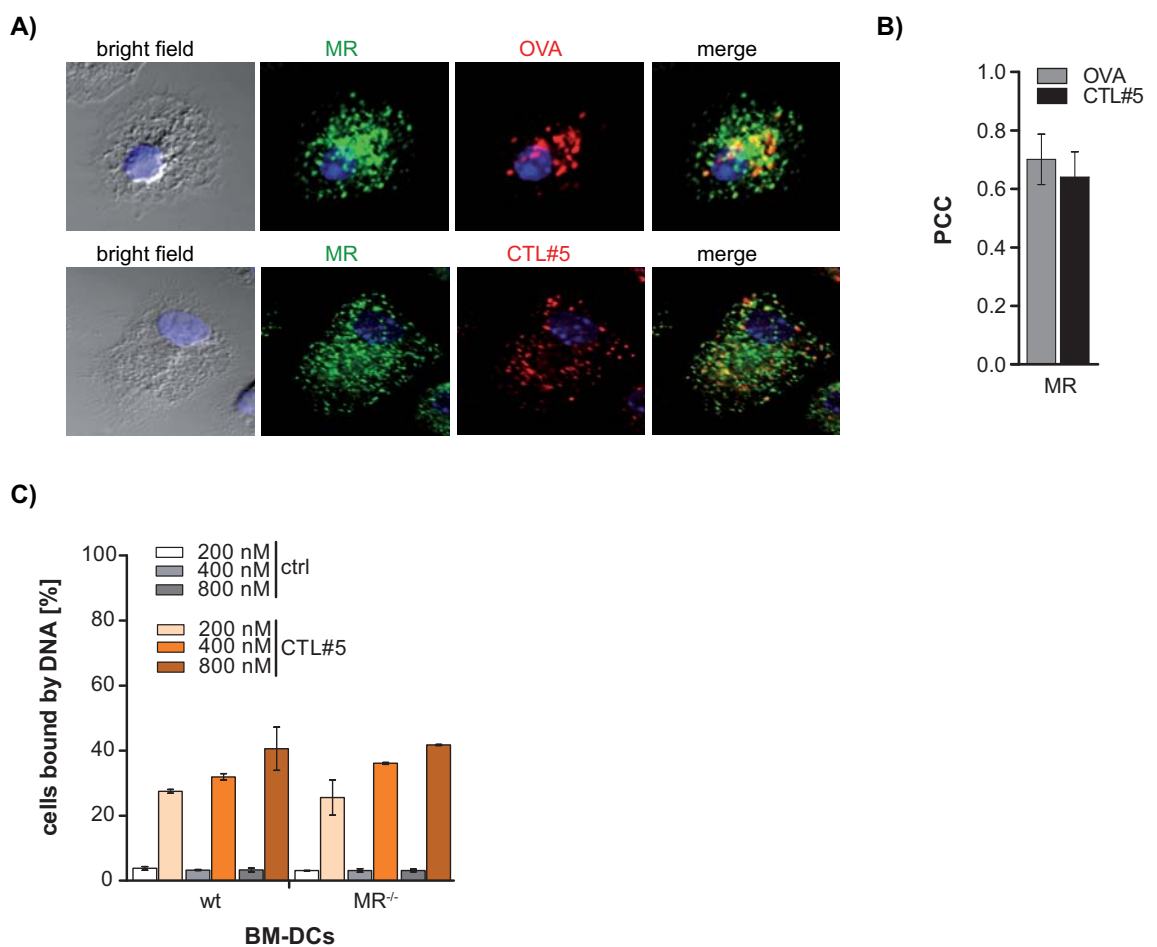
Figure 4.2.4: CTL#5 binding is not only mediated by the MR
Targeting of the MR by CTL#5 was analyzed in confocal microscopy and flow cytometry. For co-localization study, 2×10^5 BM-DCs were co-stained with OVA-Alexa Fluor 647 or CTL#5-ATTO 647N and MR antibody-Alexa Fluor 488 conjugates. Representative pictures out of at least twice performed experiments are shown **(A)**. Fluorescence intensities were quantified as Pearson's correlation coefficient (PCC) (mean ± SD) **(B)**. 4×10^5 wildtype or MR$^{-/-}$ BM-DCs were incubated with increasing concentrations of ATTO 647N-labeled CTL#5 and the amount of cells bound by CTL#5 was measured by flow cytometry and normalized to the control (ctrl) sequence (n=2, mean ± SD) **(C)**.

4.2.3 Internalization and cellular localization of BM-DC-binding aptamers

4.2.3.1 Internalization of aptamers by BM-DCs

Cell-specific aptamers were often reported to be internalized into cells[96,99,112,113]. To investigate if aptamers CTL#5, D#5 and D#7 were taken up by BM-DCs, confocal microscopy was used. 2×10^5 BM-DCs were incubated with 250 nM ATTO 647N-conjugated aptamers in DC cell medium at 37 °C for 30 minutes (CTL#5) or 10 minutes (D#5 and D#7), then, the cells were fixed in paraformaldehyde and co-stained with the membrane marker wheat germ agglutinin (WGA)-Alexa Fluor 488 and the nuclear stain DAPI. In confocal microscopy, pictures of cells at various depths within the Z-axis were taken (Z-stacks). The incubation times were chosen in accordance to the incubation times used in the SELEX approaches.

All aptamers were localized within almost every BM-DC whereby only ~2 % of cells contained the control sequence (**Figure 4.2.5**).
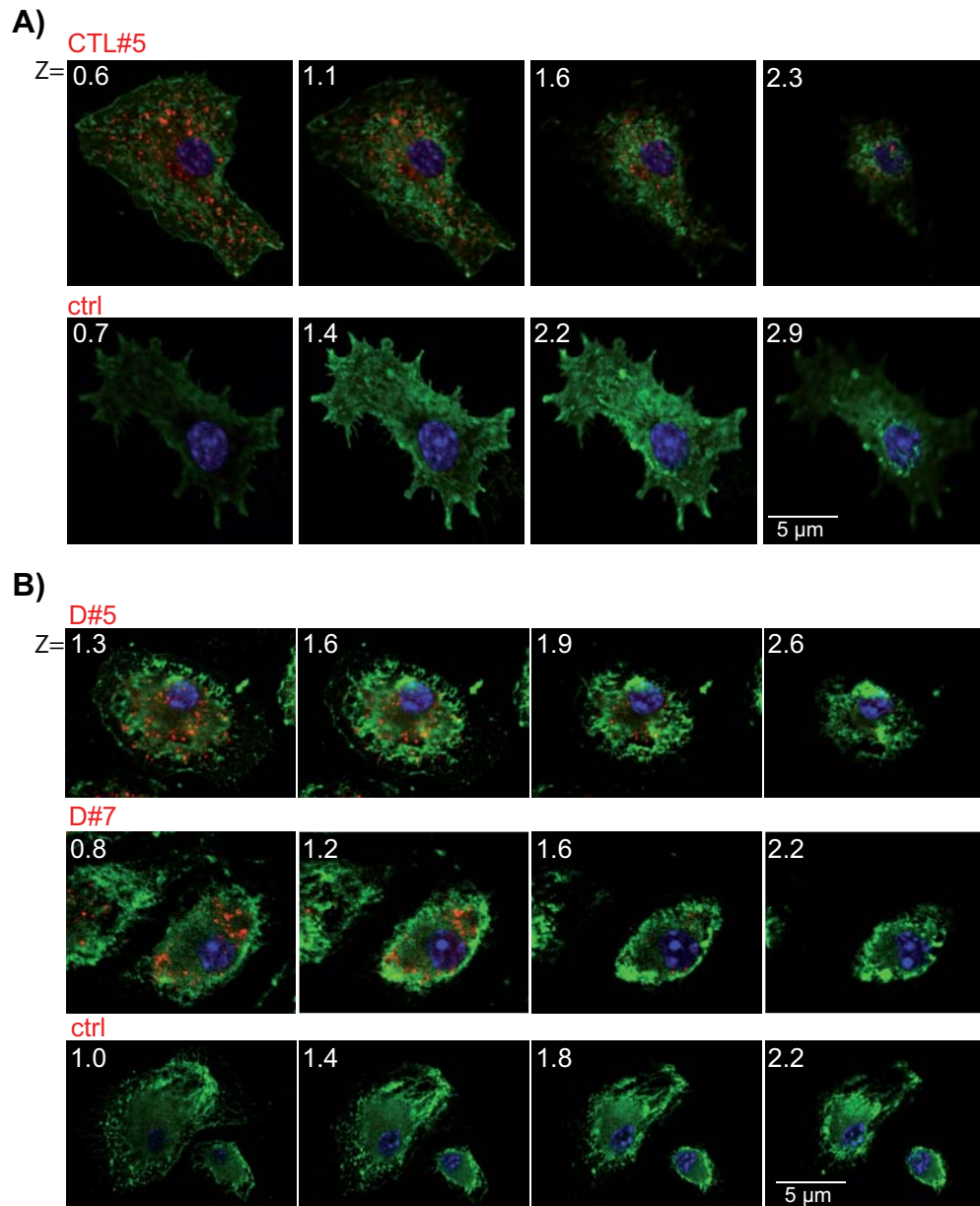
Figure 4.2.5: Aptamers internalize into BM-DCs

2×10^5 BM-DCs were incubated with 250 nM aptamers-ATTO 647N conjugates, fixed and co-stained with membrane marker wheat germ agglutinin-Alexa Fluor 488 and nuclear marker DAPI. In confocal microscopy, pictures along the Z-axis were taken (Z numbers are given in µm). CTL#5 **(A)**, D#5 and D#7 **(B)** were present as punctuate structures in the cytoplasm of BM-DCs. Representative pictures out of at least twice performed experiments are shown. ctrl=control sequence

In previous studies, it was reported that the mechanism of uptake and cellular trafficking influences antigen processing and presentation by BM-DCs[19,37,39]. For example, ligands internalized by the MR were entrapped in slowly maturing early endosomes for cross-presentation on MHC I molecules[19,38], whereas ligands taken up by DEC-205 are transported towards late endosomes or lysosomes for presentation on MHC II molecules[37,39]. Thus, the cellular localization of CTL#5, D#5 and D#7 can

influence the processing and presentation of a conjugated antigen. To investigate the cellular localization of the aptamers, confocal microscopy was applied.

4.2.3.2 Cellular localization of aptamers

Ingested antigens route through endolysosomal compartments within DCs and are finally loaded on MHC I or MHC II molecules for presentation[16] (**Section 3.3.1**). To assess the cellular localization of CTL#5, D#5 and D#7, co-localization studies in confocal microscopy were done. 2×10^5 BM-DCs were treated with 250 nM ATTO 647N-labeled aptamers in DC cell medium at 37 °C for 30 minutes (CTL#5) or 10 minutes (D#5 and D#7) and co-stained with either early endosome antigen 1 (EEA1) or lysosome-associated membrane glycoprotein-1 (LAMP-1) antibody-Alexa Fluor 488 conjugates. Co-localization was quantified by using the PCC. The incubation times were chosen in accordance to the incubation times used in the SELEX approaches.

First, co-localization studies of CTL#5 were done in comparison with the model antigen OVA. Co-localization, as indicated by shades of yellow, was observed in some punctate structures. OVA as well as CTL#5 co-localized strongly with EEA1 (**Figure 4.2.6AC**). This finding is consistent with previous studies about co-localization of OVA and EEA1 done by Burgdorf *et al.*[27] and Rauen *et al.*[19,71]. Additionally, weak correlation between OVA or CTL#5 and LAMP-1 was observed (**Figure 4.2.6BC**).
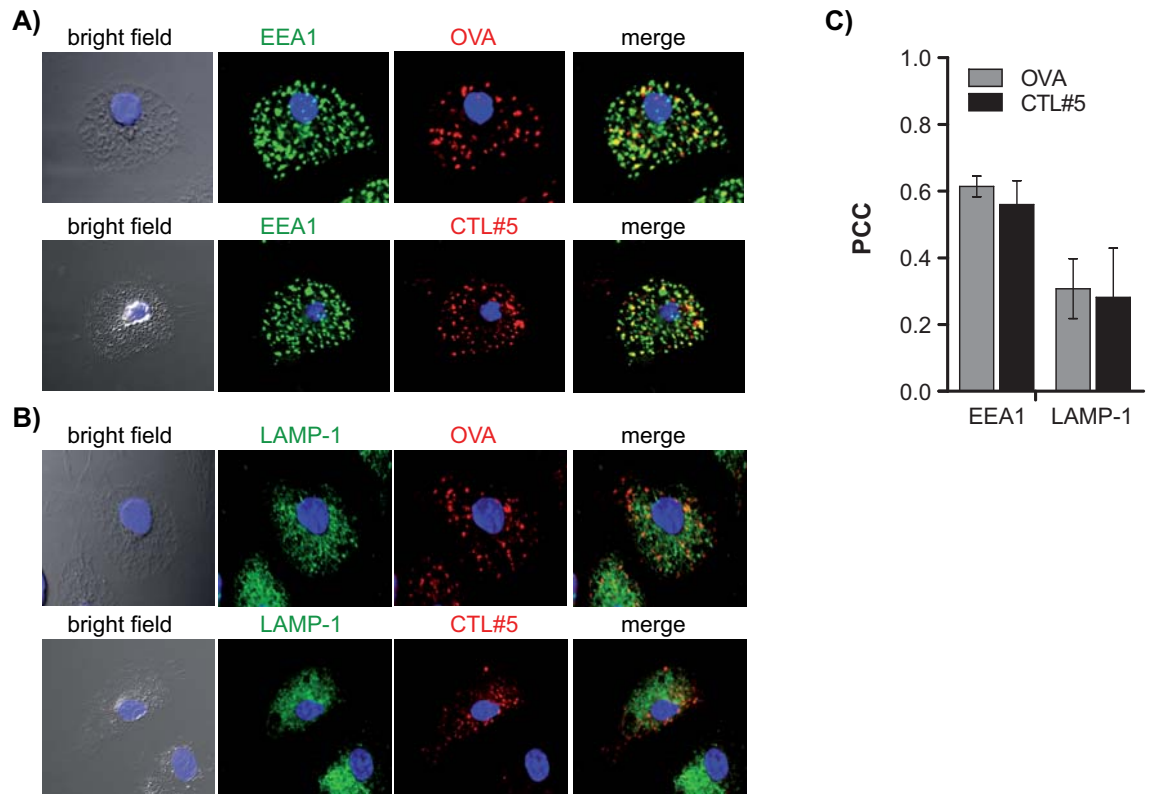
Figure 4.2.6: CTL#5 and OVA co-localize with EEA1 and LAMP-1

The cellular localization of CTL#5 and OVA was analyzed by co-localization studies in confocal microscopy. 2 x 10^5 BM-DCs were incubated with 250 nM aptamer-ATTO 647N or 250 ng/ml OVA-Alexa Fluor 647 conjugates, fixed and co-stained with early endosome marker EEA1 **(A)** or lysosome marker LAMP-1 **(B)**, both labeled with Alexa Fluor 488. Representative pictures out of at least twice performed experiments are shown. The fluorescence signals were quantified as Pearson's correlation coefficient (PCC) (mean ± SD) **(C)**.

In a similar way, cellular localization of D#5 and D#7 was analyzed. It was shown that neither D#5 nor D#7 were located in organelles containing LAMP-1 (**Figure 4.2.7**). D#5-ATTO 647N correlated weak with EEA1-Alexa Fluor 488 (**Figure 4.2.7AB**) while D#7 co-localized strongly with EEA1 (**Figure 4.2.7CD**).
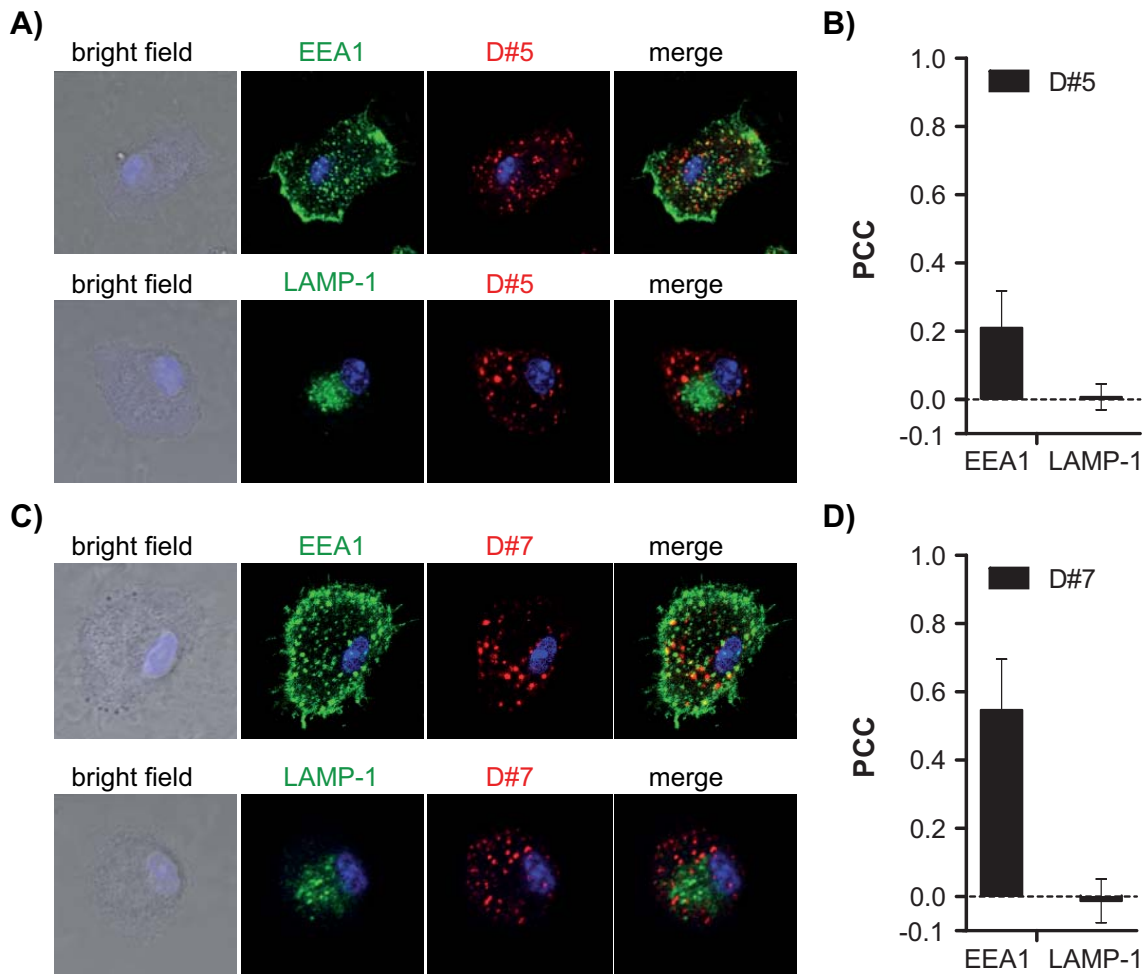
Figure 4.2.7: D#5 and D#7 co-localize with EEA1
The cellular localization of aptamers was analyzed by co-localization studies in confocal microscopy. 2 x 10^5 BM-DCs were incubated with 250 nM D#5- **(A+B)** or D#7-ATTO 647N **(C+D)** conjugates, fixed and co-stained with early endosome marker EEA1 or lysosome marker LAMP-1, both labeled with Alexa Fluor 488. Representative pictures out of at least twice performed experiments are shown. The fluorescence signals were quantified as Pearson's correlation coefficient (PCC) (mean ± SD) **(B+D)**.

The results of the co-localization studies indicated internalization of aptamers into BM-DCs and localization within endolysosomal compartments. These results underline the potency of the selected aptamers to deliver antigens into cellular compartments important for adequate processing and presentation.

4.2.4 Immunogenicity of BM-DC-binding aptamers

Cells involved in innate immunity evolved several sensors for foreign nucleic acids, termed pattern recognition receptors (PRRs). Most prominent among them are the Toll-like receptors (TLRs) 3, 7/8, 9 and 13, which are localized within endosomes. Upon recognition of nucleic acid ligands, signaling cascades are activated resulting in secretion of proinflammatory cytokines like tumor necrosis factor-α (TNF-α) or type I interferons (IFNs)[146,147] (**Figure 4.2.8**).
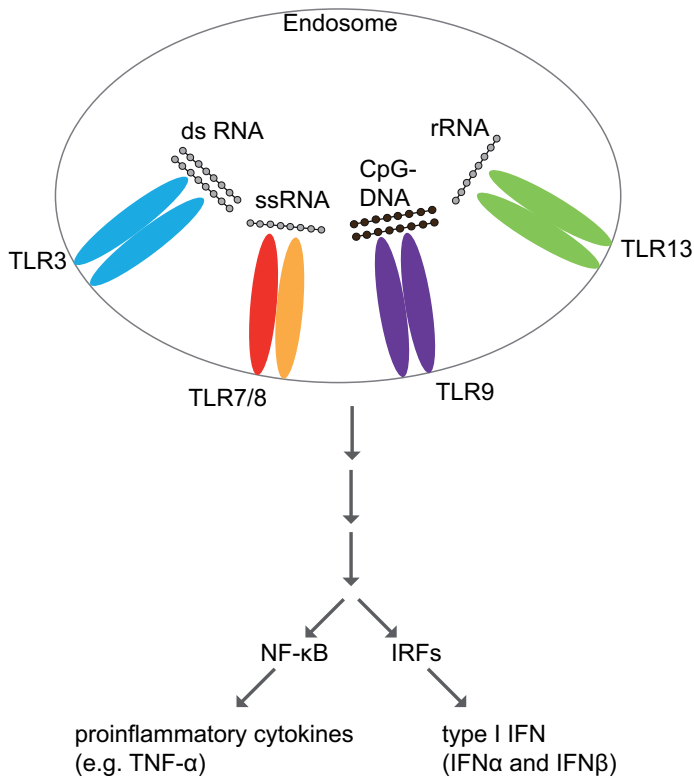
Figure 4.2.8: Schematic representation of TLR signaling
TLR 3, 7/8, 9 and 13 are localized in endosomal compartments. Upon recognition of their nucleic acid ligands, transcription factors such as nuclear factor-κB (NF-κB) and interferon-regulatory factors (IRFs) get activated. Consequence of TLR signaling is the induction of proinflammatory cytokines, e.g. tumor necrosis factor-α (TNF- α) and type I interferons (IFNs). ds=double-stranded, ss=single-stranded, r=ribosomal

To investigate if BM-DC targeting aptamers were sensed by TLRs, secretion of TNF-α was measured by homogeneous time-resolved fluorescence (HTRF) assay. It was performed in close collaboration with Prof. Eicke Latz. HTRF is based on fluorescence resonance energy transfer (FRET). Here, FRET donor and acceptor molecules were attached to anti-TNF-α antibodies and in close proximity to the molecules the fluorescence emission spectrum changes. This change is proportional to the TNF-α concentration in the sample.

Immortalized murine embryonic stem cell-derived macrophages were used to investigate TLR activation. CpG ODN 1826 is described to activate TLR9[148] and was used as positive control. In general, CpG ODNs are composed of unmethylated CpG motif (cytosine - phosphodiester or phosphorothioate - guanosine) flanked by 5' purines and 3' pyrimidines[149]. Here, to increase stability, CpG ODN 1826 has a phosphorothioate backbone. As expected, CpG ODN 1826 activated TNF-α secretion at concentrations in the nanomolar range (**Figure 4.2.9A**). The DNA library used for aptamer selection induced TNF-α production at concentrations higher than 0.5 µM (**Figure 4.2.9AB**). In comparison, all aptamers demonstrated low TLR activation only at the highest concentration of 3 µM. D#5 mediated secretion of around 220 pg/ml TNF-α

whereas CTL#5 and D#7 treatment induced less than 50 pg/ml TNF-α (**Figure 4.2.9C**). The control sequence caused secretion of approx. 100 pg/ml TNF-α. Thus, in comparison to the DNA library which induced secretion of around 2100 pg/ml TNF-α, the aptamers are 10-40 times less potent in activation of TNF-α response.
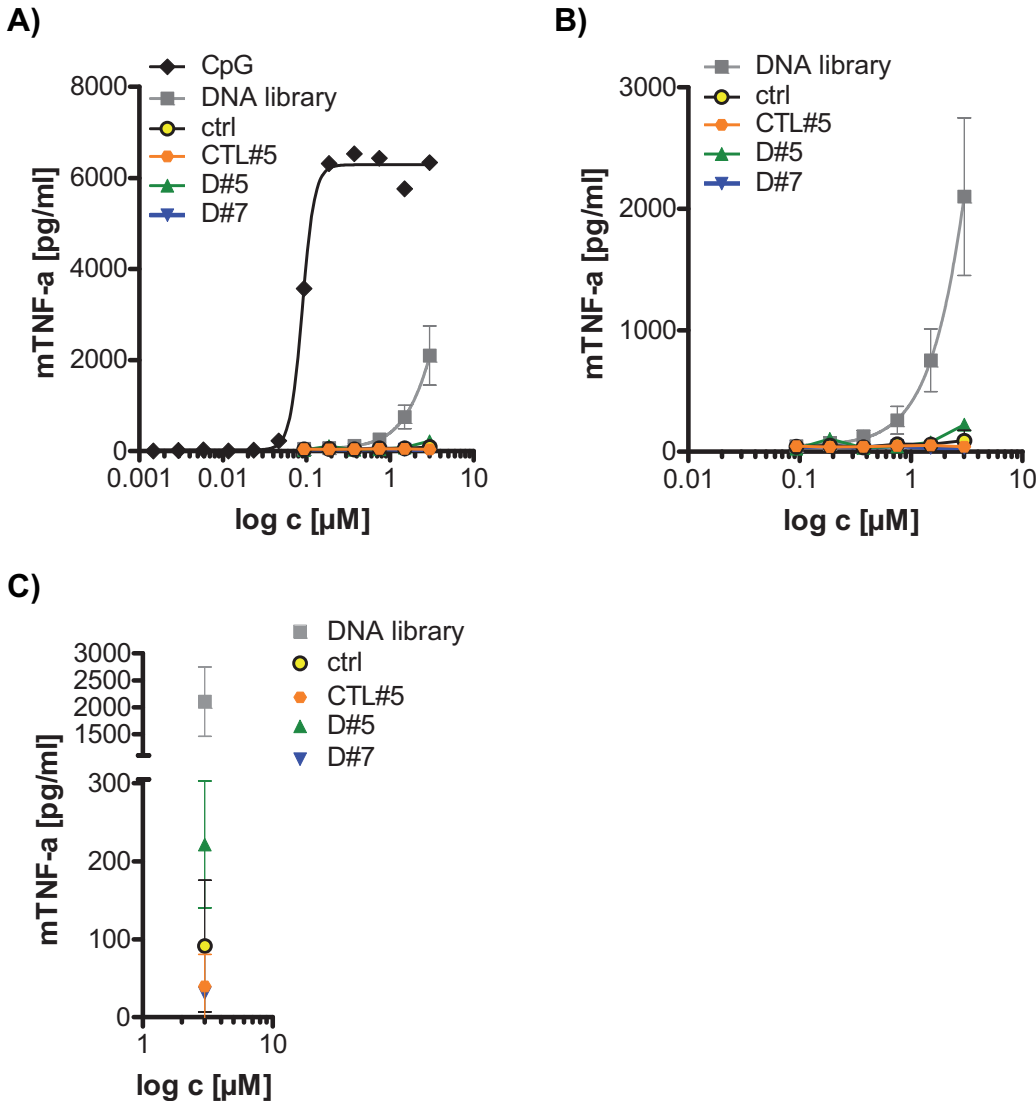
Figure 4.2.9: Aptamers induce low TNF-α secretion
Immortalized murine embryonic stem cell-derived macrophages were incubated with increasing concentrations of CpG ODN 1826 type B, naïve DNA library or aptamers **(A)** for 24 h and the concentration of TNF-α in the supernatant was determined by HTRF assay (n=4, mean ± SD). For a better comparison, the results without CpG ODN are depicted in **(B)**. The amount of TNF-α after treatment with 3 µM of DNA is shown in **(C)**. The assays were performed as blinded analyses by James Stunden, member of Prof. Latz group, University Hospitals Bonn. ctrl=control sequence.

4.3 Aptamer-targeted activation of T cell-mediated immunity

In the previous parts of this chapter, it was demonstrated that the selected aptamers exhibit all requirements to function as suitable delivery tools in an immunological context. They were shown to bind specifically to BM-DCs, get internalized, be

transported into appropriate antigen processing compartments and be non-immunogenic.

To investigate if BM-DC aptamers indeed deliver antigens to mediate targeted activation of T cells, an OVA model system was applied. This system was chosen because it is one of the most feasible ways to investigate T cell-mediated immunity. It is common knowledge that OVA possess MHC I and MHC II binding sites $OVA_{257-264}$ (MHC I peptide) and $OVA_{323-339}$ (MHC II peptide), respectively[128,129]. Accordingly, Hogquist *et al.*[150] and Barnden and co-workers[155] established transgenic mouse models producing OVA-specific CD8 or CD4 T cells. These mice develop either CD8 T cells recognizing MHC I bound $OVA_{257-264}$ or CD4 T cells specific for MHC II bound $OVA_{323-339}$ recognition.

Isolated MHC I or MHC II peptides can directly bind to MHC molecules expressed on the cell surface. Therefore, prolonged OVA peptides, namely OT-I ($OVA_{249-272}$) and OT-II ($OVA_{317-345}$), expanding either MHC I or MHC II recognition sequences were attached to the aptamers. In theory, upon binding and internalization of aptamer-OT-I or -OT-II conjugates by BM-DCs, activation of either CD8 or CD4 T cells is expected (**Figure 4.3.1**).
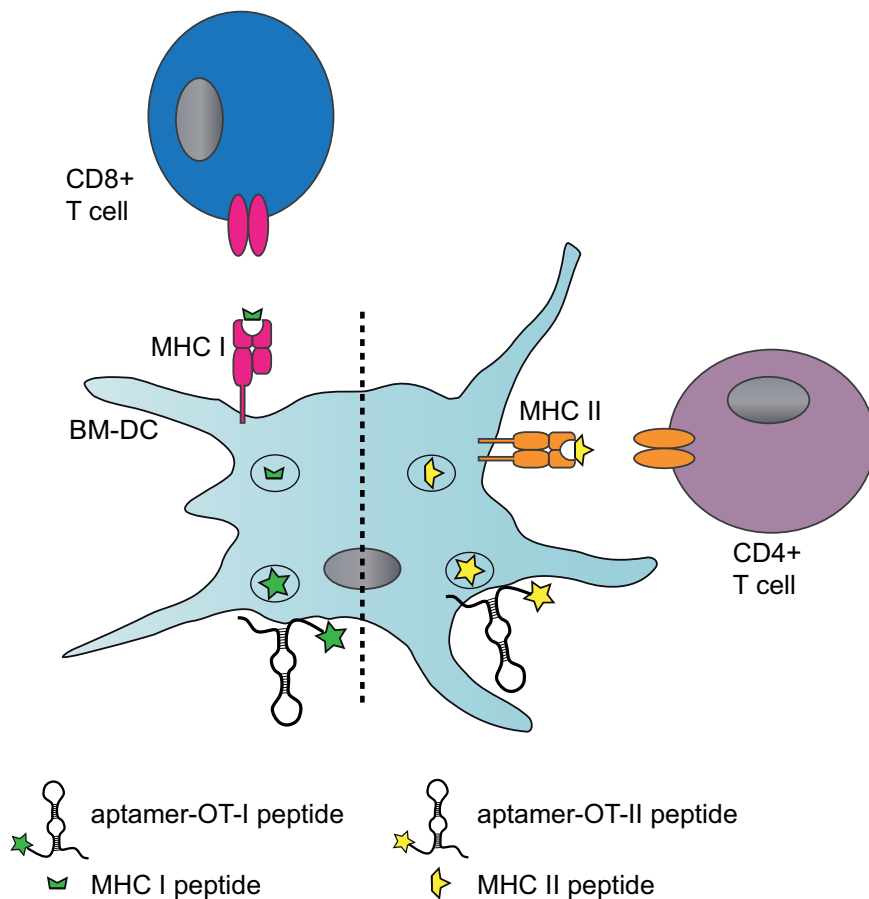
Figure 4.3.1: Schematic representation of aptamer-targeted delivery of OVA peptides to induce specific T cell-mediated immune responses

In theory, the OT-I (green star) or OT-II (yellow star) peptides that are coupled to BM-DC binding aptamers will be taken up by the BM-DCs and then digested into smaller MHC I (cutted green star) or MHC II (cutted yellow star) peptides, respectively. Finally, MHC I or MHC II peptides will be loaded on MHC I or MHC II molecules and presented to CD8 or CD4 T cells for activation of T cell-mediated immunity. MHC I peptide=OVA$_{257-264}$, MHC II peptide=OVA$_{323-339}$, OT-I peptide=OVA$_{249-272}$, OT-II peptide=OVA$_{317-345}$

Thiol-maleimide chemistry was used to conjugate aptamers with OT-I or OT-II peptides. Targeted activation of T cell immunity was finally tested by *in vitro* proliferation and cytotoxicity assays.

4.3.1 Synthesis and binding ability of aptamer-peptide conjugates

4.3.1.1 Coupling of aptamers and OVA peptides

MHC I-restricted OT-I or MHC II-binding OT-II OVA peptides were crosslinked via thiol-maleimide chemistry to aptamers CTL#5, D#5 or D#7, or the control sequence (ctrl) (**Figure 4.3.2**). To this end, 5'-disulfide modified aptamers were reduced to corresponding thiol derivatives and added to N-terminal maleimide functionalized OVA peptides. Maleimide reacts specifically with sulfhydryl groups, resulting in a stable thioether linkage.

A)

Peptides
OT-I (OVA$_{249-272}$)   VSGLEQLE|SIINFEKL|TEWTSSNV
OT-II (OVA$_{317-345}$)   SAESLK|ISQAVHAAHAEINEAGR|EVVGSA

B)
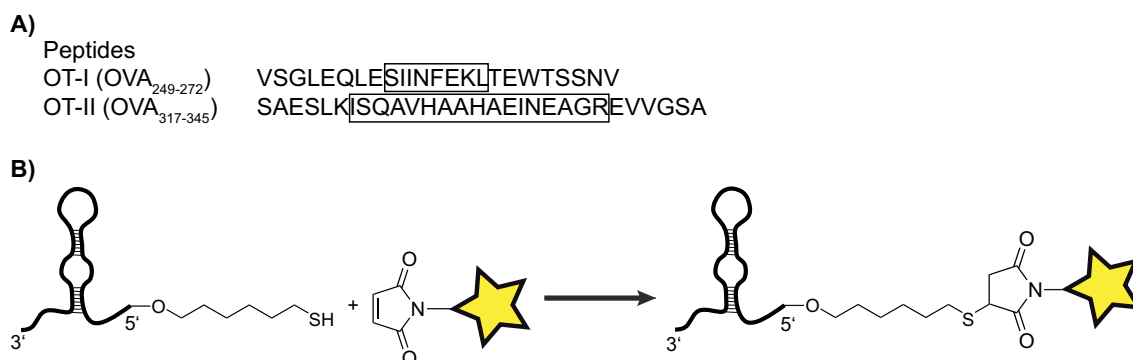
Figure 4.3.2: OVA peptides and thiol-maleimide chemistry were used to synthesize aptamer-peptide conjugates

OVA peptides expanding MHC I- or MHC II recognition sequences were used for coupling to BM-DC targeting aptamers **(A)**. MHC I peptide OVA$_{257-264}$ and MHC II peptide OVA$_{323-339}$ are highlighted in boxes. Coupling was performed by thiol-maleimide chemistry **(B)**. 5' thiol-modified DNA was conjugated to N-terminal maleimide functionalized peptides (yellow star).

After purification by reversed-phase high-performance liquid chromatography (RP-HPLC), the mass of the conjugates was determined by liquid chromatography-mass spectrometry (LC-MS). The quantities of thiol-modified DNA used for coupling, the yields and the calculated and measured monoisotopic masses are given in **Table 4-1**.

Table 4-1: Obtained yields and masses of aptamer-peptide conjugates

DNA-peptide chimera	used SH-ODN [pmol]	yield [pmol]	yield [%]	monoisotopic mass theoretical	experimental
ctrl-OT-I	8000	3320	42	27639,3	27643,4
ctrl-OT-II	8000	3720	47	27847,5	27850,3
CTL#5-OT-I	4000	2240	56	27639,3	27645,2
CTL#5-OT-II	4000	2000	50	27847,5	27853,2
D#5-OT-I	4000	2080	52	27544,2	27552,4
D#5-OT-II	4000	1920	48	27752,4	27756,5
D#7-OT-I	4000	1640	41	27945,3	27951,3
D#7-OT-II	4000	1360	34	28153,5	28162,3

All chimeras were shown to have the expected monoisotopic mass and were further characterized with regard to binding capability to BM-DCs.

4.3.1.2 Binding capability of aptamer-peptide conjugates

After the synthesis of aptamer-peptide conjugates, it was investigated if the binding ability of aptamers to BM-DCs was maintained. This was done by using a competition assay. 2 x 10^5 of 7 days differentiated BM-DCs were simultaneously incubated with 250 nM ATTO 647N-labeled aptamers and a two-fold molar excess of unlabeled

competitors in DC cell medium for 10 minutes at 37 °C. Fluorescence intensities were measured by flow cytometry and normalized to the control sequence (ctrl).

The amount of cells bound by CTL#5 (**Figure 4.3.3A**), D#5 (**Figure 4.3.3B**) or D#7 (**Figure 4.3.3C**) was strongly decreased when adding the particular aptamer or aptamer-peptide conjugates as competitors. No or low competition was induced by the control sequence, unconjugated OT-I and OT-II peptides or control-peptide conjugates.
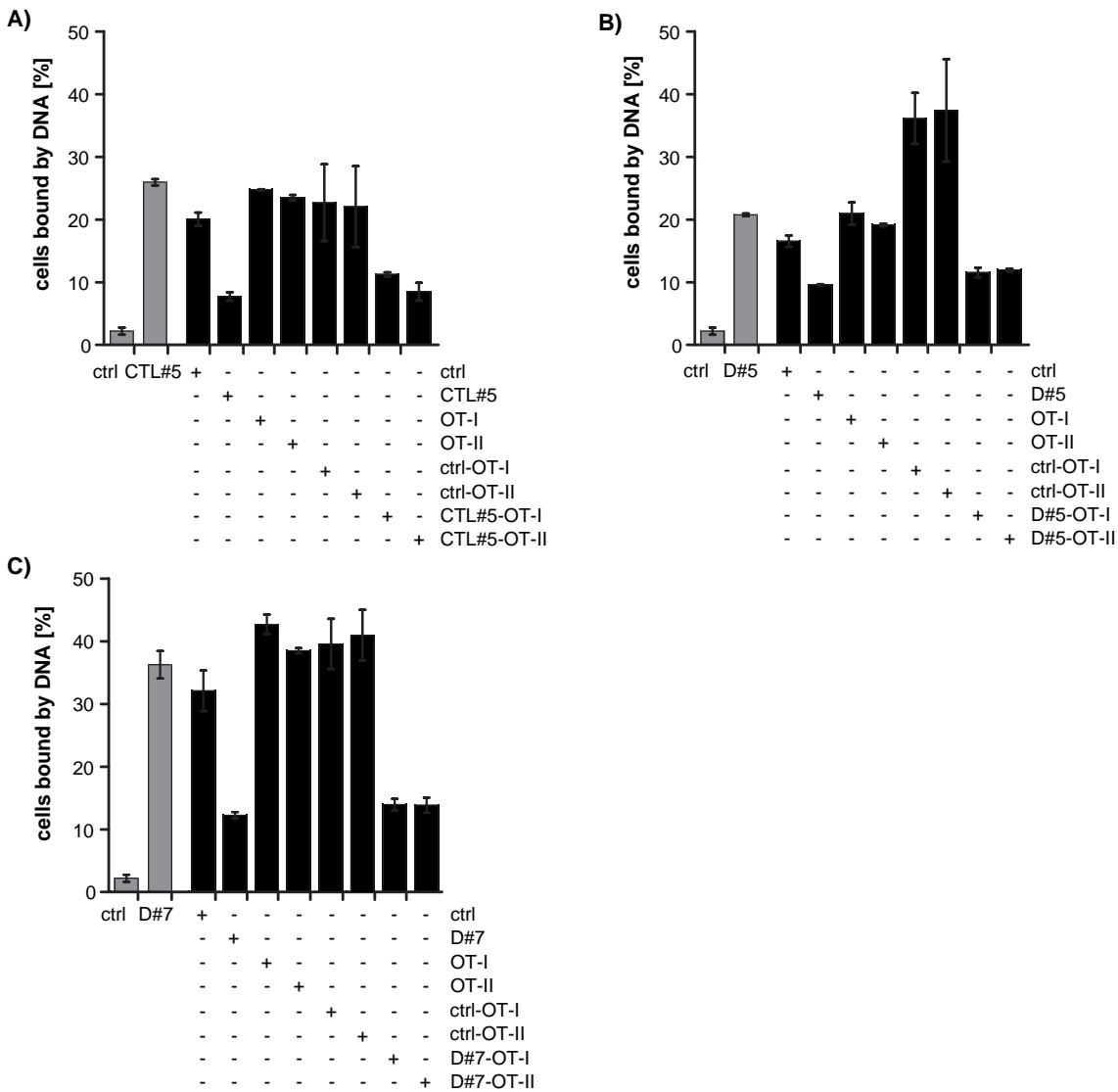
Figure 4.3.3: Binding capability of aptamers coupled to peptides is maintained
2×10^5 BM-DCs were incubated with 250 nM ATTO 647N-labeled CTL#5 **(A)**, D#5 **(B)** and D#7 **(C)** without (grey bars) or in presence of 500 nM competitors (black bars) and analyzed by flow cytometry (n=2, mean ± SD).

To conclude, all aptamers were shown to preserve their binding capability to BM-DCs within crosslinked molecules. Finally, the functionality of conjugates was investigated.

4.3.2 Activation of T cell-mediated immunity

4.3.2.1 Aptamer-targeted activation of CD4 T cells

OVA-specific CD4 T cells derived from transgenic mice[150] are activated by MHC II peptide presented on MHC II molecules by BM-DCs. To investigate if OT-II peptides delivered by aptamers mediate CD4 T cell activation, an *in vitro* proliferation assay was used. 5 x 10^4 of murine BM-DCs were either treated with MHC II or OT-II peptides, non-conjugated aptamers or aptamer-OT-II conjugates in DC cell medium for 10 minutes at 37 °C. 1 x 10^5 OVA-specific CD4 T cells were isolated from the spleen, CFSE-labeled and subsequently incubated for 72 h with the BM-DCs.

Carboxyfluorescein succinimidyl ester (CFSE) is a staining dye used to track cell division frequencies. The non-fluorescent form of CFSE enters the cell and is hydrolyzed by cellular esterases into the fluorescent form. Finally, the dye is retained within the cell through interactions of the succinimidyl mioety with primary amines and is equally distributed among daughter cells upon divisions[151]. CFSE proliferation profile of T cells was measured by flow cytometry and quantified as division index.

The results are shown in **Figure 4.3.4** and **Figure S 9.4.1-Figure S 9.4.3**. The non-proliferative population (grey peak) was obtained by adding T cells to non-treated BM-DCs. MHC II peptide compromised of only the OVA MHC II recognition amino acid sequence (**Figure 4.3.2A**), is bound directly by MHC II molecules on the surface of BM-DCs. As anticipated, 400 nM MHC II peptide strongly activated CD4 T cells (**Figure 4.3.4A**). In comparison, OT-II peptides need to be taken up by BM-DCs, processed and degraded into MHC II peptides. Without carrier, OT-II peptide was not observed to induce CD4 T cell proliferation (**Figure 4.3.4A**). In addition, no CD4 T cell activation occurred after treatment with aptamers alone (**Figure 4.3.4B**).

Crucially, all aptamer-OT-II conjugates mediated CD4 T cell activation in a concentration-dependent manner (**Figure 4.3.4C**). D#7-OT-II was the most potent activator, followed by D#5-OT-II and CTL#5-OT-II. In contrast, less T cell divisions were detectable after treatment with 25-100 nM of ctrl-OT-II, where no activation of CD4 T cells was observed at 1 nM concentration.
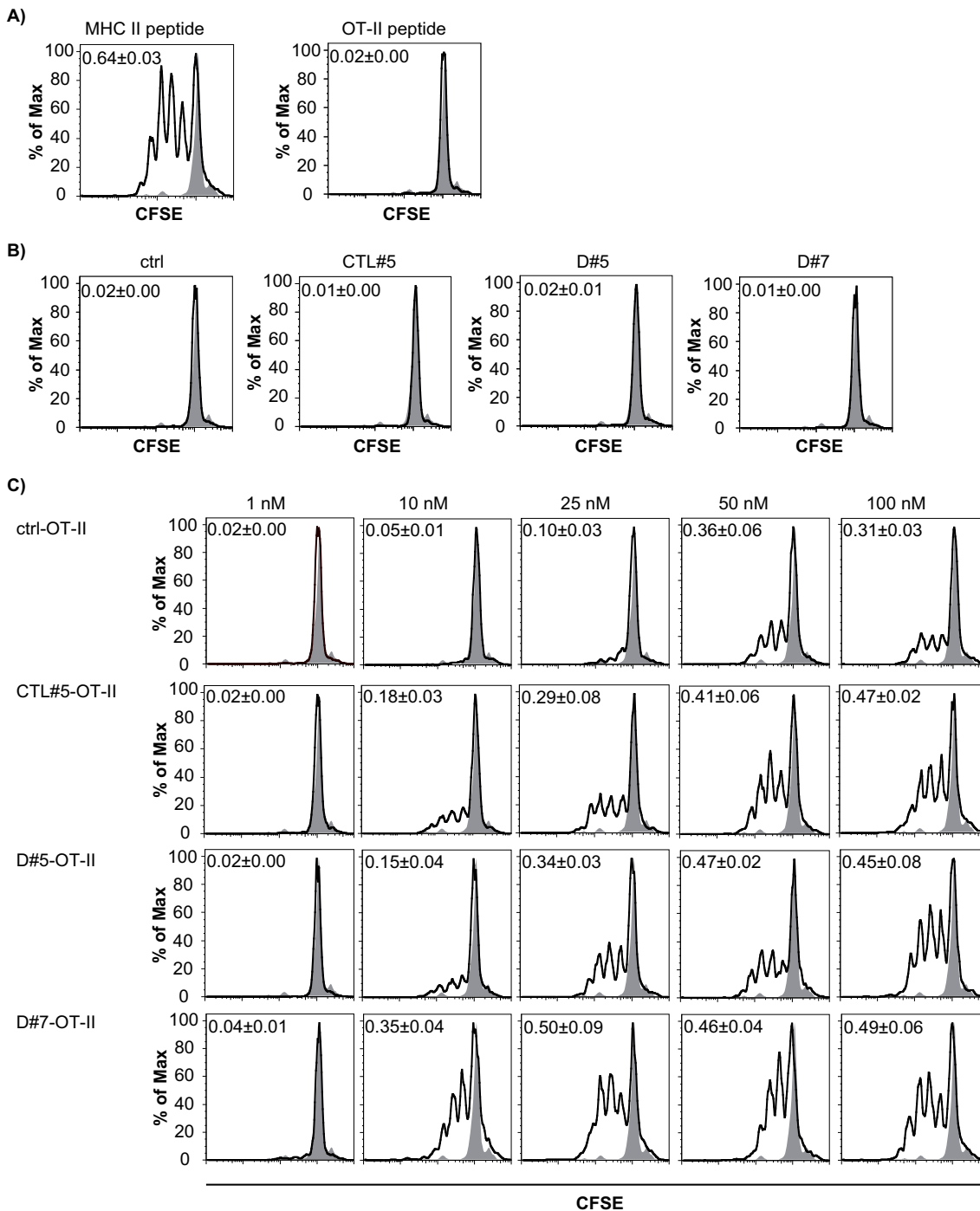
Figure 4.3.4: Aptamer-targeted delivery of OT-II peptide induces CD4 T cell activation

5 x 10^4 BM-DCs were either treated with 400 nM MHC II peptide, 100 nM OT-II peptide **(A)**, 100 nM DNA **(B)** or increasing concentrations of aptamer-peptide conjugates **(C)**. 1 x 10^5 OVA-specific CD4 T cells were labeled with CFSE and added for 72 h. The CFSE profiles were measured by flow cytometry. One FACS histogram profile of one representative experiment out of n=4 is shown, where non-proliferative population is given in grey. Numbers show division index of triplicates (mean ± SD). For more information see supplementary Figure S 9.4.1-Figure S 9.4.3. The assays were done with blinded samples.

Over the past three decades, many human and mouse studies revealed that CD4 T cells were able to acquire cytotoxic function similar to CD8 T cells[152-154]. Thus,

activation of OVA-specific CD4 T cells was further analyzed by an *in vitro* cytotoxicity assay.

4.3.2.2 Cytotoxic capacity of activated CD4 T cells

In theory, cytotoxic CD4 T cells recognize their respective antigens on MHC II molecules and induce apoptosis of the carrier cell.

To investigate if the most potent CD4 T cell activator D#7-OT-II (**Figure 4.3.4C**) induces CD4-mediated cytotoxicity, an *in vitro* cytotoxicity assay was applied. On that account, 2×10^5 BM-DCs were incubated with MHC II peptide, D#7-OT-II or ctrl-OT-II in DC cell medium for 10 minutes at 37 °C. 4×10^5 CD4 T cells were primed for 72 h by the differently treated BM-DCs, isolated and added to a mixture of differently CFSE-labeled target cells loaded with MHC II peptide and non-loaded control cells. On day 5, the target and control cells were stained with the viability marker Hoechst and analyzed by flow cytometry.

As a result, no cytotoxic capacity of CD4 T cells was detectable upon priming with MHC II peptide, ctrl-OT-II or D#7-OT-II treated BM-DCs (**Figure 4.3.5**).
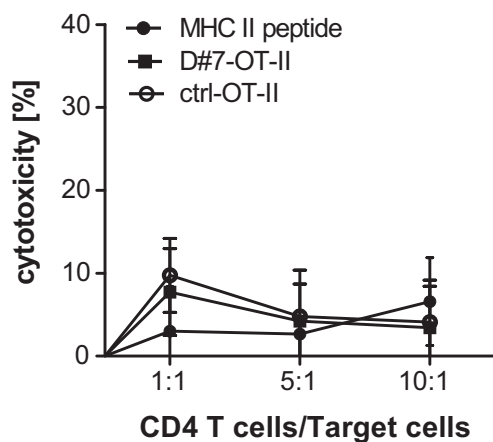
Figure 4.3.5: CD4 cytotoxicity is not induced by aptamer-peptide conjugates
2×10^5 BM-DCs were treated with 400 nM MHC II peptide, 100 nM D#7-OT-II or ctrl-OT-II conjugates. Next, 4×10^5 OVA-specific CD4 T cells were added. After 72 h, T cells were isolated by density gradient separation and incubated for another 24 h with CFSE-labeled target and control cells. Alive and dead target and control cells were distinguished by flow cytometry according to CFSE and Hoechst 33258 signals. The percentages of T cell cytotoxicity were determined (n=3, mean ± SD).

In summary, the results of the *in vitro* proliferation assay (**Figure 4.3.4**) validate the usefulness of aptamers CTL#5, D#5 and D#7 as potent mediators of specific CD4 T cell activation. However, activation of T cells by D#7-OT-II was not resulting in cytotoxic capability.

Next, it was investigated if aptamer based delivery of MHC I-restricted OVA peptides induce CD8 T cell activation.

4.3.2.3 Aptamer-targeted activation of CD8 T cells

Murine OVA-specific CD8 T cells[155] were genetically modified to recognize $OVA_{257-264}$ (MHC I peptide; **Figure 4.3.2A**) immobilized onto MHC I molecules on the surface of BM-DCs. To evaluate if aptamer-OT-I conjugates mediate targeted activation of OVA-specific CD8 T cell, an *in vitro* proliferation assay was utilized. Similarly as for CD4 T cells, 5 x 10^4 murine BM-DCs were either treated with MHC I or OT-I peptides, non-conjugated aptamers or aptamer-OT-I conjugates in DC cell medium for 10 minutes at 37 °C. 1 x 10^5 OVA-specific CD8 T cells were isolated from spleen of transgenic mice, labeled with CFSE and subsequently added for 72 h to the treated BM-DCs. CFSE proliferation profile of T cells was monitored by flow cytometry and quantified as division index.

Results are given in **Figure 4.3.6** and **Figure S 9.5.1-Figure S 9.5.3**. Profiles of non-proliferative T cells population (grey peaks) were acquired by measuring T cells incubated with non-treated BM-DCs. MHC I peptide is directly bound by MHC I molecules on the surface of BM-DCs. As expected, this peptide mediated strong CD8 proliferation at 1 nM concentration (**Figure 4.3.6A**).

In contrast, the prolonged OVA peptide, OT-I peptide, was not anticipated to have intrinsic capacity to activate CD8 T cells (**Figure 4.3.6A**), nevertheless, it was observed that at concentrations of 25-100 nM OT-I peptide induced CD8 proliferation.

As observed above for CD4 T cell activation (**Figure 4.3.4B**), CD8 T cells were not activated by BM-DCs treated with non-conjugated aptamers (**Figure 4.3.6B**).

Remarkably, all aptamer-OT-I chimeras activated CD8 T cells at different concentrations (**Figure 4.3.6C**). In comparison to ctrl-OT-I, proliferation profiles of 25-50 nM aptamer-OT-I revealed that almost all cells of starting population (grey peak) shifted to the left, in other words, underwent cell divisions. No CD8 T cell proliferation was detectable at 10 nM.

In conclusion, all aptamers mediated CD8 T cell proliferation upon delivery of OT-I peptide.
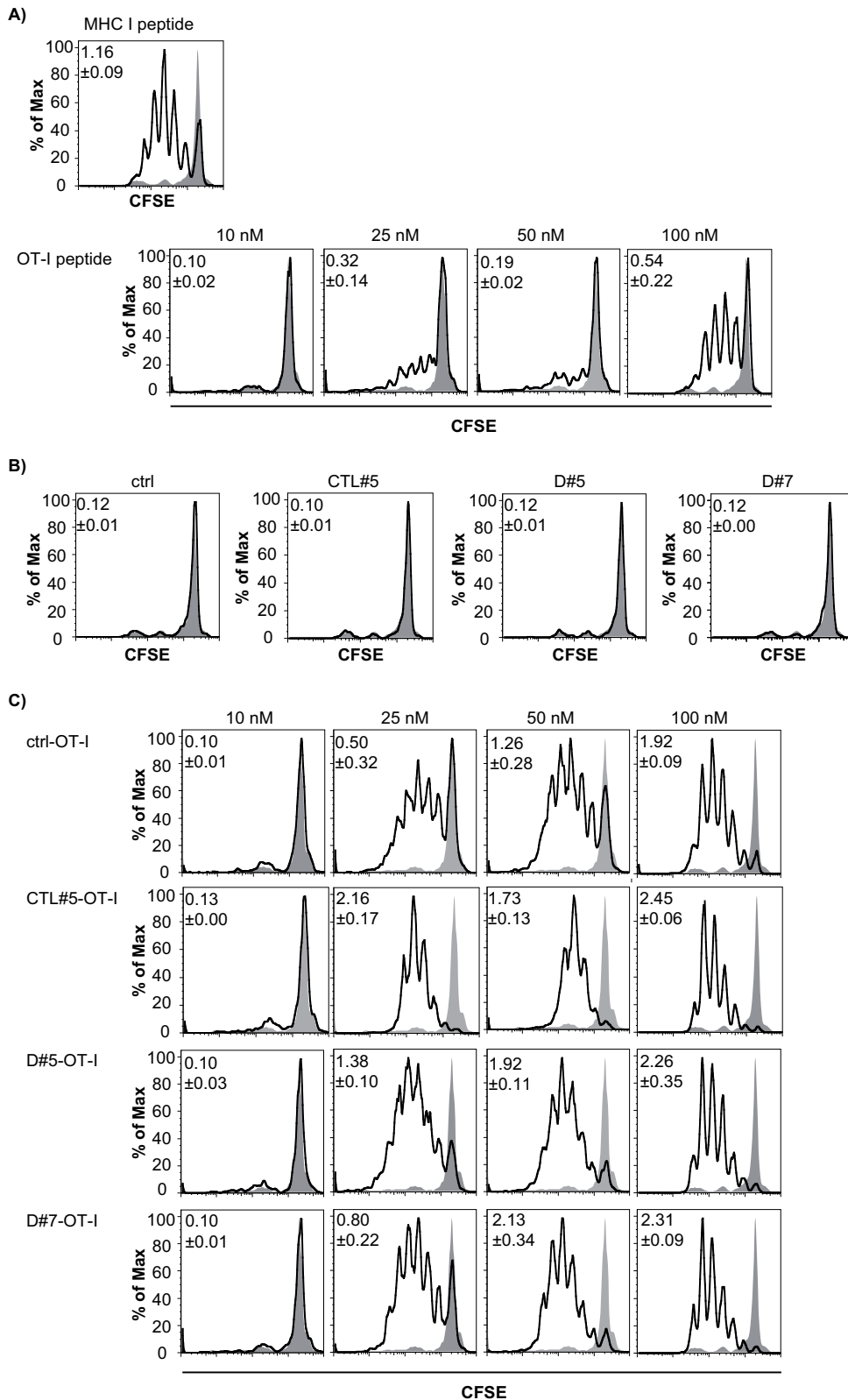
Figure 4.3.6: Aptamer-targeted delivery of OT-I peptide activates CD8 T cells
1×10^5 OVA-specific CD8 T cells were stained with CFSE and added to 5×10^4 BM-DCs treated with 1 nM MHC I peptide, different concentrations of OT-I peptide **(A)**, 100 nM DNA **(B)** or increasing concentrations of aptamer-OT-I conjugates **(C)**. CFSE profiles were measured by flow cytometry. Non-proliferated population is shown in grey. Mean division index of triplicates is given in numbers (mean ± SD). Representative results out of n=4 are shown (refer to supplementary Figure S 9.5.1-Figure S 9.5.3). The assays were done with blinded samples.

4.3.2.4 Cytotoxic capacity of activated CD8 T cells

Activation of CD8 T cells results not only in proliferation, but also in gain of cytotoxic function (**Section 3.2**). To verify that aptamer-mediated OT-I delivery results in CD8 T cell activation, an *in vitro* cytotoxicity assay was done. To this end, 4 x 10^5 OVA-specific CD8 T cells were incubated with 2 x 10^5 of differently treated BM-DCs and subsequently added to a mixture of differently CFSE-labeled target cells loaded with MHC I peptide and non-loaded control cells. Finally, the amount of alive and dead target and control cells was measured in flow cytometry by using Hoechst as viability marker and quantified as percentage of cytotoxicity.

As forecasted, 50 nM MHC I peptide induced rising CD8 T cell cytotoxicity with increasing T cell to target cell ratio (**Figure 4.3.7**). In addition, aptamer-OT-I conjugates functionalized CD8 T cells become cytotoxic effector cells. In comparison to ctrl-OT-I, cytotoxicity of aptamer-OT-I was elevated to an extent similar to MHC I peptide.
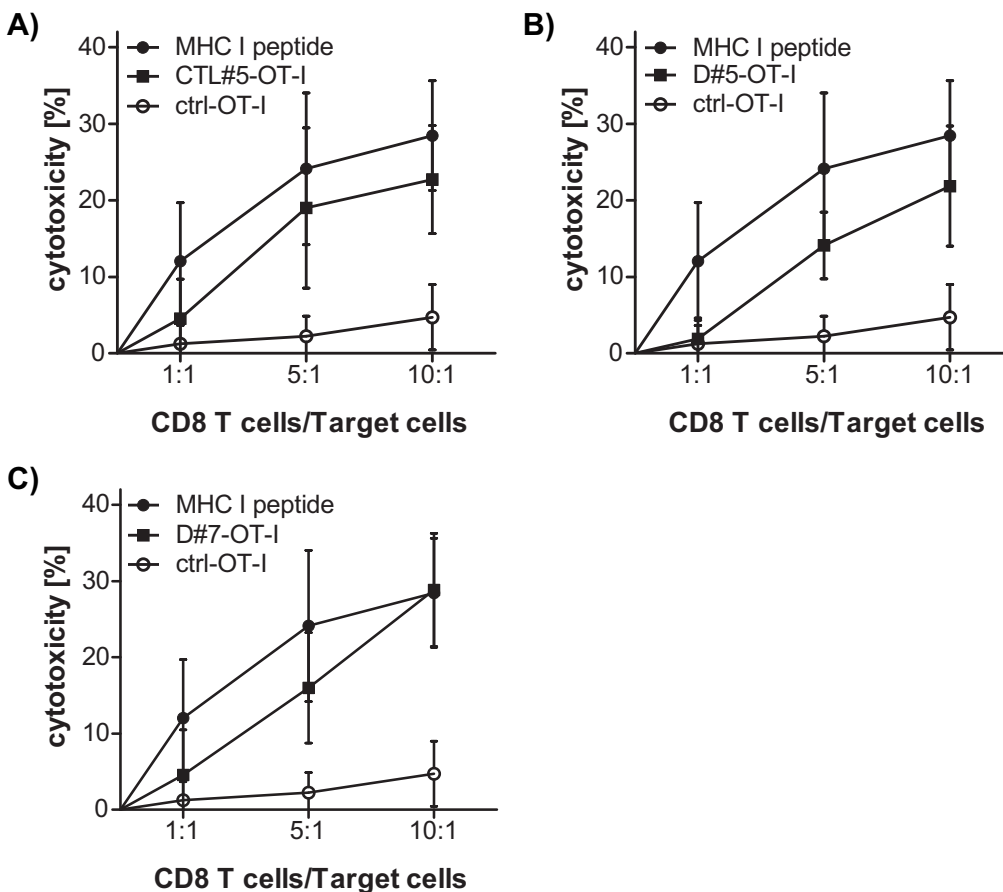
Figure 4.3.7: Aptamer-peptide conjugates induce CD8 cytotoxicity
2 x 10^5 BM-DCs were treated with 50 nM MHC I peptide or 100 nM CTL#5-OT-I **(A)**, D#5-OT-I **(B)** or D#7-OT-I **(C)** conjugates. 4 x 10^5 OVA-specific CD8 T cells were added. After 72 h, T cells were isolated and incubated with CFSE-labeled target and control cells for another 24 hours. On day 5, cells were stained with Hoechst 33258 and analyzed by flow cytometry. The percentages of T cell cytotoxicity were determined (n=2, mean ± SD). The assays were performed with blinded samples.

These data highlight that aptamer-targeted delivery of OT-I peptide indeed activates CD8 T cells.

5 Discussion

Protective immunity requires strong activation of T cells. DCs mediate the transition between innate immunity and adaptive T cell-mediated immunity allowing for such activation to occur. Hence, DC-based vaccination is an emerging field in immunotherapy. One approach for developing a DC vaccine is to conjugate antigens to carrier molecules that specifically target DCs.

Carrier molecules used thus far exhibit several limitations such as cost-intensive manufacturing, chemical stability, variations in production charges or intrinsic immunostimulatory potential. A novel promising class of carriers that might overcome these limitations are aptamers.

In the study at hand, it was investigated if aptamers are capable to mediate T cell activation through targeted delivery of antigens to DCs. Therefore, aptamers targeting DCs were selected by two different strategies. First, aptamer CTL#5 was identified by addressing recombinant proteins originated from the cell surface receptor MR in a SELEX approach. Second, aptamers D#5 and D#7 were selected without knowledge of the respective target structure by directly using BM-DCs in a cell-SELEX process.

Next, the properties of the selected aptamers were elucidated. All identified candidate aptamers were found to bind BM-DCs, were internalized and localized within appropriate antigen processing compartments and had low immunogenicity.

Finally, functionality of aptamers as DC-targeting carrier molecules was analyzed in an OVA model system. Remarkably, aptamers conjugated to antigenic OVA peptides are potent mediators of targeted activation of OVA-specific T cells.

5.1 Selection of DC-targeting aptamers

5.1.1 Protein-SELEX

DCs express a variety of endocytic receptors that are crucial for recognizing and processing antigenic structures for efficient T cell activation. Prominent examples are C-type lectin receptors, e.g. the MR[31,138] (**Section 3.3.2**). It is described that the recognition and uptake of pathogens by C-type lectin receptors determine the subsequent processing and antigen presentation[19,37]. The C-type lectin receptor MR is known to direct antigens towards cross-presentation for CD8 T cell activation[19,38]. Thus, the MR was chosen as an attractive target to identify aptamers that are internalized and localized in DCs in a similar way as MR ligands. In this work, the recombinant proteins Fc-CTL and Fc-FN, composed of domains of murine MR, were used in a

protein-SELEX approach to select BM-DC-specific aptamers. As a result, a repertoire of aptamers that bind to both Fc-CTL and Fc-FN was selected (**Section 4.1.1**).

Even though SELEX is a notionally simple method, it does not always result in aptamers with desired properties. Several factors influence the outcome of SELEX, including structural characteristics of targets, size and complexity of the starting library, choice of partitioning and elution methods and concentrations of targets and competitors[82,156].

It is plausible that the SELEX conditions chosen in this thesis influenced the results obtained. First, although a counter selection step was carried out from the 2nd to the 11th selection cycle, cross-reactive sequences binding both Fc-CTL and Fc-FN were generated (**Figure 4.1.3** and **Figure 4.1.5**). A possible explanation may be that not enough protein targets were offered during the counter selection step to catch unspecific and cross-reactive DNA binders. Consequently, after pre-incubation with the non-desirable target, non-specific binders were still present and added to the target of interest.

Second, the limited complexity of the used DNA starting library may have hampered the identification of strong Fc-FN binding sequences. Natural nucleotides exhibit constricted chemical diversity, hence the formation of complex structures necessary for target binding is limited[80]. The use of modified nucleic acid libraries containing non-canonical base pairs can be an alternative for the selection of difficult targets[111,157].

Despite the above mentioned limitations of the method, the binding to both proteins might be mediated by structural similarities. Fc-CTL as well as Fc-FN contain C-type lectin-like domains (**Figure 4.1.1A**). Although the eight CTLDs of MR differ in their function and ligand specificity, they share conserved amino acid residues to form the typical CTLD fold[35,137-140] (**Figure 5.1.1**). Presumably, cross-reactive DNA sequences may address these conserved sites.
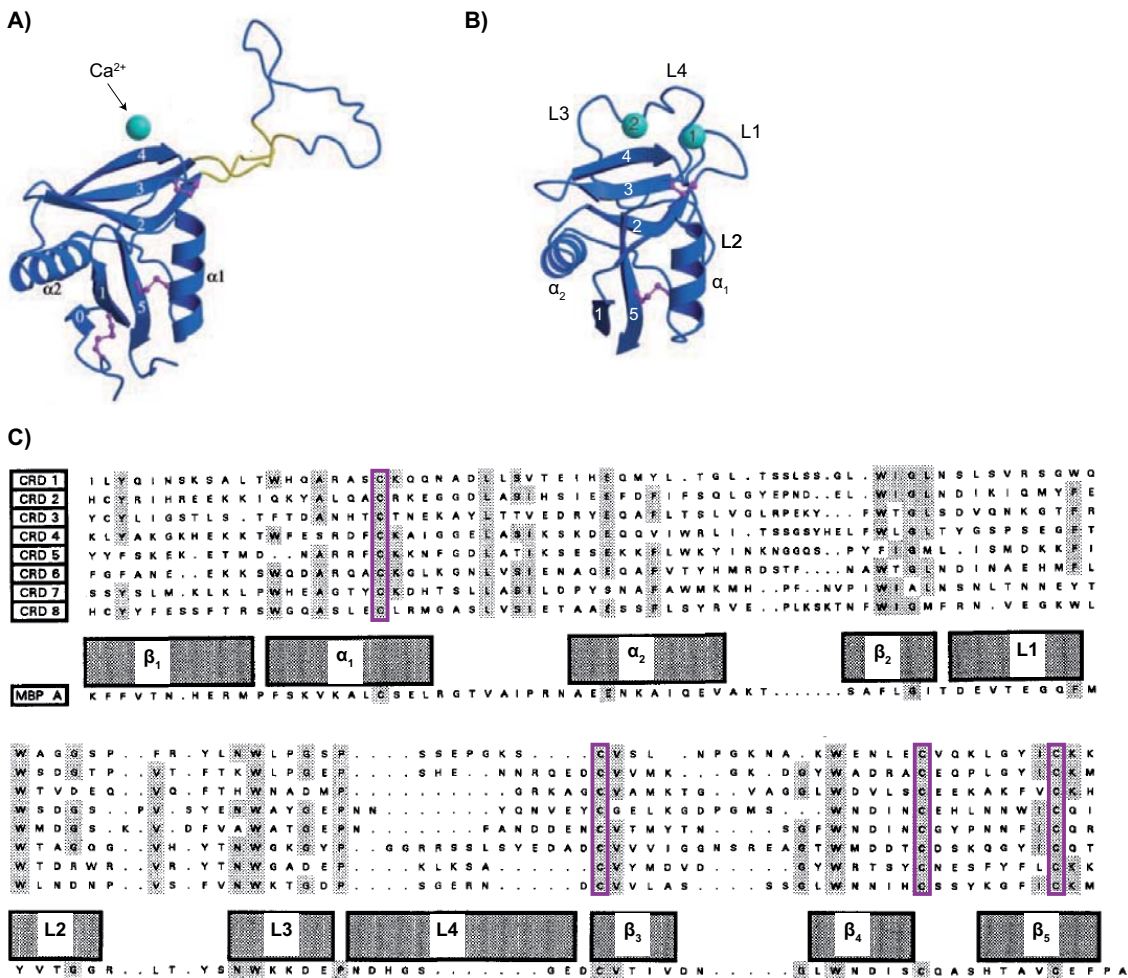
Figure 5.1.1: Structure and sequence similarities of the CTLDs of murine MR and rat mannose-binding protein-A

The ribbon diagrams of the CTLD 4 of murine MR **(A)** and the CTLD of rat mannose-binding protein-A (MBP-A) **(B)** illustrate the typical CTLD fold consisting of two α helices, two antiparallel β sheets (β strands 1-5) and four loops (L1-4). The CTLD of MBP-A is composed of two Ca^{2+} ions binding sites, whereas the CTLD 4 of MR has only one binding site. Highly conserved disulfide bonds are shown in purple and the regions connecting the external loop of CTLD 4 to the core is depicted in yellow (modified from Feinberg et al.[139]). The alignment of the eight CTLDs (CRD 1-8) and the CTLD of MBP-A reveals conserved amino acids **(C)**, shaded amino acids are conserved in five or more CTLDs. The predicted secondary structures, α helix, β strand or loop (L), are given in the boxes below the sequences. Highly conserved cysteine residues are highlighted in purple boxes (modified from Harris et al.[140]). CRD=carbohydrate-recognition domain

Nevertheless, SELEX targeting Fc-CTL resulted in the identification of aptamer CTL#5. Particularly, CTL#5 showed more than two-fold higher binding to Fc-CTL in comparison to Fc-FN (**Figure 4.1.5**) and was additionally proven to bind BM-DCs (**Figure 4.2.1**). In literature, several cell-binding aptamers were selected by protein-SELEX approaches[122,158,159]. For example, RNA aptamers recognizing prostate-specific membrane antigen (PSMA) on prostate cancer cells were identified by using the extracellular domain of PSMA in a protein-SELEX approach[158]. Remarkably, these

aptamers were functional *in vitro* and *in vivo* as selective carriers for several cargo molecules such as siRNAs or toxins[112,118,160].

5.1.2 Cell-SELEX

As outlined in the introduction, in-depth knowledge of the respective target is not necessary for cell-aptamer selection (**Section 3.5.2**). BM-DCs express a variety of molecules on their surface that are involved in modulating downstream T cell responses[13]. These molecules represent accessible targets for aptamer selection. In the present work, aptamers D#5 and D#7 that are functional in targeted activation of T cells through antigen delivery to DCs, were identified without knowledge of the respective target structures on BM-DCs (**Section 4.1.2**). This result extends previous findings in the literature. Since 1998, a growing number of aptamers recognizing mammalian cell types were identified by cell-SELEX[96,161-163]. In several studies, cancer cell lines are the target of interest[162]. For example, Tang and co-workers reported the generation of a series of aptamers as molecular probes for Burkitt lymphoma cells[164]. Moreover, one aptamer, namely TD05, was observed to be functional in targeting of lymphoma cells *in vivo*[165].

The use of somatic cells in cell-SELEX has been also reported[126,166]. Interestingly, Berezovski and co-workers enriched DNA libraries targeting either immature or mature murine BM-DCs for identification of cell state-specific biomarkers[126]. In fact, biomarkers such as protein CXorf17 homologue and serine β-lactamase-like protein were until then unknown. However, binding or functionality of individual DNA sequences was not investigated.

5.2 Properties of DC-aptamers

Aptamers CTL#5, D#5 and D#7 were found to clearly discriminate between BM-DCs and splenic T and B cells (**Figure 4.2.2**). This highlights the specificity of the selected aptamers for targets mainly expressed by BM-DCs.

However, a small amount of B cells were bound by the aptamers. Since B cells and DCs are classified as professional APCs with common functions and shared expression of surface receptors[2,27], this finding is hardly surprising. Moreover, preliminary data revealed binding of CTL#5 to murine bone marrow-derived macrophages that represent the third type of professional APC (**Figure S 9.6.1**).

This result is comparable with previous studies, which utilize the mannose receptor targeting vaccine CDX-1307, and indicate binding to DCs as well as macrophages[58]. Interestingly, binding to both cell types does not negatively influence the therapeutic

efficacy; CDX-1307 is currently tested in phase II clinical trials for treatment of muscle-invasive bladder cancer (**Table 3-1**).

Whether the binding of aptamers to other APCs might influence the outcome of downstream T cell responses, will be further investigated. This is in particular of great interest for *in vivo* applications in which the aptamers encounter all types of APCs simultaneously. However, if the binding to B cells or macrophages negatively influence aptamer-based vaccination, DCs could be alternatively treated *ex vivo* and re-implanted in patients.

5.2.1 Immunogenicity of aptamers

Repeated administration of immunogenic molecules can cause severe adverse immunological reactions ranging from dizziness, flushing and headache, to inducing the secretion of autoantibodies[77,167].

In comparison to other carrier molecules like antibodies or viruses, aptamers are described to be low or non-immunogenic[78,119]. This was confirmed for the selected aptamers in this work by the obtained results.

Here, the immunogenicity of the selected aptamers was investigated by measuring the TNF-α concentration in the supernatant of treated cells. Basically, upon recognition of nucleic acids ligands by TLR3, 7/8, 9 or 13, signaling cascades are activated which triggers the secretion of the proinflammatory cytokine TNF-α (**Figure 4.2.8**). As a result, only the naïve DNA library induced strong cytokine secretion (**Figure 4.2.9**). In theory, the library is composed of up to 10^{15}-10^{17} unique DNA sequences. Thus, it is very likely that some sequences resemble TLR ligands such as CpG rich motifs (**Figure 5.2.1**).

Similar results were obtained in previous studies done by Avci-Adali *et al.*[168]. They observed upregulation of TLR pathway-related transcripts after treating human blood cells with a DNA starting library.

ODN type	Representative sequence	Structural characteristics
D- also referred to as A-class	GGTGCAT<u>CG</u>ATGCAGGGGGG	Mixed phosphodiester/phosphorothioate backbone Single CpG motif CpG flanking region forms a palindrome Poly G tail at 3′ end
K- also referred to as B-class	TCC**ATGGA<u>CG</u>TTCCT**GAG<u>CG</u>TT	Phosphorothioate backbone Multiple CpG motifs 5′ motif most stimulatory
C	T<u>CG</u>T<u>CG</u>TT<u>CG</u>AA<u>CG</u>A<u>CG</u>TTGAT	Phosphorothioate backbone Multiple CpG motifs TCG dimer at 5′ end CpG motif imbedded in a central palindrome
P	**T<u>CG</u>T**<u>CG</u>A<u>CG</u>AT<u>CG</u>G<u>CG</u><u>CG</u><u>CG</u>CCG	Phosphorothioate backbone Two palindromes Multiple CpG motifs

Figure 5.2.1: Sequence and structural characteristics of CpG-rich oligonucleotides
In general, CpG motifs are composed of a central unmethylated CG dinucleotide flanked by 5' purines and 3' pyrimidines. Four classes of CpG-rich oligonucleotides (ODN) are described so far and are used as TLR 9 ligands in pre-clinical and clinical studies (modified after Bode *et al.*[169]). The phosphorothioate backbone increases the stability of the ODN.

Nevertheless, the conformation of aptamers might influence the immunogenicity. Other aptamers that were identified in our group to target breast cancer cells elicit elevated secretion of TNF-α (unpublished data). Consequently, immunogenicity of aptamers has to be tested for every individual sequence.

Differentiation of murine bone marrow progenitors with GM-CSF results in a mixture of immature and mature DCs[133]. Consequently, BM-DCs express moderate levels of co-stimulatory molecules like CD80, CD86 and CD40 which function as secondary signal for adequate T cell priming[71,170] (**Section 3.2.1**).

However, the situation *in vivo* is different. Under non-inflammatory steady-state conditions DCs reside as immature cells in different tissues, i.e. they lack co-stimulatory molecules. Only after receiving inflammatory stimuli, DCs mature into professional APCs and acquire the capability to activate T cells (**Section 3.3**). In turn, delivery of antigens to immature DCs in absence of inflammatory stimuli results in tolerogenicity. For instance, Bonifaz *et al.*[134] observed that T cell proliferation and subsequent deletion occurred upon antibody-mediated OVA delivery to DEC-205 on DCs in absence of inflammatory stimuli.

Consequently, the use of the described aptamers for aptamer-based antigen delivery treatments *in vivo* may offer several therapeutic possibilities (see **Section 5.4**).

5.2.2 CTL#5 specificity towards MR

C-type lectin receptors are non-canonical PRRs that enable the discrimination of self from non-self substances by cells involved in innate immunity[35] (**Section 3.3.2**). The C-type lectin receptor MR is mainly expressed by DCs and macrophages and described to direct antigens towards cross-presentation for CD8 T cell activation[19,138]. Thus, the MR is an attractive target for DC-based vaccine strategies to recruit cytotoxic CD8 T cells.

In the study at hand, recombinant Fc-CTL, composed of CTLD 4-7 from the MR (**Figure 4.1.1**), was used to identify aptamer CTL#5. Although CTL#5 was observed to co-localize strongly with MR (**Figure 4.2.4AB**), MR$^{-/-}$ DCs were bound to the same extent as wildtype DCs (**Figure 4.2.4C**). Thus, it can be assumed that DC-targeting by CTL#5 is not only mediated by MR.

A reasonable explanation might be that other C-type lectin receptors expressed on BM-DCs like DEC-205 or dectin-1 are recognized by CTL#5 (**Figure 4.2.3**). A common structure of these receptors are CTLDs[31]. Although CTLDs exhibit different ligand specificity among the receptors, they share conserved residues responsible for the typical formation of a hydrophobic fold[35,137] (**Figure 5.1.1AB**).

Previous studies demonstrated that antigens endocytosed by the MR are entrapped within slowly maturing early endosomes for cross-presentation[19,24,26]. Thus, co-localization of MR ligands with EEA1 is anticipated rather than lysosomal marker LAMP-1. Within this study, both OVA and CTL#5 were observed to co-localize weakly with LAMP-1 besides the co-localization with EEA1 (**Figure 4.2.6**). This implies that upon endocytosis, both OVA and CTL#5 are shuttled into slowly as well as rapid maturing early endosome populations. Plus, OVA and CTL#5 may be internalized by other endocytic receptors apart from the MR or by distinct mechanisms like phagocytosis. For example, targeting of other receptors of the C-type lectin family like DEC-205 are described to potentiate internalization into early endosomes that rapidly mature into late endosomes and lysosomes[37,39]. Subsequently, cargoes are immobilized onto MHC II molecules and presented to CD4 T cells.

Hence, antigens coupled to CTL#5 can be directed towards cellular compartments adequate for both MHC I and MHC II-epitope generation.

5.3 Aptamer-targeted activation of T cell-mediated immunity

5.3.1 Aptamer-targeted activation of CD4 T cells

The study at hand is the first that demonstrates aptamer-mediated CD4 T cell activation through targeting of DCs with a MHC II-restricted antigen.

CD4 T cells recognize antigenic peptides immobilized on MHC II. Basically, exogenous antigens are degraded within late endosomes or lysosomes and subsequently loaded onto MHC II in multivesicular bodies (MVBs) (**Section 3.3.1.2**). In the present study, all aptamers conjugated to the MHC II-restricted OT-II peptide mediated CD4 T cell activation in a concentration-dependent manner, as measured by *in vitro* proliferation assays (**Figure 4.3.4C**).

However, only CTL#5 was observed to co-localize with the lysosomal marker LAMP-1 (**Figure 4.2.6BC**). A possible explanation may be that recycling of MHC II from the cell surface might enable the loading or exchange of antigens within early endosomes[171,172]. MHC II molecules are thought to be continuously recycled from the plasma membrane to early endosomes and back to the membrane[27]. Some antigenic MHC II-epitopes were demonstrated to simply require unfolding and mild proteolysis that is enabled by proteases present in early endosomes[172]. These epitopes can bind to recycled MHC II and are transported to the plasma membrane for presentation.

Another possible explanation is that aptamer-OT-II conjugates are internalized by phagocytic receptors. Antigens taken up by these receptors are entrapped within phagosomes. Phagosomes are composed of elements derived from early endosomes and the ER[173,174], thus they are detectable by staining of EEA1.

A third possible explanation may be that the attached OT-II peptide influenced the trafficking and processing within DCs. In this thesis, co-localization studies were carried out with non-conjugated aptamers. Further work will concentrate on the cellular localization of aptamer-peptide conjugates.

Apart from that, ctrl-OT-II conjugates were observed to induce CD4 T cell division (**Figure 4.3.4C**). This result was not anticipated, because neither the control sequence nor unconjugated OT-II peptide elicited T cell proliferation in their singular, unconjugated form (**Figure 4.3.4AB**). Furthermore, the control sequence was not internalized by BM-DCs (**Figure 4.2.5**). However, one reason might be that the coupling of both molecules affects the internalization and processing by BM-DCs. Similar findings were obtained by the work of Wengerter *et al.*[115]. They observed minimal CD8 T cell division after treatment of splenic DCs with control sequence- as well as antibody isotype-OVA conjugates.

In general, activated CD4 T cells polarize into activator or suppressor cells that regulate other effectors of the adaptive immunity[5]. However, a growing body of literature has analyzed the ability of CD4 T cells to acquire cytotoxic activity upon activation[152-154]. In the present work, no CD4 T cell cytotoxicity was detectable in *in vitro* cytotoxicity assays (**Figure 4.3.5**). This was not unexpected; in fact, there is no general

agreement on the nature and role of cytotoxic CD4 T cells. Some studies revealed the development of cytotoxic CD4 T cells upon chronic viral infections[152], whereas others proposed their occurrence in anti-cancer immunity[153]. Moreover, there are discrepancies if cytotoxic CD4 T cells represent a specialized subset of T cells or if they are associated with the Th1 phenotype[175,176].

Therefore, future work will focus on the ability of aptamers to cause CD4 T cell polarization towards activating helper cells or suppressing regulatory T cells. First of all, it is projected to monitor the cytokine profile of the activated T cells. Secretion of different cytokines is characteristic for each effector subset, for example, Th2 cells produce high levels of IL-4[2].

In addition, the functionality of aptamer-OT-II *in vivo* will be assessed by different strategies. One strategy takes advantage of the effector function of activated CD4 T helper cells to induce differentiation of B cells into antibody-producing plasma cells[5]. Therefore, aptamer-OT-II mediated CD4 T cell activation will be assessed by determining the titer of OT-II peptide-specific antibodies in serum of mice.

Another strategy is to stain isolated CD4 T cells from spleen or serum with fluorophore labeled tetramers of MHC-peptide complexes[177,178]. In principle, activation and clonal expansion of CD4 T cells can be determined by the increasing number of cells bound to the tetramers.

5.3.2 Aptamer-targeted activation of CD8 T cells

CD8 T cells recognize antigens immobilized on MHC I molecules expressed by DCs. In the classical MHC I pathway, endogenous antigens are loaded onto MHC I molecules. However, this pathway can be bypassed by a process named cross-presentation. Exogenous antigens are thereby endocytosed by DCs and actively translocated out of slowly maturing early endosomes into the cytosol for generation of MHC I epitopes[16] (**Section 3.3.1.1**).

In the present study, aptamer-targeted delivery of OT-I peptide elicited strong CD8 T cell activation. This indicates that in accordance with the observed co-localization of all aptamers with early endosomes marker EEA1 (**Figure 4.2.6AC** and **Figure 4.2.7**), aptamer-based delivery of OT-I peptide mediated cross-presentation on MHC I molecules for efficient CD8 T cell activation (**Figure 4.3.6C**).

These results are in agreement with Wengerter *et al.*[115], where they targeted full-length OVA attached to DEC-205 specific aptamers to splenic DCs and observed proliferation of CD8 T cells. However, in other studies, OVA was demonstrated to be internalized,

processed and cross-presented by DCs in its natural unconjugated form[19,38]. It is questionable if the DEC-205 aptamers improved the effect of OVA on DCs and T cells.

Furthermore, activation of CD8 T cells was verified with *in vitro* cytotoxicity assays. In comparison to ctrl-OT-I conjugates, CD8 T cell cytotoxicity induced by aptamer-OT-I was elevated to an extent similar to MHC I peptide (**Figure 4.3.7**). This highlights the potential of aptamers to mediate efficient cytotoxic activity of CD8 T cells.

Surprisingly, in contrast to the OT-II peptide (**Figure 4.3.4A**), the OT-I peptide was observed to have an intrinsic capacity to activate CD8 T cell divisions (**Figure 4.3.6A**). Moreover, although ctrl-OT-I mediated low cytotoxic activity (**Figure 4.3.7**), it was observed to induce cell division (**Figure 4.3.6C**). Similar results were obtained with ctrl-OT-II conjugates (**Figure 4.3.4C** and **Section 5.3.1**). Despite the fact that the conjugation of the control sequence and the peptides might affect internalization and processing, incomplete activation of T cells can also be considered. Complete activation of CD8 T cells requires the continuous stimulation of all three signals, i.e. antigen, co-stimulation and inflammatory cytokines, for more than 40 hours[9]. Cell division alone is initiated by the recognition of the respective antigen loaded on MHC I and co-stimulatory stimuli, whereas cell survival and effector function depend on prolonged signaling of all three signals. Incomplete activation of T cells results in T cell anergy or clonal deletion[10] (**Section 3.2.1**). Analysis such as apoptosis or anergy assays will shed light on the effect of OT-I peptide or control-peptide conjugates on T cells.

Apart from that, it cannot be excluded that other yet unknown mechanisms lead to the observed effect.

To further investigate aptamer targeted CD8 T cell activation *in vivo*, a cytotoxicity assay in mice will be performed. On that account, mice will be immunized with aptamer-OT-I conjugates and after several days, CFSE-labeled and MHC I peptide loaded target cells and non-loaded control cells will be co-administrated. Finally, target and control cells will be isolated from the spleen and analyzed by flow cytometry.

In addition, CD8 T cell activation will be determined by staining of isolated T cells with fluorophore-labeled tetramers of MHC-peptide complexes[177,178].

5.4 Perspective for future research

The present work clearly demonstrates the functionality of aptamers for DC-based vaccination. Still, for their *in vivo* use, open questions remain.

What are the pharmacokinetic properties of the described aptamers and aptamer-peptide conjugates? Are the aptamers stable in whole blood or do they need modifications to increase their nuclease-stability or elimination half-life? How are the aptamers distributed *in vivo*? Depending on the administration, the nucleic acid composition, modifications and conjugates, aptamers are described to exhibit widespread half-lifes ranging from 10 minutes to more than 75 hours in mammals[179]. Future work will explore if the selected aptamers need to be modified to increase their stability *in vivo* (**Section 3.5.2**).

What is the optimal route of administration? In previous work, the impact of administration on the immune response was demonstrated[178]. Vaccination with mannosylated peptides in mice, for example, was more effective in CD8 activation upon intradermal injection in comparison to subcutaneous administration[71]. This result might be due to the fact that the layers of the skin are inhabited by DCs with different presenting capacities or that intradermal injected vaccines are longer available for efficient T cell priming[180]. Therefore, the optimal route of administration has to be determined in mouse models.

What are the optimal conditioning and activation stimuli? Concerning the very low immunogenic potential of the selected aptamers, aptamer-based targeting of DCs may offer several therapeutic possibilities. Depending on how the non-immunogenic aptamers are administrated, DCs become activating or tolerogenic (**Figure 3.3.1**).

On the one hand, aptamer-based delivery of cargo molecules in presence of inflammatory stimuli could induce T cell-mediated immunity for prevention or treatment of infection or cancer. This is done in particular by the co-delivery of adjuvants like pIC (polyinosinic:polycytidylic acid)[115,181]. However, the type of adjuvant has to be chosen carefully, because PRR ligands themselves influence the outcome of adaptive immune responses[182].

In addition, DC-aptamers can be conjugated to aptamers antagonizing receptors that negatively regulate T cell effector functions such as CTLA-4 aptamers[122].

On the other hand, aptamer-based DC vaccines administrated without inflammatory stimuli might be useful for the prevention or treatment of allograft rejections or autoimmune diseases. Lack of such stimuli facilitates the development of tolerogenic DCs. Tolerogenic DCs are deficient in adequate signaling for T cell activation or they only deliver co-inhibitory signals[18]. As a consequence, auto-reactive or allo-reactive T cells interacting with tolerogenic DCs become anergic or are deleted.

Moreover, aptamer-based delivery of siRNAs, miRNAs or antagomiRs could change cellular phenotypes. Cancer or chronic inflammation facilitates the occurrence of tolerogenic DCs and macrophages[183,184]. Inhibition of miR-22 and miR-503, for example, was reported to restore the activating capacity of DCs within tumor microenvironments[185]. We are in the process of investigating aptamer-based silencing of miR-125a in human macrophages associated with granulomatous diseases[184].

What is the optimal dose and frequency of aptamer-based DC vaccination? Even though repeated administration of vaccines increases the frequencies of memory T cells, overstimulation is reported to cause T cell deletion[186]. Similar observations were done after treatment with high doses of peptide vaccines[187]. Therefore, the optimal dose and vaccination schedule have to be determined in mouse models.

Which antigen should be conjugated? A wide range of cancer antigens and auto-antigens associated with autoimmune diseases have been identified in the last decades[188-190]. The choice of aptamer cargo molecule is dependent on the desired therapeutic effect. Within this study, it was clearly demonstrated that all aptamers delivered MHC I epitopes as well as MHC II epitopes (**Section 5.3.1** and **5.3.2**). This feature could be beneficial for future treatments. For example, Tsuji *et al.*[191] recently reported that the cancer testis antigen NY-ESO-1 which contains both MHC I and MHC II epitopes, enhances T cell responses. This is hardly surprising. In fact, most CD8 T cell responses require activation of CD4 T helper cells by the same APC[2] (**Section 3.2**).

Future work will elucidate if aptamer-based delivery of such antigens boosts CD4 and CD8 T cell responses.

5.5 Concluding remarks

The present work demonstrates the potential of aptamers to function as delivery tools in an immunological context. The investigated DC-aptamers were selected with and without knowledge of the target structures. Noteworthy, both selections yielded aptamers that are potent DC-based vaccines *in vitro*. All aptamers direct antigens into eligible processing compartments for efficient antigen presentation and T cell activation.

These results widen the knowledge about the potential applicability of aptamers as DC-targeting carriers and pave the way for the development of aptamer-based DC vaccines for *in vivo* applications.

6   Materials

6.1 Equipment

Table 6-1 Equipment

Equipment	Manufacturer
FACS Canto II	BD
FACS LSR II	BD
FluoView FV1000 confocal laser scanning microscope	Olympus
Genoplex UV transilluminator	VWR
HPLC 1260 series, C18 Eclipse column	Agilent
LC-MS: HPLC 1100 series/Easy-nLC esquire HCT	Agilent/Bruker
Liquid scintillation counter WinSpectral 1414	Perkin Elmer
LSM 710 confocal laser scanning microscope	Zeiss
Nanodrop 2000c Spectrophotometer	Thermo Scientific
NanoQuant Infinite M200 Spectrophotometer	Tecan
PCR Mastercycler personal	Eppendorf
Phosphorimager FLA-3000	Fujifilm
Pipets	Eppendorf
SpeedVac	Thermo Scientific
Water purification system	TKA/Thermo Scientific

6.2 Consumables

Table 6-2 Consumables

Consumable	Supplier
Amicon Ultra-0.5 Centrifugal Filter Devices 10 K	Millipore
Cell culture plates	Sarstedt; TPP; Greiner Bio One
FACS tubes, 5 ml, 12 mm	Sarstedt
Falcon cell strainer 40 µm	Sarstedt
G25 columns	GE Healthcare
Nitrocellulose membrane (Protran 0.45 µm)	Schleicher and Schuell
Pipet tips	Sarstedt
Reaction tubes	Sarstedt; Eppendorf

6.3 Chemicals and reagents

Table 6-3 Chemicals and reagents

Reagent	Supplier
1,1,1,3,3,3-hexafluoro-2-propanol (HFIP)	Sigma Aldrich
1,4-Dithiothreitol (DTT)	Roth
4',6-diamidino-2-phenylindole (DAPI)	Sigma Aldrich
Acetic acid	Merck
Acetonitril	Fluka
Agar	Sigma Aldrich
Agarose	Merck; Genaxxon
Ammoniumacetate	Gruessing
Ammoniumperoxodisulfate (APS)	Roth
Ampicillin sodium salt	AppliChem
Bis-Acrylamid, Rotiphorese	Roth
Bovine serum albumin (BSA, nuclease and protease free)	Calbiochem
Bromophenol blue	Merck
β-mercaptoethanol	Roth
Carboxyfluorescein succinimidyl ester (CFSE)	BD
Cell culture media	PAA
Chloroform	AppliChem
Calf intestinal alkaline phosphatase (CIAP)	Promega
Coomassie Brilliant Blue G250	Biorad
Di-sodiumhydrogenphosphate-dihydrate	Merck
DNA ladders	Fermentas; Thermo Scientific
dNTPs/NTPs	Larova
DPBS	Gibco
Dynabeads Protein G	Invitrogen
Ethanol abs.	Sigma Aldrich
Ethdiumbromide	Roth
Ethylendiamintetraacetic acid (EDTA)	AppliChem
FCS Clone	PAA
Ficoll-Paque Premium 1.084	GE Healthcare
Fluorogel mounting medium	EMS
Formaldehyde	Fluka
ɣ-^{32}P-ATP	Perkin Elmer
Glycine	Roth
Hoechst 33258	Invitrogen
Inorganic pyrophosphatase (IPP)	Roche
Isopropanol	Merck

Lambda Exonuclease	Fermentas
Low fat dry milk powder	Roth
Magnesiumchloride-hexahydrate	AppliChem
Mouse serum	PAA
N,N,N',N'-tetramethylethylendiamide (TEMED)	Roth
Ovalbumin (OVA)-Alexa Fluor 647	Life Technologies
Penicillin [10000 U/ml]/Streptomycin [10 mg/ml]	PAA
Phenol	Roth
Potassium chloride (KCl)	Gruessing
RNasin ribonuclease inhibitor	Promega
Rotiphorese sequencing gel concentrate	Roth
Prolong diamond antifade mountant	Life technologies
Protein ladders	Sigma Aldrich; Fermentas
Pwo polymerase	Genaxxon
Sodium chloride (NaCl)	AppliChem
Sodium dodecylsulfate (SDS)	Roth
Sodiumacetate	Gruessing
Superscript II reverse transcriptase	Thermo Scientific
T4 polynucleotide kinase (PNK)	NEB
T7 Y639F RNA-polymerase	Inhouse production
Taq polymerase	In house production; Promega
Tricine	Roth
Triethylamine (TEA)	Sigma Aldrich
Triethylammonium acetat (TEAA)	Sigma Aldrich
Tris	Roth
Triton-X 100	Merck
Trypsin [0.05%]/EDTA [0.5M]	Thermo Scientific
Urea	AppliChem
Wheat germ agglutinin-Alexa Fluor 488	Invitrogen

6.4 Commercially available kits

Table 6-4 Kits

Kit	Supplier
NucleoSpin Extract II Gel and PCR Clean-up	Macherey and Nagel
NucleoSpin plasmid	Macherey and Nagel
TOPO TA Cloning	Invitrogen
TruSeq DNA PCR-Free LT	Illumina

6.5 Buffers and solutions

1 x Phosphate buffered saline (PBS)

137 mM NaCl, 2.7 mM KCl, 6.5 mM Na_2HPO_4, 1.47 mM NaH_2OP_4, pH 7.4

6.5.1 Gel electrophoresis

1 x TBE

90 mM Tris pH 8.0, 90 mM Borat, 2 mM EDTA

1 x DNA loading buffer

25 mM Tris pH 8.0, 25 % glycerol, 25 mM EDTA, bromophenol blue

1 x RNA loading buffer

50 % formamide, 0.013 % SDS, 0.25 mM EDTA, bromophenol blue

10 x PAA loading buffer

60 % formamide, 5 % SDS, 0.25 mM EDTA, bromphenol blue

3 x Tricine SDS gel buffer

3 M Tris, 0.3 % SDS, pH 8.45

1 x Tricine SDS cathode buffer

0.1 M Tris, 0.1 M tricine, 0.1 % SDS, pH 8.25

1 x Tricine SDS anode buffer

0.2 M Tris, dissolved in ddH_2O, pH 8.9

4 x non-reducing sample buffer

150 mM Tris pH 6.8, 30 % glycerol, 12 % SDS, bromophenol blue

4 x Laemmli buffer

150 mM Tris pH 6.8, 30 % glycerol, 12 % SDS, 15 % β-mercaptoethanol, bromophenol blue

10 x SDS running buffer

250 mM Tris, 2 M glycine, 1 % SDS

Coomassie staining solution

10 % acetic acid, Coomassie Brilliant Blue G250

Coomassie destaining solution

10 % acetic acid

6.5.2 Bacteria culture

Agarose plates w/ ampicillin

3.8 g agarose, 5 g LB broth, 250 ml ddH$_2$O, 250 µl 100 mg/ml ampicillin

LB medium w/ ampicillin

10 g LB broth, 500 ml ddH$_2$O, 500 µl 100 mg/ml ampicillin

6.5.3 Flow cytometry

FACS buffer

0.1 % BSA, 0.005 % NaN$_3$ in PBS

6.5.4 SELEX

Selection buffer protein-SELEX

PBS, 1 mM MgCl$_2$, 1 mM CaCl$_2$, 0.01 mg/ml BSA

Selection buffer cell-SELEX

DPBS (Gibco pH 7.0-7.2), 1 mM MgCl$_2$, 0.01 mg/ml BSA

Wash buffer

Selection buffer w/o BSA

6.5.5 Cell culture

DC culture medium (DC-medium)

IMDM, 10 % heat inactivated FCS, 50 µM β-mercaptoethanol, 100 U/ml penicillin, 0.1 mg/ml streptomycin, 2.5 % R1/J558 supernatant w/ GM-CSF

Macrophage culture medium (macrophage-medium)

IMDM, 10 % heat inactivated FCS, 50 µM β-mercaptoethanol, 100 U/ml penicillin, 0.1 mg/ml streptomycin, 2.5 % R1/J558 supernatant w/ M-CSF

T cell medium

RPMI 1640, 10 % heat inactivated FCS, 50 µM β-mercaptoethanol, 100 U/ml penicillin, 0.1 mg/ml streptomycin, 2 mM L-glutamine

6.6 Oligonucleotides

All oligonucleotides, including 5'-thiol-C6 and 5'-ATTO 647N modified aptamers and control sequences (ctrl), were purchased from Ella Biotech GmbH (Martinsried). The DNA was supplied HPLC-purified and lyophilized.

Table 6-5 Oligonucleotides

Name	Sequence 5'-3'
D3 DNA library	GCTGTGTGACTCCTGCAA-N43-GCAGCTGTATCTTGTCTCC
D3 fwd Primer	GCTGTGTGACTCCTGCAA
D3 rev Primer, 5'-phosphorylated	GGAGACAAGATACAGCTGC
CTL#5	GCTGTGTGACTCCTGCAATGCAATCTAGCTGACAATGGGG GGGAAGAATGTGGGTGGGTGGCAGCTGTATCTTGTCTCC
D#5	GCTGTGTGACTCCTGCAACGCATTTGGGTGGGATTGTTATT TGGGTCGGGATTGGCAGTTGCAGCTGTATCTTGTCTCC
D#7	GCTGTGTGACTCCTGCAACGTGGGTGGGTTTATATTCGGT GGTGGTGGGGGTGGTACTGTTGCAGCTGTATCTTGTCTCC
ctrl (CTL#5sc)	GCTGTGTGACTCCTGCAAGTGGTGTTAAGAGGTGAGGTAT AACGCGGAATGGTGCGAGGCGCAGCTGTATCTTGTCTCC
D3 NGS primer	
F1	ATCACGGCTGTGTGACTCCTGCAA
R1	ATCACGGGAGACAAGATACAGCTGC
F2	CGATGTGCTGTGTGACTCCTGCAA
R2	CGATGTGGAGACAAGATACAGCTGC
F3	TTAGGCGCTGTGTGACTCCTGCAA
R3	TTAGGCGGAGACAAGATACAGCTGC
F4	TGACCAGCTGTGTGACTCCTGCAA
R4	TGACCAGGAGACAAGATACAGCTGC
F5	ACAGTGGCTGTGTGACTCCTGCAA
R5	ACAGTGGGAGACAAGATACAGCTGC
F6	GCCAATGCTGTGTGACTCCTGCAA
R6	GCCAATGGAGACAAGATACAGCTGC
F7	CAGATCGCTGTGTGACTCCTGCAA
R7	CAGATCGGAGACAAGATACAGCTGC
F8	ACTTGAGCTGTGTGACTCCTGCAA
R8	ACTTGAGGAGACAAGATACAGCTGC
F9	GATCAGGCTGTGTGACTCCTGCAA
R9	GATCAGGGAGACAAGATACAGCTGC
F10	TAGCTTGCTGTGTGACTCCTGCAA
R10	TAGCTTGGAGACAAGATACAGCTGC
F11	GGCTACGCTGTGTGACTCCTGCAA
R11	GGCTACGGAGACAAGATACAGCTGC
F12	CTTGTAGCTGTGTGACTCCTGCAA
R12	CTTGTAGGAGACAAGATACAGCTGC
A50 library (DNA/RNA)	ATAGCTAATACGACTCACTATAGGGAGAGGAGGGAAGTCT ACATCTT-N50-TTTCTGGAGTTGACGAAGCTT/ GGGAGAGGAGGGAAGUCUACAUCUU-N50-

	UUUCUGGAGUUGACGAAGCUU
A50 fwd Primer	ATAGCTAATACGACTCACTATAGGGAGAGGAGGGAAGTCT ACATCTT
A50 rev Primer	AAGCTTCGTCAACTCCAGAAA

6.7 Mouse strains

Table 6-6 Mouse strains

Mouse strain	Description
C57/BL6J	Wildtype strain, Haplotype H-2K^b
MR$^{-/-}$	C57/BL6 background, stop codon inserted at the MR start codon of Exon 1, preventing its expression[192]
OTI Rag2$^{-/-}$	C57/BL6 background, CD8 T cells express TCR specific for OVA$_{257-264}$ on MHC I, no endogenous TCR expression because of recombinant activating gene 2 (Rag2) deficiency[155]
OTII	C57/BL6 background, CD4 T cells express TCR specific for OVA$_{323-339}$ on MHC II[150]

6.8 Proteins

Table 6-7 Ovalbumin (OVA) peptides

Protein	Sequence (N-C)	Supplier
MHC I peptide (OVA$_{257-264}$)	SIINFEKL	Tebu-Bio
MHC II peptide (OVA$_{323-339}$)	ISQAVHAAHAEINEAGR	Tebu-Bio
OT-I peptide	VSGLEQLESIINFEKLTEWTSSNV	Panatecs
OT-II peptide	SAESLKISQAVHAAHAEINEAGREVVGSA	Panatecs

N-terminal functionalized maleimide OT-I and OT-II peptides were also purchased from Panatecs. OT-I and OT-II peptides were supplied HPLC-purified and lyophilized.

Table 6-8 Proteins

Protein	Supplier
Activated Protein C (aPC), Xigris	Lilly
Humanes Alpha Thrombin	Cellsystems
Humanes Cytohesin 1 Sec 7 (Cyt1 Sec7)	In house production
Humanes Erk2	In house production
Protein G	Invitrogen

6.9 Antibodies

Table 6-9 Antibodies

Antibody	Supplier
B220 (CD45RA)-eFluor450, Clone RA3-6B2	eBioscience
B220 (CD45RA)-FITC, Clone T6D11	Miltenyi
CD4-PerCP-Cy5.5, Clone Gk 1.5	Biolegend
CD8α-eFluor450, Clone 53-6.7	eBioscience
CD8α-PE, Clone 53-6.7	eBioscience
EEA1, Clone H-300	Santa Cruz
LAMP-1, Clone 1D4B	BD
MR-Alexa Fluor 488, Clone MR5D3	AbD Serotec
Rabbit-Alexa Fluor 488	Life Technologies
Rat-Alexa Fluor 488	Life Technologies

7   Methods

If not noted otherwise, all experimental steps were done at room temperature.

7.1 Handling of nucleic acids

7.1.1 General handling and storage

Purchased lyophilized nucleic acids were dissolved in ddH$_2$0 according to the manufacturer manuals. The concentration was determined by UV spectrometry at 260 and 280 nm and the quality checked by agarose gel electrophoresis. For long-term storage, nucleic acids were kept at -20 °C.

To determine the labeling efficiency, ATTO 647 N-labeled DNA was separated by gel electrophoresis and the fluorescence was monitored by Phosphorimager FLA-3000 (Fujifilm).

7.1.2 Agarose gel electrophoresis

4 % agarose gels were used to monitor purchased nucleic acids, PCR products, generated single-stranded DNA or transcribed 2'F-RNA. To this end, 4 g agarose was dissolved in 100 ml TBE buffer and boiled for several minutes in the microwave. 40 ml was poured into the gel cast and stained with ethidiumbromide at a 1:10000 dilution.

Samples were diluted in DNA or RNA loading buffer, where RNA loading buffer was used for single-stranded DNA or 2'F-RNA to enable optimal separation. Gels were run in TBE buffer at 130 V for 25 minutes and bands were visualized by UV transilluminator (VWR) and evaluated by comparison with the standard DNA ladder.

7.1.3 Polyacrylamide gel electrophoresis (PAGE)

Polyacrylamide gel electrophoresis was used to separate nucleic acids for monitoring labeling efficiency of ^{32}P-labeling. A 10 % gel was prepared as described below (**Table 7-1**) and poured into the gel cast. After polymerization for at least 1 hour, the gel was placed into a running chamber filled with 1 x TBE buffer. The gel was pre-run for 30 minutes at 370 V and 15 W. Before loading the samples, the pockets were cleared with 1 x TBE. Samples were diluted in PAA loading buffer and boiled for 3 minutes at 95 °C. The gel was run for 45 minutes at 370 V and 15 W.

Table 7-1 Pipetting scheme for one 10 % polyacrylamide gel

Solution	Volume
Rotiphorese sequencing gel concentrate	28 ml
8.3 M Urea	35 ml
8.3 M Urea in 10 x TBE	7 ml
10 % APS	560 µl
TEMED	28 µl

Radioactivity was monitored by Phosphorimager FLA-3000 (Fujifilm).

7.1.4 Polymerase chain reaction (PCR)

The following pipetting scheme and PCR program were used to amplify DNA.

Table 7-2 Pipetting scheme for one PCR reaction

Reagent	Stock concentration	Volume [µl]	Final concentration
Taq reaction buffer	10 x	10	1 x
$MgCl_2$	100 mM	2	2 mM
dNTPs	25 mM each	0.8	0.2 mM
D3 fwd primer	100 µM	1	1 µM
D3 rev primer	100 µM	1	1 µM
Taq polymerase	2.5 U/µl	2	5 U
DNA template			1-10 nM
ddH_2O		ad 100 µl	

5'-phosphorylated reverse primers were used to enable single strand displacement by lambda exonuclease digestion.

Table 7-3 PCR program

Step	Time [min]	Temperature [°C]
Activation of Taq (first cycle)	5	95
Denaturation	1	95
Annealing	1	64
Elongation	1.5	72
Final elongation (last cycle)	3	72
Storage	∞	4

PCR products were purified with the commercially available NucleoSpin clean-up kit from Machery and Nagel. In brief, 3 PCR reactions were pooled for 1 silica column and eluted with 2 x 25 µl ddH$_2$0.

7.1.5 Reverse transcription-PCR (RT-PCR)

The following pipetting scheme and PCR program were used to reverse transcribe 2'F-RNA and amplify the obtained DNA.

Table 7-4 Pipetting scheme for one RT-PCR reaction

Reagent	Stock concentration	Volume [µl]	Final concentration
Taq reaction buffer	10 x	10	1 x
First strand buffer	5 x	4	0.2 x
MgCl$_2$	100 mM	1.5	1.5 mM
DTT	100 mM	2	2 mM
dNTPs	25 mM each	1.2	0.3 mM
A50 fwd primer	100 µM	1	1 µM
A50 rev primer	100 µM	1	1 µM
Taq polymerase	2.5 U/µl	2	5 U
Reverse Transcriptase	200 U/µl	1	2 U
DNA template			1-10 nM
ddH$_2$0		ad 100 µl	

Table 7-5 RT-PCR program

Step	Time [min]	Temperature [°C]
Reverse transcription	10	54
Denaturation	1	95
Annealing	1	60
Elongation	1.5	72
Final elongation (last cycle)	3	72
Storage	∞	4

7.1.6 Single strand displacement by lambda exonuclease digestion

Lambda exonuclease selectively digests the 5'-phosphorylated strand of double-stranded DNA and thereby generates single-stranded DNA. The following reaction mixture (**Table 7-6**) was incubated for 45 minutes at 37 °C and the reaction was stopped by heating the samples for 15 minutes at 80 °C.

Table 7-6 Pipetting scheme for one digestion reaction

Reagent	Stock concentration	Volume [µl]	Final concentration
Lambda exonuclease reaction buffer	10 x	5	1 x
Purified PCR product		45	
Lambda exonuclease	10 U/µl	1	10 U

Single-stranded DNA was purified with the commercially available NucleoSpin clean-up kit from Machery and Nagel. In brief, 2 digestion reactions were pooled for 1 silica column and eluted with 2 x 20 µl ddH$_2$0. The concentration was determined by UV-spectrometry at 260 and 280 nm.

7.1.7 *In vitro* transcription

The following pipetting scheme was used to transcribe DNA into 2'F-RNA. The T7 RNA-polymerase mutant Y639F was used to enable the introduction of 2'F-pyrimidines. The reaction mixture was incubated for 4 hours at 37 °C and purified by phenol/chloroform extraction and ethanol precipitation.

Table 7-7 Pipetting scheme for one *in vitro* transcription reaction

Reagent	Stock concentration	Volume [µl]	Final concentration
Tris pH 7.9	200 mM	20	40 mM
MgCl$_2$	100 mM	15	15 mM
DTT	100 mM	5	5 mM
ATP	100 mM	0.5	0.5 mM
GTP	100 mM	0.5	0.5 mM
2'F-dUTP	100 mM	2	2 mM
2'F-dCTP	100 mM	2	2 mM
RNasin	40 U/µl	1	40 U
T7 Y639F RNA-polymerase	10 U/µl	5	50 U
IPP	2 U/µl	0.2	0.4 U
DNA template			1-10 nM
ddH$_2$0		ad 100 µl	

7.1.8 Phenol/Chloroform extraction and ethanol precipitation

Phenol/Chloroform extraction and ethanol precipitation was used to isolate DNA or 2'F-RNA sequences from BM-DCs during cell-SELEX.

One volume of phenol was mixed with one volume of nucleic acid solution by extensive vortexing. After spinning the samples at maximum speed for 3 minutes, the upper phase was transferred into a new tube. Two volumes of chloroform were added and the samples mixed and centrifuged. Again, the upper phase was transferred into a new tube for ethanol precipitation. DNA was precipitated with 1/10 volume 3 M NaOAc pH 5.4 and 3 volumes of cold ethanol absolute for at least 10 minutes at -80 °C. Afterwards the samples were centrifuged at maximum speed for 20 minutes and the pellets washed with 70 % cold ethanol. After spinning at maximum speed for 5 minutes, the pellets were air-dried and resuspended in 50 µl ddH$_2$0.

7.1.9 Quantification

Concentrations of nucleic acids were determined by using the NanoQuant infinite 200 (Tecan) or Nanodrop 2000c (Thermo Scientific) devices. In principle, absorption of nucleic acids at 260 nm was measured and correlated to the respective concentration by using the Lambert-Beer law. Ratio of absorbance at 260 nm and 280 nm determined the purity of nucleic acid solutions.

7.1.10 ^{32}P-labeling of nucleic acids

For radioactive filter retention assay or binding assay, single-stranded DNA or dephosphorylated 2'F-RNA (**Table 7-8**) was labeled with ^{32}P at the 5'-end by using the T4 polynucleotide kinase (PNK). The following reaction mixture (**Table 7-9**) was incubated for 1 hour at 37 °C and subsequently desalted by passing through a G25 column.

Table 7-8 Pipetting scheme of one dephosphorylation reaction

Reagent	Stock concentration	Volume [µl]	Final concentration
CIAP reaction buffer	10 x	5	1 x
BSA	10 mg/ml	5	1 mg/ml
2'F-RNA			1.5 µM
RNasin	40 U/µl	0.5	20 U
CIAP	20 U/µl	0.85	17 U
ddH$_2$0		ad 50 µl	
Incubate for 15 minutes at 37 °C			
CIAP	20 U/µl	0.425	8.5 U
Incubate for 15 minutes at 55 °C			
EDTA	0.5 M	0.5 µl	5 mM
Incubate for 10 minutes at 75 °C			
ddH$_2$0		ad 100 µl	

Table 7-9 Pipetting scheme for one ^{32}P-labeling reaction

Reagent	Stock concentration	Volume [µl]	Final concentration
T4 PNK reaction buffer	10 x	2	1 x
ɣ-^{32}P-ATP	10 µCi/µl	1	10 µCi
DNA or 2'F-RNA	1 µM	10	10 pmol
T4 PNK	10 U/µl	2	20 U
ddH$_2$0		5	

Labeling efficiency was monitored by polyacrylamide gel electrophoresis.

7.1.11   Cloning and sequencing

Cloning reaction was done in accordance with the manufacturer's protocol (TOPO-TA cloning kit, Invitrogen). In brief, freshly prepared PCR product was ligated into pCR2.1-TOPO vectors and cloned into OneShot Mach1-T1 chemical competent *E. coli*. Bacteria were plated on 10 cm agarose plates supplemented with 100 µg/ml ampicillin. After overnight incubation at 37 °C, single bacteria colonies were picked and cultivated in 5 ml LB-medium supplemented with 100 µg/ml ampicillin overnight under vigorous shaking (150 rpm).

Plasmids were prepared by using the commercially available Nucleospin plasmid kit from Machery and Nagel. In brief, 5 ml overnight culture solution was centrifuged and the plasmids isolated from the pellet by alkaline lysis reaction. Finally, the plasmids were purified by using a silica column.

For sequencing, 30 ng of single sequences in a final volume of 20 µl was sent to GATC biotech AG (Köln). The appropriate M13-RP primer for sequencing was provided by GATC.

7.1.12 Next-generation sequencing (NGS)

PCR amplified DNA libraries obtained by SELEX were used for preparation of NGS samples. In four steps DNA is generated which contains index and adaptor sequences. Differently indexed DNA can be sequenced in one run and be assigned in later data analysis. Added adaptors enable the immobilization and processing of the sample by the Sequencing instrument.

Table 7-10 NGS Indices

Index	Sequence 5'-3'
1	ATCACG
2	CGATGT
3	TTAGGC
4	TGACCA
5	ACAGTG
6	GCCAAT
7	CAGATC
8	ACTTGA
9	GATCAG
10	TAGCTT
11	GGCTAC
12	CTTGTA

First, NGS indices were introduced by utilizing index-containing D3 primers (**Table 6-5**). The following pipetting scheme was used for one PCR reaction (**Table 7-11**; PCR program see **Table 7-3**).

Table 7-11 Pipetting scheme for one PCR reaction for NGS preparation

Reagent	Stock concentration	Volume [µl]	Final concentration
Pwo reaction buffer	10 x	10	1 x
dNTPs	25 mM each	0.8	0.2 mM
fwd primer D3 F	100 µM	1	1 µM
rev primer D3 R	100 µM	1	1 µM
Pwo polymerase	2.5 U/µl	1 µl	2.5 U
DNA template			1-10 nM
ddH$_2$0		ad 100 µl	

Second, the PCR products were mixed and phosphorylated at the 5'-end using the T4 polynucleotide kinase (PNK). The following mixture (**Table 7-12**) was incubated for 1 hour at 37 °C and vigorous shaking at 650 rpm.

Table 7-12 Pipetting scheme for 5'-phosphorylating of NGS samples

Reagent	Stock concentration	Volume [µl]	Final concentration
T4 PNK reaction buffer	10 x	6	1 x
ATP	100 mM	0.6	1 mM
Mixed DNA			1-1.2 µg
T4 PNK	10 U/µl	0.5	5 U
ddH$_2$0		ad 60 µl	

The samples were purified with the commercially available NucleoSpin clean-up kit from Machery and Nagel and concentrated in SpeedVac (Thermo Scientific).

Third, adapters were ligated by using the TruSeq DNA PCR-Free LT kit, commercially available from Illumina. The following steps according to the manufacture's protocol were applied: End Repair, Adenylation and (enzymatic) Adaptor Ligation. Here, adaptor no. 12 was used.

Fourth, the desired DNA which contained indices and adapters on both ends, was isolated by using preparative agarose gel electrophoresis and the commercially available NucleoSpin clean-up kit from Machery and Nagel. Briefly, the samples were diluted in DNA loading buffer, loaded on 2-2.5 % agarose gels and run for 1 hour at 100 V. The desired band was cut and purified by a silica column.

The quantification of the samples and the final NGS run on the Illumina HiSeq 1500 instrument was performed by members of Prof. Schultze's group, LIMES institute Bonn. NGS data was analyzed by AptaIT GmbH (München).

7.2 Working with proteins and peptides

7.2.1 General handling and storage

All proteins and peptides were dissolved in DPBS (Gibco) or PBS and kept on ice or at 4 °C in use. Proteins were stored at -20 °C for long-term storage.

OT-I and OT-II peptides were dissolved in degased DPBS at a final concentration of 1 mM and analyzed on Tricine-SDS gels.

Proteins and peptides were quantified by UV spectrometry at 280 and 205 nm using NanoDrop 2000c, Thermo Scientific.

7.2.2 SDS polyacrylamide gel electrophoresis (SDS PAGE)

Classical Glycine-SDS PAGE was used to analyze the coupling efficiency of Fc-CTL and Fc-FN to Protein G magnetic beads. 1-5 µg of proteins were eluted from the beads by adding 0.1 M glycine pH 2.5 for 2 minutes. Protein solution was neutralized with 1.5 M Tris pH 8.8 and diluted in Laemmli buffer. The samples were heated at 95 °C for 5 minutes and loaded on 12.5 % Glycine-SDS-gel (**Table 7-13**). After running the gel for 45 minutes at 175 V, 300 mA and 25 W in SDS running buffer, the proteins were stained with Coomassie staining solution for 10 seconds at maximum power in the microwave. The gel was destained with Coomassie destaining solution for 30 seconds at maximum power in the microwave. This step was repeated until the protein bands became clearly visible. The gel was visualized by UV transilluminator (VWR). The bands were compared with the standard protein ladder.

Table 7-13 Pipetting scheme for one 12.5 % Glycine-SDS gel

Reagent	Stock concentration	Volume [µl]	Final concentration
12.5 % Glycine-SDS gel			
Tris pH 8.8	1.5 M	1500	375 mM
ddH$_2$0		1940	
Bis-Acrylamide	30 %	2500	12.5 %
SDS	10 %	60	0.1 %
TEMED		6	
APS	10 %	60	0.1 %
4 % stacking gel			
Tris pH 6.8	1 M	500	250 mM
ddH$_2$0		1220	
Bis-Acrylamide	30 %	270	4 %
SDS	10 %	10	0.05 %
TEMED		2.5	
APS	10 %	10	0.05 %

The purity of the purchased OT-I and OT-II peptides as well as the coupling to the aptamers were analyzed by Tricine-SDS PAGE[193]. 1-5 µg of peptides were diluted in nonreducing sample buffer and heated for 5 minutes at 95 °C. The samples were loaded on 16 % Tricine-SDS gel (**Table 7-14**) and run for 1 hour 45 minutes at 175 V, 300 mA and 25 W in Tricine SDS Anode and Cathode buffer. Here, in the vertical electrophoresis apparatus (Biorad) the anode buffer was the lower electrode buffer and the cathode buffer was the upper one. The gel was stained with Coomassie blue as described before. DNA was visualized by staining the gel with 1:10000 ethidiumbromide in TBE buffer for 10 minutes.

Table 7-14 Pipetting scheme for one 16 % Tricine-SDS gel

Reagent	Stock concentration	Volume [µl]	Final concentration
16 % Tricine-SDS gel			
Tricine SDS gel buffer	3 x	2000	1
ddH$_2$0		200	
Bis-Acrylamide	30 %	3200	16 %
Glycerole	100 %	600	10 %
TEMED		6	
APS	10 %	60	0.1 %
10 % spacer gel			
Tricine SDS gel buffer	3 x	800	1 x
ddH$_2$0		800	
Bis-Acrylamide	30 %	800	10 %
TEMED		2.4	
APS	10 %	24	0.1 %
4 % stacking gel			
Tricine SDS gel buffer	3 x	800	1 x
ddH$_2$0		1280	
Bis-Acrylamide	30 %	320	4 %
TEMED		2.4	
APS	10 %	24	0.1 %

7.2.3 Production of fusionproteins Fc-CTL and Fc-FN

Fusionproteins Fc-CTL and Fc-FN, and IgG$_1$ Fc protein were kindly provided by Prof. Sven Burgdorf, LIMES institute Bonn. Protein production and functionality testing was conducted by the members of Prof. Burgdorf's group.

Basically, HEK293T cells were transfected with the previously described[130,131] plasmids pIgplus-CTLD4-7 or pIgplus-CR-FNII-CTLD1-3, or pFuse-hIgG1-Fc2 purchased from Invitrogen. After 5 days of cultivation the supernatant was collected and Fc-CTL, Fc-FN or IgG$_1$ Fc proteins were purified by immobilization on a protein G column. The proteins were stored in PBS at 4 or -20 °C for long-term storage.

Functionality of the proteins was analyzed as previously described[131]. In brief, ovalbumin and collagen R were coated onto wells of 96-well plates and incubated with either Fc-CTL or Fc-FN. Binding was assessed by adding anti-hIgG$_1$ antibody

horseradish conjugate and peroxidase substrate. Absorbance was measured at 450 and 620 nm.

7.3 Handling of mice and cells

7.3.1 Mice

C57BL/6J, MR^{-/-}, OTI RAG2^{-/-} and OTII mice were bred in the central animal facility of the LIMES institute under specific pathogen-free conditions. Mice between 8-16 weeks were used in accordance with local animal experimental guidelines.

7.3.2 Cell culture

Cells were cultured under standard conditions (37 °C, 5 % CO_2, 95 % humidity). Cells were handled under sterile conditions according to S1 lab regulations. BM-DCs were centrifuged for 5 min at 200 x g, splenocytes for 10 min at 300 x g.

7.3.3 Isolation and cultivation of bone marrow-derived dendritic cells (BM-DC) and macrophages (BM-macrophages)

Wildtype or MR^{-/-} mice were sacrificed and the femur and tibia extracted. The bone marrow was flushed out with PBS and filtered through a 40 µm nylon membrane. The cells of the bone marrow were cultivated in DC-medium or macrophage-medium for 7 days. After 3-4 days the medium was changed.

7.3.4 Isolation and cultivation of splenocytes

The mouse (C57/BL6J, OTI RAG2^{-/-} or OTII) was sacrificed and the spleen extracted. The spleen was mashed with a syringe plunger into cold PBS and filtered through a 40 µm nylon membrane. The cells were centrifuged and resuspended in T-cell medium.

7.3.5 Human peripheral blood mononuclear cells (PBMCs)

Human PBMCs were kindly provided by Prof. Joachim Schultze, LIMES institute Bonn. Cells were isolated and cultured as previously described[184,194] by the members of Prof. Schultze's group. In brief, human blood PBMCs were obtained from healthy donor at the Institute for Experimental Hematology and Transfusion Medicine of the University Hospitals Bonn (local ethics votes no. 288/13). CD14^{+} blood monocytes were either differentiated with GM-CSF alone or GM-CSF supplemented with IL-4, IFN-ɣ or TPP

stimuli (TNF-α/PGE$_2$/P3C) to generate baseline macrophages, M1 or M2 macrophages, DCs or TPP macrophages (see **Figure S 9.8.1**).

7.4 SELEX

7.4.1 Coupling of Fc-fusionproteins to Protein G magnetic beads

Fc-CTL and Fc-FN were coupled to magnetic beads Protein G conjugates. 10 mg beads were washed thrice with 50 mM NaOAc pH 5. 200 µg proteins were added for 30 minutes and vigorous shaking at 400 rpm. The mixture was thereby resuspended every 5 minutes. The samples were finally washed thrice with PBS and stored in 2 ml PBS supplemented with 0.01 mg/ml BSA at 4 °C until use.
Coupling efficiency was analyzed by SDS polyacrylamide gel electrophoresis.

7.4.2 Protein SELEX

The SELEX procedure was started by incubation of 1 nmol D3 DNA library with 400 µg Fc-CTL- or Fc-FN-beads in a total volume of 100 µl selection buffer for 30 min at 37 °C. The beads were resuspended every 5 minutes. After washing with wash buffer the bound DNA was eluted in 65 µl ddH$_2$O 3 min at 80 °C and amplified. After lambda exonuclease digestion the DNA was purified by silica column and eluted in a total volume of 30 µl ddH$_2$O. 18 µl eluate was introduced in the subsequent rounds of SELEX. From the second round counter selection was carried out, i.e. enriched DNA was pre-incubated with 400 µg of the other Fc-fusionprotein-beads. To gradually enhance the stringency of the selection process, the two washing cycles from round 1 were increased by two per selection round, ending with 24 at round 11.

7.4.3 Cell-SELEX

Before every selection experiment the cultivated BM-DCs were detached by using PBS, containing 2 mM EDTA, and seeded in 6 cm petri dishes. After reattachment the cells were washed twice with wash buffer. The naïve D3 DNA or A50 2'F-RNA library and enriched libraries were denaturated by heating 5 min at 95 °C and immediately added to the selection buffer. The naïve D3 DNA library was supplemented with the mixture of enriched libraries of the 3rd round of protein-SELEX targeting Fc-CTL and Fc-FN. The SELEX procedure was started by incubation of 1 nmol naïve library with 5 x 10^6 BM-DCs in a total volume of 2 ml selection buffer for 30 min at 37 °C. The cells were rotated gently every 5 minutes. After washing the cells with wash buffer, they were scraped and the bound oligonucleotides eluted in ddH$_2$O 5 min at 95 °C. The

nucleic acids were isolated by phenol/chloroform extraction and ethanol precipitation and amplified. The DNA was digested by lambda exonuclease and purified by silica column. The 2'F-RNA was transcribed by using 2'F-pyrimidines and purified by phenol/chloroform extraction and ethanol precipitation. To gradually increase the selection pressure, the amount of cells were decreased, starting from 1×10^6 (round 4-5) to 7.5×10^5 (round 6-10). Additionally, the concentration of oligonucleotides and the incubation time were reduced from 500 pmol (round 2) to 250 pmol (round 3-10) and 20 min (round 7) to 10 min (round 9-10), respectively.

7.5 Characterization assays

7.5.1 Flow cytometry binding assay

4×10^5 BM-DCs were seeded in 24-well plates and cultivated under standard conditions for at least one hour. The cells were washed once with wash buffer (DPBS, 1 mM MgCl$_2$) and subsequently incubated for 10 minutes at 37 °C with ATTO 647N-labeled aptamers diluted in 200 μl DC-medium in total. The cells were scraped and transferred into FACS tubes containing 2 ml wash buffer. The samples were centrifuged for 5 minutes at 200 x g and the supernatant discarded. The cell pellets were washed again with 1 ml wash buffer. Mean fluorescence intensities (MFI) were acquired by BD FACS Canto II or LSR II and analyzed by FlowJo software (BD).
Binding analysis of BM-macrophages was done as mentioned above.

The binding specificity of the aptamers was determined as follows. 2×10^5 BM-DCs were seeded in 24-well plates and incubated with 500 nM ATTO 647N-labeled aptamers for 30 minutes at 37 °C. Splenocytes were isolated from wildtype mice and 2×10^5 cells were transferred into FACS tubes for incubation with 500 nM ATTO 647N-labeled aptamers. BM-DCs were washed as mentioned above. Splenocytes were washed once with 1 ml wash buffer and subsequently stained with 1:200 antibodies-mixes (anti-CD8α/CD4/B220 (CD45RA)) in FACS buffer for 20 minutes at 4 °C. In parallel, BM-DCs were kept at 4 °C. Finally, splenocytes were washed with 1 ml FACS buffer.

The competition of aptamers by aptamer-peptide conjugates was determined as follows. 2×10^5 BM-DCs were transferred into FACS tubes and incubated with 250 nM ATTO 647N-labeled aptamers in absence or presence of 500 nM competitors for 10 minutes at 37 °C. BM-DCs were washed as mentioned above.

7.5.2 Radioactive binding assay

7.5.2.1 Filter retention assay

The interaction of DNA with proteins was monitored by radioactive filter retention assay. ^{32}P-DNA was incubated with increasing concentrations of proteins in 25 µl protein-SELEX selection buffer for 30 minutes at 37 °C. In the meantime, the nitrocellulose membrane was soaked in 0.4 M KOH for 15-20 minutes and subsequently rinsed with PBS. The dot blot unit and the vacuum manifold were assembled. The membrane was equilibrated with 200 µl wash buffer (PBS, 1 mM MgCl$_2$, 1 mM CaCl$_2$) and 20 µl sample was loaded. Afterwards, the membrane was washed 4 times with 200 µl wash buffer. 0.8 µl ^{32}P-DNA was spotted on a dry membrane to allow the quantification of the percentage of DNA bound to the proteins. Radioactivity was acquired on the Phosphorimager FLA-3000 (Fujifilm) and quantified by using AIDA image software (raytest).

7.5.2.2 Cell binding assay using Cherenkov protocol

0.5×10^5 BM-DCs were seeded in 24-well plates and cultivated under standard conditions for at least one hour. The cells were washed once with wash buffer (DPBS, 1 mM MgCl$_2$) and subsequently incubated for 10 minutes at 37 °C with 1 pmol ^{32}P-DNA or ^{32}P-2'F-RNA diluted in 500 µl cell-SELEX selection buffer in total. The incubation buffer was collected in 1.5 ml reaction tubes as fraction I. The cells were washed twice with 500 µl wash buffer and both fractions were collected (fraction II and III). The cells were detached by adding 500 µl Trypsin/EDTA for several minutes at 37 °C and collected as fraction IV. Radioactivity was measured on the Liquid scintillation counter WinSpectral (Perkin Elmer) using the Cherenkov protocol. The percentage of bound ^{32}P-DNA or ^{32}P-2'F-RNA was calculated with the following formula:

$$\% \ bound \ DNA = \left[\frac{fraction \ IV}{fraction \ I + fraction \ II + fraction \ III + fraction \ IV} \right] * 100$$

7.5.3 Confocal microscopy

2×10^5 BM-DCs were seeded onto cover slips in 12-well plates and cultivated under standard conditions for at least one hour. The cells were washed once with wash buffer (DPBS, 1 mM MgCl$_2$) and subsequently incubated for 30 minutes at 37 °C with 250 nM ATTO 647N-labeled CTL#5 or for 10 minutes at 37 °C with 250 nM ATTO 647N-labeled D#5 or D#7 diluted in 300 µl DC-medium in total. The cells were washed thrice with wash buffer and once with 1 ml DPBS. After fixation in 4 % paraformaldehyde

diluted in DPBS for 20 minutes, cells were washed thrice with DPBS and permeabilized in 0.1 % Triton X-100 in DPBS for 5 minutes. The cells were washed thrice with DPBS and blocked in 10 % milk in DPBS for 1 hour. Primary antibodies were diluted in DPBS at a dilution of 1:100. The cells were stained for 45 minutes and subsequently washed thrice with DPBS. Secondary antibodies were diluted 1:400 in DPBS. The cells were stained for 45 minutes and subsequently washed thrice with DPBS. The nuclei were stained with 1:1000 1 mg/ml DAPI in DPBS for 5 minutes and washed once with DPBS and twice with 2 ml ddH$_2$O. Finally, cover slips were mounted onto slides with Fluorogel or Prolong Diamond mouting medium.

The co-localization studies of CTL#5 was done in comparison with OVA. Here, the cells were stained for 30 minutes at 37 °C with 250 ng/ml OVA-Alexa Fluor 647.

In internalization studies the membranes were stained after fixation with WGA-Alexa Fluor 488 (1.5 µl 1 mg/ml WGA-AF488 in 500 µl DPBS) for 10 minutes.

Confocal microscopy data for CTL#5 were acquired by FluoView FV1000 confocal laser scanning microscope (Olympus), and for D#5 and D#7 by LSM 710 confocal laser scanning microscope (Zeiss). Co-localization was quantified by Olympus FluoView or Zeiss Zen software.

7.5.4 TNF-α HTRF assay

In accordance with the manufacturer guidelines (Cisbio) TNF-α homogeneous time-resolved fluorescence (HTRF) assay was performed by James Stunden, member of Prof. Latz group, University Hospitals Bonn. In brief, immortalized murine embryonic stem cell-derived macrophages were treated with increasing concentrations of oligonucleotides for 24 hours. Subsequently, cell supernatants were stained with two different anti-TNF-α antibodies attached to either fluorescence energy transfer (FRET) donor or acceptor molecules. In close proximity of these molecules the fluorescence emission spectrum changes and this change is proportional to the TNF-α concentration in the sample.

7.6 Generation of aptamer-peptide conjugates

7.6.1 Thiol-maleimide coupling

5'-thiol-C6 oligonucleotides were purchased from Ella Biotech, dissolved in degased ddH$_2$O at a final concentration of 100 µM and stored at -20 °C. The oligonucleotides

were reduced with a 2000-fold molar excess of freshly prepared DTT in 1 M TEAA pH 8.3-8.5, heated up for 3 min at 70 °C following 1 h incubation at room temperature. The reduced oligonucleotides were desalted using an Amicon 10 K column into degased ddH$_2$O and subsequently incubated with a 55-fold molar excess of N-maleimide-peptides. The reaction mixture was incubated overnight at 4 °C and purified by reverse-phase HPLC on a C18 column using a linear gradient of 100 mM HFIP and 10 mM TEA. The collected fractions were analyzed by LC-MS and the concentration quantified with UV spectrometry.

7.7 Functional assays

7.7.1 *In vitro* proliferation assay

5 x 10^4 BM-DCs were seeded in 96-well plates and cultivated under standard conditions for at least one hour. OTI or OTII T cells (OVA-specific CD8 or CD4 T cells) were isolated from spleen and stained with 1 µM CFSE in PBS for 15 min at 37 °C. The T cells were washed three times with 4 °C cold PBS and centrifuged. Meanwhile, MHC I or MHC II peptides, aptamers, aptamer-peptide conjugates and OT-I or OT-II peptides were diluted in DC-medium and added to the BM-DCs for 10 min at 37 °C. Subsequently, the supernatants from BM-DCs were removed and 1 x 10^5 OTI or OTII T cells in 100 µl T cell medium were added. After 24 hours, 200 µl T cell medium was given per well and the cells were incubated for another 48 hours. Finally, the T cells were stained with anti-CD4 or anti-CD8alpha antibodies-fluorophore conjugates and analyzed by flow cytometry. The antibodies were diluted 1:400 in FACS buffer supplemented with mouse serum at a 1:100 dilution.

7.7.2 *In vitro* cytotoxicity assay

2 x 10^5 BM-DCs were seeded in 24-well plates and cultivated under standard conditions for at least one hour. OTI or OTII T cells (OVA-specific CD8 or CD4 T cells) were isolated from spleen and centrifuged at 300 x g for 10 min. Meanwhile, MHC I or MHC II peptides, aptamers, aptamer-peptide conjugates and OT-I or OT-II peptides were diluted in DC-medium and added to the BM-DCs for 10 min at 37 °C. Subsequently, the supernatants from BM-DCs were removed and 4 x 10^5 OTI or OTII T cells in 400 µl T cell medium were added. After 24 hours, 2 ml T cell medium was given per well and the cells were incubated for another 48 hours. On day 4, T cells were isolated using Ficoll density gradient centrifugation. Splenocytes derived from wildtype mice were stained with different concentrations of CFSE and used as target or control

cells. Target cells stained with 0.1 µM CFSE and loaded with 2 µM MHC I or MHC II peptides, and control cells stained with 1 µM CFSE were mixed equally and added in different T cells:mixed cells ratios. After 24 hours, cells were labeled with Hoechst 33258 and analyzed by flow cytometry. The cytotoxic activity was calculated with the following formula:

$$\% \, cytotoxicity = 100 - [100 * (p \, target)/(p \, control)/(n \, target)/(n \, control)],$$

where p and n indicates if target and control cells were incubated for 24 hours without T cells (no (n) T cells) or with primed (p) T cells.

7.8 Experimental analysis

7.8.1 Statistics

If not otherwise noted, data for statistical quantification were acquired from individual experiments repeated at least two times. Samples of individual experiments were prepared at least in duplicates. Mean and standard deviation values were calculated with Microsoft Office Excel 2007.

8   References

1   Hoption Cann, S. A., van Netten, J. P. & van Netten, C. Dr William Coley and tumour regression: a place in history or in the future. *Postgrad Med J* 79, 672-680 (2003).

2   Murphy, K., Travers, P., Walport, M. *Janeway's Immunobiology*. 7th edn, 928 (Garland Science, 2007).

3   Kawai, T. & Akira, S. The role of pattern-recognition receptors in innate immunity: update on Toll-like receptors. *Nat Immunol* 11, 373-384, doi:10.1038/ni.1863 (2010).

4   Janeway, C. A., Jr. & Medzhitov, R. Innate immune recognition. *Annu Rev Immunol* 20, 197-216, doi:10.1146/annurev.immunol.20.083001.084359 (2002).

5   Behrens, G. *et al.* Helper T cells, dendritic cells and CTL Immunity. *Immunol Cell Biol* 82, 84-90, doi:10.1111/j.1440-1711.2004.01211.x (2004).

6   Chambers, C. A. & Allison, J. P. Costimulatory regulation of T cell function. *Curr Opin Cell Biol* 11, 203-210 (1999).

7   Cheuk, A. T., Mufti, G. J. & Guinn, B. A. Role of 4-1BB:4-1BB ligand in cancer immunotherapy. *Cancer Gene Ther* 11, 215-226, doi:10.1038/sj.cgt.7700670 (2004).

8   Curtsinger, J. M. & Mescher, M. F. Inflammatory cytokines as a third signal for T cell activation. *Curr Opin Immunol* 22, 333-340, doi:10.1016/j.coi.2010.02.013 (2010).

9   Curtsinger, J. M., Johnson, C. M. & Mescher, M. F. CD8 T cell clonal expansion and development of effector function require prolonged exposure to antigen, costimulation, and signal 3 cytokine. *J Immunol* 171, 5165-5171 (2003).

10   Xing, Y. & Hogquist, K. A. T-cell tolerance: central and peripheral. *Cold Spring Harb Perspect Biol* 4, doi:10.1101/cshperspect.a006957 (2012).

11   Green, D. R., Droin, N. & Pinkoski, M. Activation-induced cell death in T cells. *Immunol Rev* 193, 70-81 (2003).

12   Lanzavecchia, A. & Sallusto, F. Understanding the generation and function of memory T cell subsets. *Curr Opin Immunol* 17, 326-332, doi:10.1016/j.coi.2005.04.010 (2005).

13   Banchereau, J. & Steinman, R. M. Dendritic cells and the control of immunity. *Nature* 392, 245-252, doi:10.1038/32588 (1998).

14   Delamarre, L., Pack, M., Chang, H., Mellman, I. & Trombetta, E. S. Differential lysosomal proteolysis in antigen-presenting cells determines antigen fate. *Science* 307, 1630-1634, doi:10.1126/science.1108003 (2005).

15   Liu, K. & Nussenzweig, M. C. Origin and development of dendritic cells. *Immunol Rev* 234, 45-54, doi:10.1111/j.0105-2896.2009.00879.x (2010).

16   Mellman, I. & Steinman, R. M. Dendritic cells: specialized and regulated antigen processing machines. *Cell* 106, 255-258 (2001).

17   Kaisho, T. & Akira, S. Toll-like receptors and their signaling mechanism in innate immunity. *Acta Odontol Scand* 59, 124-130 (2001).

18   Steinman, R. M., Hawiger, D. & Nussenzweig, M. C. Tolerogenic dendritic cells. *Annu Rev Immunol* 21, 685-711, doi:10.1146/annurev.immunol.21.120601.141040 (2003).

19   Burgdorf, S., Kautz, A., Bohnert, V., Knolle, P. A. & Kurts, C. Distinct pathways of antigen uptake and intracellular routing in CD4 and CD8 T cell activation. *Science* 316, 612-616, doi:10.1126/science.1137971 (2007).

20   Platt, C. D. *et al.* Mature dendritic cells use endocytic receptors to capture and present antigens. *Proc Natl Acad Sci U S A* 107, 4287-4292, doi:10.1073/pnas.0910609107 (2010).

21   Sommer, S. The importance of immune gene variability (MHC) in evolutionary ecology and conservation. *Front Zool* 2, 16, doi:10.1186/1742-9994-2-16 (2005).

22   Bouvier, M. Accessory proteins and the assembly of human class I MHC molecules: a molecular and structural perspective. *Mol Immunol* 39, 697-706 (2003).

23   Fremont, D. H., Hendrickson, W. A., Marrack, P. & Kappler, J. Structures of an MHC class II molecule with covalently bound single peptides. *Science* 272, 1001-1004 (1996).

24   Schuette, V. & Burgdorf, S. The ins-and-outs of endosomal antigens for cross-presentation. *Curr Opin Immunol* 26, 63-68, doi:10.1016/j.coi.2013.11.001 (2014).

25   Blanchard, N. *et al.* Endoplasmic reticulum aminopeptidase associated with antigen processing defines the composition and structure of MHC class I peptide repertoire in normal and virus-infected cells. *J Immunol* 184, 3033-3042, doi:10.4049/jimmunol.0903712 (2010).

26   Lakadamyali, M., Rust, M. J. & Zhuang, X. Ligands for clathrin-mediated endocytosis are differentially sorted into distinct populations of early endosomes. *Cell* 124, 997-1009, doi:10.1016/j.cell.2005.12.038 (2006).

27   Roche, P. A. & Furuta, K. The ins and outs of MHC class II-mediated antigen processing and presentation. *Nat Rev Immunol* 15, 203-216, doi:10.1038/nri3818 (2015).

28   O'Brien, C., Flower, D. R. & Feighery, C. Peptide length significantly influences in vitro affinity for MHC class II molecules. *Immunome Res* 4, 6, doi:10.1186/1745-7580-4-6 (2008).

29   Klein, L., Munz, C. & Lunemann, J. D. Autophagy-mediated antigen processing in CD4(+) T cell tolerance and immunity. *FEBS Lett* 584, 1405-1410, doi:10.1016/j.febslet.2010.01.008 (2010).

30   Lim, J. P. & Gleeson, P. A. Macropinocytosis: an endocytic pathway for internalising large gulps. *Immunol Cell Biol* 89, 836-843, doi:10.1038/icb.2011.20 (2011).

31   Figdor, C. G., van Kooyk, Y. & Adema, G. J. C-type lectin receptors on dendritic cells and Langerhans cells. *Nat Rev Immunol* 2, 77-84, doi:10.1038/nri723 (2002).

32   van Vliet, S. J., Garcia-Vallejo, J. J. & van Kooyk, Y. Dendritic cells and C-type lectin receptors: coupling innate to adaptive immune responses. *Immunol Cell Biol* 86, 580-587, doi:10.1038/icb.2008.55 (2008).

33   Osorio, F. & Reis e Sousa, C. Myeloid C-type lectin receptors in pathogen recognition and host defense. *Immunity* 34, 651-664, doi:10.1016/j.immuni.2011.05.001 (2011).

34   East, L. & Isacke, C. M. The mannose receptor family. *Biochim Biophys Acta* 1572, 364-386 (2002).

35   McGreal, E. P., Martinez-Pomares, L. & Gordon, S. Divergent roles for C-type lectins expressed by cells of the innate immune system. *Mol Immunol* 41, 1109-1121, doi:10.1016/j.molimm.2004.06.013 (2004).

36   Frenz, T. *et al.* Antigen presenting cell-selective drug delivery by glycan-decorated nanocarriers. *Eur J Pharm Biopharm* 95, 13-17, doi:10.1016/j.ejpb.2015.02.008 (2015).

37   Chatterjee, B. *et al.* Internalization and endosomal degradation of receptor-bound antigens regulate the efficiency of cross presentation by human dendritic cells. *Blood* 120, 2011-2020, doi:10.1182/blood-2012-01-402370 (2012).

38   Burgdorf, S., Lukacs-Kornek, V. & Kurts, C. The mannose receptor mediates uptake of soluble but not of cell-associated antigen for cross-presentation. *J Immunol* 176, 6770-6776 (2006).

39   Mahnke, K. *et al.* The dendritic cell receptor for endocytosis, DEC-205, can recycle and enhance antigen presentation via major histocompatibility complex class II-positive lysosomal compartments. *J Cell Biol* 151, 673-684 (2000).

40   Bol, K. F., Schreibelt, G., Gerritsen, W. R., de Vries, I. J. & Figdor, C. G. Dendritic Cell-Based Immunotherapy: State of the Art and Beyond. *Clin Cancer Res* 22, 1897-1906, doi:10.1158/1078-0432.CCR-15-1399 (2016).

41   Kreutz, M., Tacken, P. J. & Figdor, C. G. Targeting dendritic cells--why bother? *Blood* 121, 2836-2844, doi:10.1182/blood-2012-09-452078 (2013).

42   Banchereau, J., Schuler-Thurner, B., Palucka, A. K. & Schuler, G. Dendritic cells as vectors for therapy. *Cell* 106, 271-274 (2001).

43   Figdor, C. G., de Vries, I. J., Lesterhuis, W. J. & Melief, C. J. Dendritic cell immunotherapy: mapping the way. *Nat Med* 10, 475-480, doi:10.1038/nm1039 (2004).

44   Kastenmuller, W., Kastenmuller, K., Kurts, C. & Seder, R. A. Dendritic cell-targeted vaccines--hope or hype? *Nat Rev Immunol* 14, 705-711, doi:10.1038/nri3727 (2014).

45   Kantoff, P. W. *et al.* Sipuleucel-T immunotherapy for castration-resistant prostate cancer. *N Engl J Med* 363, 411-422, doi:10.1056/NEJMoa1001294 (2010).

46   Makarov, D. V., Loeb, S., Getzenberg, R. H. & Partin, A. W. Biomarkers for prostate cancer. *Annu Rev Med* 60, 139-151, doi:10.1146/annurev.med.60.042307.110714 (2009).

47   Anassi, E. & Ndefo, U. A. Sipuleucel-T (provenge) injection: the first immunotherapy agent (vaccine) for hormone-refractory prostate cancer. *P T* 36, 197-202 (2011).

48   Hammerstrom, A. E., Cauley, D. H., Atkinson, B. J. & Sharma, P. Cancer immunotherapy: sipuleucel-T and beyond. *Pharmacotherapy* 31, 813-828, doi:10.1592/phco.31.8.813 (2011).

49   Bui, C. N. *et al.* Budget Impact of Enzalutamide for Chemotherapy-Naive Metastatic Castration-Resistant Prostate Cancer. *J Manag Care Spec Pharm* 22, 163-170, doi:10.18553/jmcp.2016.22.2.163 (2016).

50   Commission, E. *Pharmaceuticals - Community register*, <http://ec.europa.eu/health/documents/community-register/html/h867.htm> (2015).

51   Raich-Regue, D. *et al.* Differential effects of monophosphoryl lipid A and cytokine cocktail as maturation stimuli of immunogenic and tolerogenic dendritic cells for immunotherapy. *Vaccine* 30, 378-387, doi:10.1016/j.vaccine.2011.10.081 (2012).

52   Gilboa, E. DC-based cancer vaccines. *J Clin Invest* 117, 1195-1203, doi:10.1172/JCI31205 (2007).

53   Morelli, A. E. & Thomson, A. W. Tolerogenic dendritic cells and the quest for transplant tolerance. *Nat Rev Immunol* 7, 610-621, doi:10.1038/nri2132 (2007).

54   Amos, S. M. *et al.* Autoimmunity associated with immunotherapy of cancer. *Blood* 118, 499-509, doi:10.1182/blood-2011-01-325266 (2011).

55   Ludewig, B. *et al.* Immunotherapy with dendritic cells directed against tumor antigens shared with normal host cells results in severe autoimmune disease. *J Exp Med* 191, 795-804 (2000).

56   Roskrow, M. A. *et al.* Autoimmune disease induced by dendritic cell immunization against leukemia. *Leuk Res* 23, 549-557 (1999).

57   Leleux, J., Atalis, A. & Roy, K. Engineering immunity: Modulating dendritic cell subsets and lymph node response to direct immune-polarization and vaccine efficacy. *J Control Release* 219, 610-621, doi:10.1016/j.jconrel.2015.09.063 (2015).

58   Morse, M. A. *et al.* CDX-1307: a novel vaccine under study as treatment for muscle-invasive bladder cancer. *Expert Rev Vaccines* 10, 733-742, doi:10.1586/erv.11.20 (2011).

59   Dangles, V. *et al.* Tumor-associated antigen human chorionic gonadotropin beta contains numerous antigenic determinants recognized by in vitro-induced CD8+ and CD4+ T lymphocytes. *Cancer Immunol Immunother* 50, 673-681, doi:10.1007/s00262-001-0248-0 (2002).

60   Morse, M. A. *et al.* Phase I study utilizing a novel antigen-presenting cell-targeted vaccine with Toll-like receptor stimulation to induce immunity to self-antigens in cancer patients. *Clin Cancer Res* 17, 4844-4853, doi:10.1158/1078-0432.CCR-11-0891 (2011).

61   Riedmann, E. M. CDX-1401 combined with TLR agonist: positive phase 1 results. *Hum Vaccin Immunother* 8, 1742 (2012).

62   Dhodapkar, M. V. *et al.* Induction of antigen-specific immunity with a vaccine targeting NY-ESO-1 to the dendritic cell receptor DEC-205. *Sci Transl Med* 6, 232ra251, doi:10.1126/scitranslmed.3008068 (2014).

63   Cheong, C. *et al.* Improved cellular and humoral immune responses in vivo following targeting of HIV Gag to dendritic cells within human anti-human DEC205 monoclonal antibody. *Blood* 116, 3828-3838, doi:10.1182/blood-2010-06-288068 (2010).

64   Idoyaga, J. *et al.* Comparable T helper 1 (Th1) and CD8 T-cell immunity by targeting HIV gag p24 to CD8 dendritic cells within antibodies to Langerin, DEC205, and Clec9A. *Proc Natl Acad Sci U S A* 108, 2384-2389, doi:10.1073/pnas.1019547108 (2011).

65   Flynn, B. J. *et al.* Immunization with HIV Gag targeted to dendritic cells followed by recombinant New York vaccinia virus induces robust T-cell immunity in nonhuman primates. *Proc Natl Acad Sci U S A* 108, 7131-7136, doi:10.1073/pnas.1103869108 (2011).

66   Dong, H. *et al.* Induction of protective immunity against Mycobacterium tuberculosis by delivery of ESX antigens into airway dendritic cells. *Mucosal Immunol* 6, 522-534, doi:10.1038/mi.2012.92 (2013).

67   Tacken, P. J. *et al.* No advantage of cell-penetrating peptides over receptor-specific antibodies in targeting antigen to human dendritic cells for cross-presentation. *J Immunol* 180, 7687-7696 (2008).

68   Ramakrishna, V. *et al.* Mannose receptor targeting of tumor antigen pmel17 to human dendritic cells directs anti-melanoma T cell responses via multiple HLA molecules. *J Immunol* 172, 2845-2852 (2004).

69   Ni, L. *et al.* Concomitant activation and antigen uptake via human dectin-1 results in potent antigen-specific CD8+ T cell responses. *J Immunol* 185, 3504-3513, doi:10.4049/jimmunol.1000999 (2010).

70   Saluja, S. S. *et al.* Targeting human dendritic cells via DEC-205 using PLGA nanoparticles leads to enhanced cross-presentation of a melanoma-associated antigen. *Int J Nanomedicine* 9, 5231-5246, doi:10.2147/IJN.S66639 (2014).

71   Rauen, J. *et al.* Enhanced cross-presentation and improved CD8+ T cell responses after mannosylation of synthetic long peptides in mice. *PLoS One* 9, e103755, doi:10.1371/journal.pone.0103755 (2014).

72   Rosalia, R. A. *et al.* Dendritic cells process synthetic long peptides better than whole protein, improving antigen presentation and T-cell activation. *Eur J Immunol* 43, 2554-2565, doi:10.1002/eji.201343324 (2013).

73   Hartung, E. *et al.* Induction of potent CD8 T cell cytotoxicity by specific targeting of antigen to cross-presenting dendritic cells in vivo via murine or human XCR1. *J Immunol* 194, 1069-1079, doi:10.4049/jimmunol.1401903 (2015).

74   Vingert, B. *et al.* The Shiga toxin B-subunit targets antigen in vivo to dendritic cells and elicits anti-tumor immunity. *Eur J Immunol* 36, 1124-1135, doi:10.1002/eji.200535443 (2006).

75   Thomann, J. S. *et al.* Antitumor activity of liposomal ErbB2/HER2 epitope peptide-based vaccine constructs incorporating TLR agonists and mannose receptor targeting. *Biomaterials* 32, 4574-4583, doi:10.1016/j.biomaterials.2011.03.015 (2011).

76   Gangadhar, T. C. & Vonderheide, R. H. Mitigating the toxic effects of anticancer immunotherapy. *Nat Rev Clin Oncol* 11, 91-99, doi:10.1038/nrclinonc.2013.245 (2014).

77   Gilboa, E., McNamara, J., 2nd & Pastor, F. Use of oligonucleotide aptamer ligands to modulate the function of immune receptors. *Clin Cancer Res* 19, 1054-1062, doi:10.1158/1078-0432.CCR-12-2067 (2013).

78   Nimjee, S. M., Rusconi, C. P. & Sullenger, B. A. Aptamers: an emerging class of therapeutics. *Annu Rev Med* 56, 555-583, doi:10.1146/annurev.med.56.062904.144915 (2005).

79   Lehmann, C. H. *et al.* Direct Delivery of Antigens to Dendritic Cells via Antibodies Specific for Endocytic Receptors as a Promising Strategy for Future Therapies. *Vaccines (Basel)* 4, doi:10.3390/vaccines4020008 (2016).

80   Mayer, G. The chemical biology of aptamers. *Angew Chem Int Ed Engl* 48, 2672-2689, doi:10.1002/anie.200804643 (2009).

81   Hermann, T. & Patel, D. J. Adaptive recognition by nucleic acid aptamers. *Science* 287, 820-825 (2000).

82   Stoltenburg, R., Reinemann, C. & Strehlitz, B. SELEX--a (r)evolutionary method to generate high-affinity nucleic acid ligands. *Biomol Eng* 24, 381-403, doi:10.1016/j.bioeng.2007.06.001 (2007).

83   Tuerk, C. & Gold, L. Systematic evolution of ligands by exponential enrichment: RNA ligands to bacteriophage T4 DNA polymerase. *Science* 249, 505-510 (1990).

84   Ellington, A. D. & Szostak, J. W. In vitro selection of RNA molecules that bind specific ligands. *Nature* 346, 818-822, doi:10.1038/346818a0 (1990).

85   Hamedani, N. S. *et al.* Capture and Release (CaR): a simplified procedure for one-tube isolation and concentration of single-stranded DNA during SELEX. *Chem Commun (Camb)* 51, 1135-1138, doi:10.1039/c4cc08233h (2015).

86   Rhie, A. *et al.* Characterization of 2'-fluoro-RNA aptamers that bind preferentially to disease-associated conformations of prion protein and inhibit conversion. *J Biol Chem* 278, 39697-39705, doi:10.1074/jbc.M305297200 (2003).

87   Hamedani, N. S. & Muller, J. Capillary Electrophoresis for the Selection of DNA Aptamers Recognizing Activated Protein C. *Methods Mol Biol* 1380, 61-75, doi:10.1007/978-1-4939-3197-2_5 (2016).

88   Raddatz, M. S. *et al.* Enrichment of cell-targeting and population-specific aptamers by fluorescence-activated cell sorting. *Angew Chem Int Ed Engl* 47, 5190-5193, doi:10.1002/anie.200800216 (2008).

89   Stoltenburg, R., Reinemann, C. & Strehlitz, B. FluMag-SELEX as an advantageous method for DNA aptamer selection. *Anal Bioanal Chem* 383, 83-91, doi:10.1007/s00216-005-3388-9 (2005).

90   Bridonneau, P., Chang, Y. F., Buvoli, A. V., O'Connell, D. & Parma, D. Site-directed selection of oligonucleotide antagonists by competitive elution. *Antisense Nucleic Acid Drug Dev* 9, 1-11 (1999).

91   Mayer, G. *et al.* Controlling small guanine-nucleotide-exchange factor function through cytoplasmic RNA intramers. *Proc Natl Acad Sci U S A* 98, 4961-4965, doi:10.1073/pnas.091100698 (2001).

92   Avci-Adali, M., Paul, A., Wilhelm, N., Ziemer, G. & Wendel, H. P. Upgrading SELEX technology by using lambda exonuclease digestion for single-stranded DNA generation. *Molecules* 15, 1-11, doi:10.3390/molecules15010001 (2010).

93   Schutze, T. *et al.* Probing the SELEX process with next-generation sequencing. *PLoS One* 6, e29604, doi:10.1371/journal.pone.0029604 (2011).

94   Muller, J. *et al.* An exosite-specific ssDNA aptamer inhibits the anticoagulant functions of activated protein C and enhances inhibition by protein C inhibitor. *Chem Biol* 16, 442-451, doi:10.1016/j.chembiol.2009.03.007 (2009).

95   Huizenga, D. E. & Szostak, J. W. A DNA aptamer that binds adenosine and ATP. *Biochemistry* 34, 656-665 (1995).

96   Mayer, G., Pofahl, M., Schöler, K. M. U., Haßel, S. *Cell-Specific Aptamers for Nano-medical Applications*. Vol. 29 261-283 (Springer Berlin Heidelberg, 2013).

97   Mann, D., Reinemann, C., Stoltenburg, R. & Strehlitz, B. In vitro selection of DNA aptamers binding ethanolamine. *Biochem Biophys Res Commun* 338, 1928-1934, doi:10.1016/j.bbrc.2005.10.172 (2005).

98   Bock, L. C., Griffin, L. C., Latham, J. A., Vermaas, E. H. & Toole, J. J. Selection of single-stranded DNA molecules that bind and inhibit human thrombin. *Nature* 355, 564-566, doi:10.1038/355564a0 (1992).

99   Opazo, F. *et al.* Modular Assembly of Cell-targeting Devices Based on an Uncommon G-quadruplex Aptamer. *Mol Ther Nucleic Acids* 4, e251, doi:10.1038/mtna.2015.25 (2015).

100   Shamah, S. M., Healy, J. M. & Cload, S. T. Complex target SELEX. *Acc Chem Res* 41, 130-138, doi:10.1021/ar700142z (2008).

101   Ku, T. H. *et al.* Nucleic Acid Aptamers: An Emerging Tool for Biotechnology and Biomedical Sensing. *Sensors (Basel)* 15, 16281-16313, doi:10.3390/s150716281 (2015).

102   Vance, S. A. & Sandros, M. G. Zeptomole detection of C-reactive protein in serum by a nanoparticle amplified surface plasmon resonance imaging aptasensor. *Sci Rep* 4, 5129, doi:10.1038/srep05129 (2014).

103   Bruno, J. G. *et al.* Development of a fluorescent enzyme-linked DNA aptamer-magnetic bead sandwich assay and portable fluorometer for sensitive and rapid leishmania detection in sandflies. *J Fluoresc* 24, 267-277, doi:10.1007/s10895-013-1315-6 (2014).

104   Sun, H. *et al.* Oligonucleotide aptamers: new tools for targeted cancer therapy. *Mol Ther Nucleic Acids* 3, e182, doi:10.1038/mtna.2014.32 (2014).

105   Sundaram, P., Kurniawan, H., Byrne, M. E. & Wower, J. Therapeutic RNA aptamers in clinical trials. *Eur J Pharm Sci* 48, 259-271, doi:10.1016/j.ejps.2012.10.014 (2013).

106   Trujillo, C. A., Nery, A. A., Alves, J. M., Martins, A. H. & Ulrich, H. Development of the anti-VEGF aptamer to a therapeutic agent for clinical ophthalmology. *Clin Ophthalmol* 1, 393-402 (2007).

107   Meyer, C., Hahn, U. & Rentmeister, A. Cell-specific aptamers as emerging therapeutics. *J Nucleic Acids* 2011, 904750, doi:10.4061/2011/904750 (2011).

108   Mi, J. *et al.* In vivo selection of tumor-targeting RNA motifs. *Nat Chem Biol* 6, 22-24, doi:10.1038/nchembio.277 (2010).

109   Cheng, C., Chen, Y. H., Lennox, K. A., Behlke, M. A. & Davidson, B. L. In vivo SELEX for Identification of Brain-penetrating Aptamers. *Mol Ther Nucleic Acids* 2, e67, doi:10.1038/mtna.2012.59 (2013).

110   Sefah, K. *et al.* In vitro selection with artificial expanded genetic information systems. *Proc Natl Acad Sci U S A* 111, 1449-1454, doi:10.1073/pnas.1311778111 (2014).

111   Tolle, F., Brandle, G. M., Matzner, D. & Mayer, G. A Versatile Approach Towards Nucleobase-Modified Aptamers. *Angew Chem Int Ed Engl* 54, 10971-10974, doi:10.1002/anie.201503652 (2015).

112   Chu, T. C. *et al.* Aptamer:toxin conjugates that specifically target prostate tumor cells. *Cancer Res* 66, 5989-5992, doi:10.1158/0008-5472.CAN-05-4583 (2006).

113   Xiao, Z., Shangguan, D., Cao, Z., Fang, X. & Tan, W. Cell-specific internalization study of an aptamer from whole cell selection. *Chemistry* 14, 1769-1775, doi:10.1002/chem.200701330 (2008).

114   Yan, A. C. & Levy, M. Aptamers and aptamer targeted delivery. *RNA Biol* 6, 316-320 (2009).

115   Wengerter, B. C. *et al.* Aptamer-targeted antigen delivery. *Mol Ther* 22, 1375-1387, doi:10.1038/mt.2014.51 (2014).

116   Farokhzad, O. C. *et al.* Nanoparticle-aptamer bioconjugates: a new approach for targeting prostate cancer cells. *Cancer Res* 64, 7668-7672, doi:10.1158/0008-5472.CAN-04-2550 (2004).

117   McNamara, J. O., 2nd *et al.* Cell type-specific delivery of siRNAs with aptamer-siRNA chimeras. *Nat Biotechnol* 24, 1005-1015, doi:10.1038/nbt1223 (2006).

118   Kim, E. *et al.* Prostate cancer cell death produced by the co-delivery of Bcl-xL shRNA and doxorubicin using an aptamer-conjugated polyplex. *Biomaterials* 31, 4592-4599, doi:10.1016/j.biomaterials.2010.02.030 (2010).

119   Drolet, D. W. *et al.* Pharmacokinetics and safety of an anti-vascular endothelial growth factor aptamer (NX1838) following injection into the vitreous humor of rhesus monkeys. *Pharm Res* 17, 1503-1510 (2000).

120   Da Pieve, C., Blackshaw, E., Missailidis, S. & Perkins, A. C. PEGylation and biodistribution of an anti-MUC1 aptamer in MCF-7 tumor-bearing mice. *Bioconjug Chem* 23, 1377-1381, doi:10.1021/bc300128r (2012).

121   Parry, R. V. *et al.* CTLA-4 and PD-1 receptors inhibit T-cell activation by distinct mechanisms. *Mol Cell Biol* 25, 9543-9553, doi:10.1128/MCB.25.21.9543-9553.2005 (2005).

122   Santulli-Marotto, S., Nair, S. K., Rusconi, C., Sullenger, B. & Gilboa, E. Multivalent RNA aptamers that inhibit CTLA-4 and enhance tumor immunity. *Cancer Res* 63, 7483-7489 (2003).

123   Prodeus, A. *et al.* Targeting the PD-1/PD-L1 Immune Evasion Axis With DNA Aptamers as a Novel Therapeutic Strategy for the Treatment of Disseminated Cancers. *Mol Ther Nucleic Acids* 4, e237, doi:10.1038/mtna.2015.11 (2015).

124   McNamara, J. O. *et al.* Multivalent 4-1BB binding aptamers costimulate CD8+ T cells and inhibit tumor growth in mice. *J Clin Invest* 118, 376-386, doi:10.1172/JCI33365 (2008).

125   Pastor, F., Kolonias, D., McNamara, J. O., 2nd & Gilboa, E. Targeting 4-1BB costimulation to disseminated tumor lesions with bi-specific oligonucleotide aptamers. *Mol Ther* 19, 1878-1886, doi:10.1038/mt.2011.145 (2011).

126   Berezovski, M. V., Lechmann, M., Musheev, M. U., Mak, T. W. & Krylov, S. N. Aptamer-facilitated biomarker discovery (AptaBiD). *J Am Chem Soc* 130, 9137-9143, doi:10.1021/ja801951p (2008).

127   Hui, Y., Shan, L., Lin-Fu, Z. & Jian-Hua, Z. Selection of DNA aptamers against DC-SIGN protein. *Mol Cell Biochem* 306, 71-77, doi:10.1007/s11010-007-9555-x (2007).

128   Rotzschke, O. *et al.* Exact prediction of a natural T cell epitope. *Eur J Immunol* 21, 2891-2894, doi:10.1002/eji.1830211136 (1991).

129   McFarland, B. J., Sant, A. J., Lybrand, T. P. & Beeson, C. Ovalbumin(323-339) peptide binds to the major histocompatibility complex class II I-A(d) protein using two functionally distinct registers. *Biochemistry* 38, 16663-16670 (1999).

130   Linehan, S. A., Martinez-Pomares, L., da Silva, R. P. & Gordon, S. Endogenous ligands of carbohydrate recognition domains of the mannose receptor in murine macrophages, endothelial cells and secretory cells; potential relevance to inflammation and immunity. *Eur J Immunol* 31, 1857-1866, doi:10.1002/1521-4141(200106)31:6<1857::AID-IMMU1857>3.0.CO;2-D (2001).

131   Martinez-Pomares, L. *et al.* Carbohydrate-independent recognition of collagens by the macrophage mannose receptor. *Eur J Immunol* 36, 1074-1082, doi:10.1002/eji.200535685 (2006).

132   Lutz, M. B., Inaba, K., Schuler, G. & Romani, N. Still Alive and Kicking: In-Vitro-Generated GM-CSF Dendritic Cells! *Immunity* 44, 1-2, doi:10.1016/j.immuni.2015.12.013 (2016).

133   Lutz, M. B. *et al.* An advanced culture method for generating large quantities of highly pure dendritic cells from mouse bone marrow. *J Immunol Methods* 223, 77-92 (1999).

134   Bonifaz, L. *et al.* Efficient targeting of protein antigen to the dendritic cell receptor DEC-205 in the steady state leads to antigen presentation on major histocompatibility complex class I products and peripheral CD8+ T cell tolerance. *J Exp Med* 196, 1627-1638 (2002).

135   Heckel, A. & Mayer, G. Light regulation of aptamer activity: an anti-thrombin aptamer with caged thymidine nucleobases. *J Am Chem Soc* 127, 822-823, doi:10.1021/ja043285e (2005).

136   Lennarz, S., Heider, E., Blind, M. & Mayer, G. An aptamer to the MAP kinase insert region. *ACS Chem Biol* 10, 320-327, doi:10.1021/cb5005756 (2015).

137   Weis, W. I., Taylor, M. E. & Drickamer, K. The C-type lectin superfamily in the immune system. *Immunol Rev* 163, 19-34 (1998).

138   Martinez-Pomares, L. The mannose receptor. *J Leukoc Biol* 92, 1177-1186, doi:10.1189/jlb.0512231 (2012).

139   Feinberg, H. *et al.* Structure of a C-type carbohydrate recognition domain from the macrophage mannose receptor. *J Biol Chem* 275, 21539-21548, doi:10.1074/jbc.M002366200 (2000).

140   Harris, N., Super, M., Rits, M., Chang, G. & Ezekowitz, R. A. Characterization of the murine macrophage mannose receptor: demonstration that the downregulation of receptor expression mediated by interferon-gamma occurs at the level of transcription. *Blood* 80, 2363-2373 (1992).

141   Patra, A. *et al.* 2'-Fluoro RNA shows increased Watson-Crick H-bonding strength and stacking relative to RNA: evidence from NMR and thermodynamic data. *Angew Chem Int Ed Engl* 51, 11863-11866, doi:10.1002/anie.201204946 (2012).

142   Manoharan, M. *et al.* Unique gene-silencing and structural properties of 2'-fluoro-modified siRNAs. *Angew Chem Int Ed Engl* 50, 2284-2288, doi:10.1002/anie.201006519 (2011).

143   Su, Z. *et al.* Next-generation sequencing and its applications in molecular diagnostics. *Expert Rev Mol Diagn* 11, 333-343, doi:10.1586/erm.11.3 (2011).

144   Blank, M. Next-Generation Analysis of Deep Sequencing Data: Bringing Light into the Black Box of SELEX Experiments. *Methods Mol Biol* 1380, 85-95, doi:10.1007/978-1-4939-3197-2_7 (2016).

145   Zinchuk, V., Wu, Y. & Grossenbacher-Zinchuk, O. Bridging the gap between qualitative and quantitative colocalization results in fluorescence microscopy studies. *Sci Rep* 3, 1365, doi:10.1038/srep01365 (2013).

146   O'Neill, L. A., Golenbock, D. & Bowie, A. G. The history of Toll-like receptors - redefining innate immunity. *Nat Rev Immunol* 13, 453-460, doi:10.1038/nri3446 (2013).

147   Paludan, S. R. & Bowie, A. G. Immune sensing of DNA. *Immunity* 38, 870-880, doi:10.1016/j.immuni.2013.05.004 (2013).

148   Ballas, Z. K. *et al.* Divergent therapeutic and immunologic effects of oligodeoxynucleotides with distinct CpG motifs. *J Immunol* 167, 4878-4886 (2001).

149   Bauer, S., Pigisch, S., Hangel, D., Kaufmann, A. & Hamm, S. Recognition of nucleic acid and nucleic acid analogs by Toll-like receptors 7, 8 and 9. *Immunobiology* 213, 315-328, doi:10.1016/j.imbio.2007.10.010 (2008).

150   Barnden, M. J., Allison, J., Heath, W. R. & Carbone, F. R. Defective TCR expression in transgenic mice constructed using cDNA-based alpha- and beta-chain genes under the control of heterologous regulatory elements. *Immunol Cell Biol* 76, 34-40, doi:10.1046/j.1440-1711.1998.00709.x (1998).

151   Quah, B. J., Warren, H. S. & Parish, C. R. Monitoring lymphocyte proliferation in vitro and in vivo with the intracellular fluorescent dye carboxyfluorescein diacetate succinimidyl ester. *Nat Protoc* 2, 2049-2056, doi:10.1038/nprot.2007.296 (2007).

152   Appay, V. The physiological role of cytotoxic CD4(+) T-cells: the holy grail? *Clin Exp Immunol* 138, 10-13, doi:10.1111/j.1365-2249.2004.02605.x (2004).

153   Haabeth, O. A. *et al.* How Do CD4(+) T Cells Detect and Eliminate Tumor Cells That Either Lack or Express MHC Class II Molecules? *Front Immunol* 5, 174, doi:10.3389/fimmu.2014.00174 (2014).

154   Penaloza-MacMaster, P. *et al.* Vaccine-elicited CD4 T cells induce immunopathology after chronic LCMV infection. *Science* 347, 278-282, doi:10.1126/science.aaa2148 (2015).

155   Hogquist, K. A. *et al.* T cell receptor antagonist peptides induce positive selection. *Cell* 76, 17-27 (1994).

156   Wang, J., Rudzinski, J. F., Gong, Q., Soh, H. T. & Atzberger, P. J. Influence of target concentration and background binding on in vitro selection of affinity reagents. *PLoS One* 7, e43940, doi:10.1371/journal.pone.0043940 (2012).

157   Gold, L. *et al.* Aptamer-based multiplexed proteomic technology for biomarker discovery. *PLoS One* 5, e15004, doi:10.1371/journal.pone.0015004 (2010).

158   Lupold, S. E., Hicke, B. J., Lin, Y. & Coffey, D. S. Identification and characterization of nuclease-stabilized RNA molecules that bind human prostate cancer cells via the prostate-specific membrane antigen. *Cancer Res* 62, 4029-4033 (2002).

159   Hicke, B. J. *et al.* Tenascin-C aptamers are generated using tumor cells and purified protein. *J Biol Chem* 276, 48644-48654, doi:10.1074/jbc.M104651200 (2001).

160   Dassie, J. P. *et al.* Systemic administration of optimized aptamer-siRNA chimeras promotes regression of PSMA-expressing tumors. *Nat Biotechnol* 27, 839-849, doi:10.1038/nbt.1560 (2009).

161   Morris, K. N., Jensen, K. B., Julin, C. M., Weil, M. & Gold, L. High affinity ligands from in vitro selection: complex targets. *Proc Natl Acad Sci U S A* 95, 2902-2907 (1998).

162   Zhang, Y., Chen, Y., Han, D., Ocsoy, I. & Tan, W. Aptamers selected by cell-SELEX for application in cancer studies. *Bioanalysis* 2, 907-918, doi:10.4155/bio.10.46 (2010).

163   Ohuchi, S. Cell-SELEX Technology. *Biores Open Access* 1, 265-272, doi:10.1089/biores.2012.0253 (2012).

164   Tang, Z. *et al.* Selection of aptamers for molecular recognition and characterization of cancer cells. *Anal Chem* 79, 4900-4907, doi:10.1021/ac070189y (2007).

165   Mallikaratchy, P. R. *et al.* A multivalent DNA aptamer specific for the B-cell receptor on human lymphoma and leukemia. *Nucleic Acids Res* 39, 2458-2469, doi:10.1093/nar/gkq996 (2011).

166   Guo, K. T., Schafer, R., Paul, A., Ziemer, G. & Wendel, H. P. Aptamer-based strategies for stem cell research. *Mini Rev Med Chem* 7, 701-705 (2007).

167   Mitchell, D. A. *et al.* Severe adverse immunologic reaction in a patient with glioblastoma receiving autologous dendritic cell vaccines combined with GM-CSF and dose-intensified temozolomide. *Cancer Immunol Res* 3, 320-325, doi:10.1158/2326-6066.CIR-14-0100 (2015).

168   Avci-Adali, M., Steinle, H., Michel, T., Schlensak, C. & Wendel, H. P. Potential capacity of aptamers to trigger immune activation in human blood. *PLoS One* 8, e68810, doi:10.1371/journal.pone.0068810 (2013).

169   Bode, C., Zhao, G., Steinhagen, F., Kinjo, T. & Klinman, D. M. CpG DNA as a vaccine adjuvant. *Expert Rev Vaccines* 10, 499-511, doi:10.1586/erv.10.174 (2011).

170   Labeur, M. S. *et al.* Generation of tumor immunity by bone marrow-derived dendritic cells correlates with dendritic cell maturation stage. *J Immunol* 162, 168-175 (1999).

171   Walseng, E., Bakke, O. & Roche, P. A. Major histocompatibility complex class II-peptide complexes internalize using a clathrin- and dynamin-independent endocytosis pathway. *J Biol Chem* 283, 14717-14727, doi:10.1074/jbc.M801070200 (2008).

172   Tewari, M. K., Sinnathamby, G., Rajagopal, D. & Eisenlohr, L. C. A cytosolic pathway for MHC class II-restricted antigen processing that is proteasome and TAP dependent. *Nat Immunol* 6, 287-294, doi:10.1038/ni1171 (2005).

173   Gagnon, E. *et al.* Endoplasmic reticulum-mediated phagocytosis is a mechanism of entry into macrophages. *Cell* 110, 119-131 (2002).

174   Vieira, O. V. *et al.* Modulation of Rab5 and Rab7 recruitment to phagosomes by phosphatidylinositol 3-kinase. *Mol Cell Biol* 23, 2501-2514 (2003).

175   Marshall, N. B. & Swain, S. L. Cytotoxic CD4 T cells in antiviral immunity. *J Biomed Biotechnol* 2011, 954602, doi:10.1155/2011/954602 (2011).

176   Hahn, S. *et al.* Down-modulation of CD4+ T helper type 2 and type 0 cells by T helper type 1 cells via Fas/Fas-ligand interaction. *Eur J Immunol* 25, 2679-2685, doi:10.1002/eji.1830250942 (1995).

177   Bercovici, N., Duffour, M. T., Agrawal, S., Salcedo, M. & Abastado, J. P. New methods for assessing T-cell responses. *Clin Diagn Lab Immunol* 7, 859-864 (2000).

178   Ohlfest, J. R. *et al.* Vaccine injection site matters: qualitative and quantitative defects in CD8 T cells primed as a function of proximity to the tumor in a murine glioma model. *J Immunol* 190, 613-620, doi:10.4049/jimmunol.1201557 (2013).

179   Bouchard, P. R., Hutabarat, R. M. & Thompson, K. M. Discovery and development of therapeutic aptamers. *Annu Rev Pharmacol Toxicol* 50, 237-257, doi:10.1146/annurev.pharmtox.010909.105547 (2010).

180   Romani, N. *et al.* Targeting skin dendritic cells to improve intradermal vaccination. *Curr Top Microbiol Immunol* 351, 113-138, doi:10.1007/82_2010_118 (2012).

181   Bonifaz, L. C. *et al.* In vivo targeting of antigens to maturing dendritic cells via the DEC-205 receptor improves T cell vaccination. *J Exp Med* 199, 815-824, doi:10.1084/jem.20032220 (2004).

182   Agrawal, S. *et al.* Cutting edge: different Toll-like receptor agonists instruct dendritic cells to induce distinct Th responses via differential modulation of extracellular signal-regulated kinase-mitogen-activated protein kinase and c-Fos. *J Immunol* 171, 4984-4989 (2003).

183   Seliger, B. & Massa, C. The dark side of dendritic cells: development and exploitation of tolerogenic activity that favor tumor outgrowth and immune escape. *Front Immunol* 4, 419, doi:10.3389/fimmu.2013.00419 (2013).

184   Xue, J. *et al.* Transcriptome-based network analysis reveals a spectrum model of human macrophage activation. *Immunity* 40, 274-288, doi:10.1016/j.immuni.2014.01.006 (2014).

185   Min, S. *et al.* Multiple tumor-associated microRNAs modulate the survival and longevity of dendritic cells by targeting YWHAZ and Bcl2 signaling pathways. *J Immunol* 190, 2437-2446, doi:10.4049/jimmunol.1202282 (2013).

186   Wherry, E. J. T cell exhaustion. *Nat Immunol* 12, 492-499 (2011).

187   Leggatt, G. R. Peptide Dose and/or Structure in Vaccines as a Determinant of T Cell Responses. *Vaccines (Basel)* 2, 537-548, doi:10.3390/vaccines2030537 (2014).

188   Blankenstein, T., Coulie, P. G., Gilboa, E. & Jaffee, E. M. The determinants of tumour immunogenicity. *Nat Rev Cancer* 12, 307-313, doi:10.1038/nrc3246 (2012).

189   Liu, C. C., Yang, H., Zhang, R., Zhao, J. J. & Hao, D. J. Tumour-associated antigens and their anti-cancer applications. *Eur J Cancer Care (Engl)*, doi:10.1111/ecc.12446 (2016).

190   Roep, B. O. & Peakman, M. Antigen targets of type 1 diabetes autoimmunity. *Cold Spring Harb Perspect Med* 2, a007781, doi:10.1101/cshperspect.a007781 (2012).

191   Tsuji, T. *et al.* Antibody-targeted NY-ESO-1 to mannose receptor or DEC-205 in vitro elicits dual human CD8+ and CD4+ T cell responses with broad antigen specificity. *J Immunol* 186, 1218-1227, doi:10.4049/jimmunol.1000808 (2011).

192   Lee, S. J. *et al.* Mannose receptor-mediated regulation of serum glycoprotein homeostasis. *Science* 295, 1898-1901, doi:10.1126/science.1069540 (2002).

193   Schagger, H. Tricine-SDS-PAGE. *Nat Protoc* 1, 16-22, doi:10.1038/nprot.2006.4 (2006).

194   Nino-Castro, A. *et al.* The IDO1-induced kynurenines play a major role in the antimicrobial effect of human myeloid cells against Listeria monocytogenes. *Innate Immun* 20, 401-411, doi:10.1177/1753425913496442 (2014).

9 Supplementary data

9.1 DNA sequences obtained from Fc-FN SELEX

Table S 9-1: FN sequences

sequence FN#	DNA-sequence
1	CGCGCGGCTTAGGTGGTTGGTTCTTTTGGTGGTTCTTGTGGTG
2	CCCCGGAAATTGCGTACTTGTATCGGTCCTTTATCTTGTTGTG
4	CCACGAGTATTTGCTGGGTCCTGGTGGCGTGGGTTTTTGTGATGCA
8	CGGCGCGGGGATATGGGGTACGTGTTCTGGTCCTCTTACATTG
9	CGGGTTTGCTCTTGGTTAGTGCTTGTGGTGGTGTGCGACTTGG
12	GGGGATTCTGTTTTTTTTTTGTAACTCGGGGTTGGGTATCGTTG
14	CCTGTTCTGTGTTTATGTATTGTTGTTATAGTTGTGTTTCCTG
15	CGTGGGCTGGGATTTATTGGGGTTTGTGCTTGTTTGTTAGGCT
17	CTGGTGTATGTTCTTTGTGTGGTTTATTGATTTATTTTTCCGG
18	CCCCATGCGCTTCTTGCTCCGCTCGGTCTCCTTGTCCGCCTTG
19	GGCGGGAAGGTTTGTGTATTGCGTGGTGAAGGCTCCGTGATGT
20	CGGTGGCCGTGGTTTCTTCGTGTGGTTGTGTTTTTCGTCCTTG
23	GCGGGGGCAGTGTTAAGTCGTTTAGGTGGTGGTCGTGTGGTGG
25	CCCGCTGTGTTTCCTTCTGTGATGTTTCGTTCGTTTGTTTGCC

9.2 DNA sequences derived from Fc-CTL SELEX

Table S 9-2: CTL unique sequences

sequence CTL#	DNA-sequence
1	GCCAGTATTTTGATTTCTTTGGGCGGGGGGGAATTTATGTGG
2	CAGTCCACGAGGGGAGGTGGGAATTTTTTTGGGTGGTTTTGTC
3	GCCGGGTGGGAGTGCTCTCTGTTGCATGTGGGTGGGTAGCGTG
4	GGCGCCACGCTTGTTGTGGGCGGGAGTGGTGGGAAACTACGTG
11	CGGTACTGTGGGGGGGTGGGTCGGGAAGAACGGCGCCAGGCGT
14	CCGTGCGTGGGAGGGTGTGATTTTCCTGGGGTGGGAGCATGGG
17	CGAGCGTGGGGGGGGTGGGTTTCGGGAGCTCCGGGAGCACTTTG
18	CACTGGATTCGTTGGGGTTCTTTTGGGGGATATTCCGGGGTGG
19	GCACCGTGGGCGGGCTATACTTCTTTTCATTTGGGTGGGAGGTGCA
20	GGTCCAATCGTTGGGGTTTGGGGCGTTCACTTCATCGGGGCGG
22	CAGGGGAGGTGGGTTTTTTGGGTAGTTTTGGATCAATGGCCCG

9.3 NGS analysis of DNA sequences obtained by cell-SELEX

Table S9-3: Sequences obtained by cell-SELEX and their NGS frequencies

Classical cloning and sequencing			NGS							
				frequency [%]						
	sequence D#	random region	pattern #	selection cycle						
				1	2	3	4	7	10
sequence family 1	2	GCATGTTTGGGTGGGATATTGGCGTGTTTGGGTTGGGACTGCT	1	8,33E-05	8,10E-04	6,65E-03	0,05	0,68	3,81
	3	GCATGTTTGGGTGGGATATTGGCGTGTTTGGGTTGGGACTGCT	1	8,33E-05	8,10E-04	6,65E-03	0,05	0,68	3,81
	5	CGCATTTGGGTGGGATTGTTATTTGGGTCGGGATTGGCAGTT	1	0,00	0,00	2,83E-03	0,01	0,14	0,99
	8	CGCATTTGGGTGGGATTGTTATTTGGGTCGGGATTGGCAGTT	1	0,00	0,00	2,83E-03	0,01	0,14	0,99
sequence family 2	4	GTGGGCGGGTTTATATTCGGTGGTGGTGGGGGTGGTTCTGTT	2	0,00	0,00	0,00	6,17E-04	0,06	0,13
	7	CGTGGGTGGGTTTATATTCGGTGGTGGTGGGGGTGGTACTGTT	2	0,00	0,00	7,64E-05	1,55E-03	0,21	1,32
	23	CGTGGGCGGGTTTATATTTGGTGGTGGTGGGGGTGGTACTGTT	2	0,00	0,00	7,64E-05	1,04E-03	0,16	0,69
	28	CGTGGGTGGGTTTATATTCGGTGGTGGTGGGGGTGGTACTGTT	2	0,00	0,00	7,64E-05	1,55E-03	0,21	1,32
unique	1	CCCCACCAACTCGACCAAGTCGCTGCTCCTCTTCCTTGTGTTG	-	0,00	0,00	0,00	0,00	0,00	0,00
	6	CAACGGACCCTGGGATGTATTCGTCTCTCTCGCCGCCCACCCC	-	0,00	0,00	0,00	0,00	0,00	0,00
	9	CCGTCCCCCCCGTTGTGTTCCTACTCTCGCCCTACACGAACCG	-	0,00	0,00	0,00	0,00	0,00	0,00
	10	CCGTTCTCGTCGTCCTGTATGCGCCTGTTCGTCTCCTGTTCCT	-	0,00	0,00	0,00	0,00	0,00	0,00
	11	GACGGGGCGGTTGTTTTTTCTGGTTTTCGGTATGTTGTGTGTG	-	0,00	0,00	0,00	0,00	0,00	0,00
	13	CCTCCTCATTGCTTGTTCTCGCCTTGATCGTCCCTGGCCCGTT	-	0,00	0,00	0,00	3,94E-05	3,79E-05	0,00
	14	CCCTCACTGTAGTCCTGACTTGTCGTATTCCCGGTTTTCTTGT	-	0,00	0,00	0,00	0,00	0,00	0,00
	15	CCCTGGCCCCCTCACTCCCCGTCATTTGTTCTATGCCCGCGCC	-	0,00	0,00	0,00	2,63E-05	1,89E-04	4,57E-05
	16	CCCGGCTCTCCCCATTGGTCTGTGCTCTTTCCTCCGTTCGCCC	-	0,00	0,00	0,00	1,71E-04	5,87E-04	9,60E-04
	17	CCCCCGCCTCTCGAGCATTTACCACCCGGGCGCTTCACGTTTG	-	0,00	0,00	0,00	0,00	0,00	0,00
	18	CCCGTTTGGTATATCGCGCATTTTGGTCCCGTTCCTTGTTTGT	-	1,39E-05	0,00	0,00	0,00	0,00	0,00

19	CAGGGGAGGTGGGTTTCTTTGGGTTGTTTGTGAAGTGGGGTGT	57	2,78E-05	8,10E-04	2,06E-03	7,31E-03	0,05	0,07
20	CCCGACCCCATCCGGTATTTTGTGTAATCTAGTCTCTTTGTGT	554	0,00	0,00	0,00	1,18E-04	4,16E-04	4,16E-03
21	CCCGACCGACGCTGTATTTTCGCCACCACGCTCGACCACCCCT	171	0,00	0,00	0,00	1,31E-05	5,68E-05	0,00
22	CCCGACCCGCCGCTTTTTCCCTCTTCCGTCACCTCCTTTCGAT	-	0,00	0,00	0,00	0,00	3,79E-05	6,40E-04
24	GCGTCGGATTGGTGTTGTGGTCTTTGGGTTTTGGTTTGTGTGT	-	0,00	0,00	0,00	0,00	1,89E-05	0,00
26	CCAGGGGAGGATGGGCGGGCTTTTCGTTGTCTTCTGTGTCGCT	18	8,33E-05	8,10E-04	3,74E-03	9,07E-03	0,09	0,36
27	GCGGTTCTGTGTGTGGGTGGGTGGGTGGTAATATTGTCTCGCT	3	6,95E-05	2,03E-03	7,95E-03	0,05	0,68	2,07
29	TCCCTCTTTGCATCTCCCGTATACCCCGCCCTTTAACCGTGTG	-	0,00	0,00	0,00	0,00	0,00	0,00
30	TGGGGGTTGGGTGGGTTGGGTGTCGATTGCGTCTCTCTTCTTG	-	0,00	0,00	0,00	0,00	0,00	0,00
31	CAGGGGAGGAGGGTGGGCAGAGGTGTTTAGTGTGTCCGGGTTT	61	0,00	0,00	0,00	1,31E-05	1,06E-03	4,11E-03
32	CCACCGCGCTGATCTTGCTCCCTTCCGTCCGTCCGTTCCTCCC	306	1,39E-05	0,00	1,53E-04	4,46E-04	2,73E-03	8,45E-03
33	CCCTCGACAGCCTTCTCGTCCTCTGTATTGGGCCATCCTCCC	-	0,00	0,00	0,00	0,00	1,89E-05	0,00
34	CCTAGTACATTTCATCCGCCTCGTTGTCGCCCCTTCCCGCCGT	-	0,00	0,00	0,00	0,00	0,00	0,00
35	CGGTTTGGTGTGTGGTTCGCGAGTACGTTTCCTTCTCGACTTG	-	0,00	0,00	0,00	0,00	0,00	0,00
36	CGGGTGCTTTGTTGTATGTTGTGTGTGGGCTTTTTTGGTGTGG	-	0,00	0,00	0,00	0,00	0,00	0,00

**Table S 9-4 Consensus sequences and number of sequences of the 15 most abundant NGS patterns**

NGS pattern No.	consensus sequence	number of sequences
1	GCATGTTTGGGTGGGATATTGGCGTGTTTGGGTTGGGACTGCT	101544
2	CGTGGGCGGGTTTATATTCGGTGGTGGTGGGGGTGGTACTGTT	97341
3	GCGGTTCTGTGTGTGGGTGGGTGGGTGGTAATATTGTCTCGCT	60744
4	GGGGAGGTGGGTGGGTTGGCCTTCACGTTATCTTTTGGTGGTT	29284
5	CGCATTTGGGTGGGATTGTTATTTGGGTCGGGATTGGCAGTT	28834
6	CCAGGGGAGGATGGGAGGGTTTTTTTCGGATTCTTGTCGTGCT	26437
7	CGTGGTATGTGGTGGGTGGTGGGGTGGTAGTTGGGTGGACGGT	20588
8	CAGGGGAGGTGGGTGATTGGGTTGTTTTTCGCGGACGTGAGGT	17022
9	GCGTGTTGGGTGGGGGTGGGAGGTGGTTTCTTCTACTTGGTGG	15788
10	CGAGTTTCTGAGGGTGGGTGGGTGGTTATTAGTCGAGGTTGCA	14867
11	TGGGGTGGGTGGTCGGGGTTGTGGTTGGTTTCTCTTTAAGGGT	14472
12	CCAGGGTGGGATGGGTATTTTGAGGTGGAGGTGGGGGTTGGTT	13792
13	GGGTGTTGTGGGGTGGGGCGGTGGGTGTGAGTGTCGGCAGCTG	13764
14	TGTGGTTCGGTAGGTCGGGGAGGGTGGTGGGTTATGCGGCGGG	13593
15	CACAGGGGAGGTCGGGCGGGTTGTCTGCTTTCTTGGGTCGGTT	13429

9.4 Aptamer-targeted activation of CD4 T cells
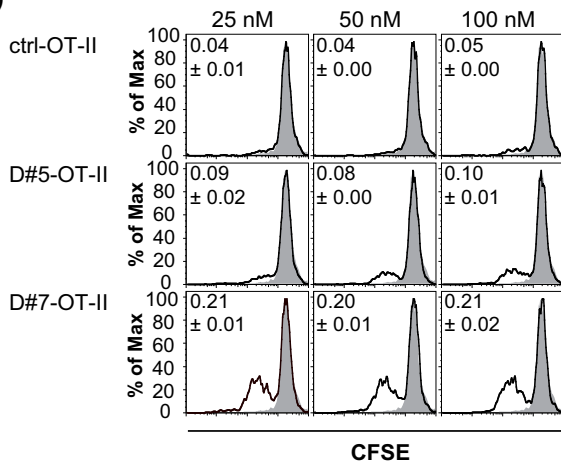
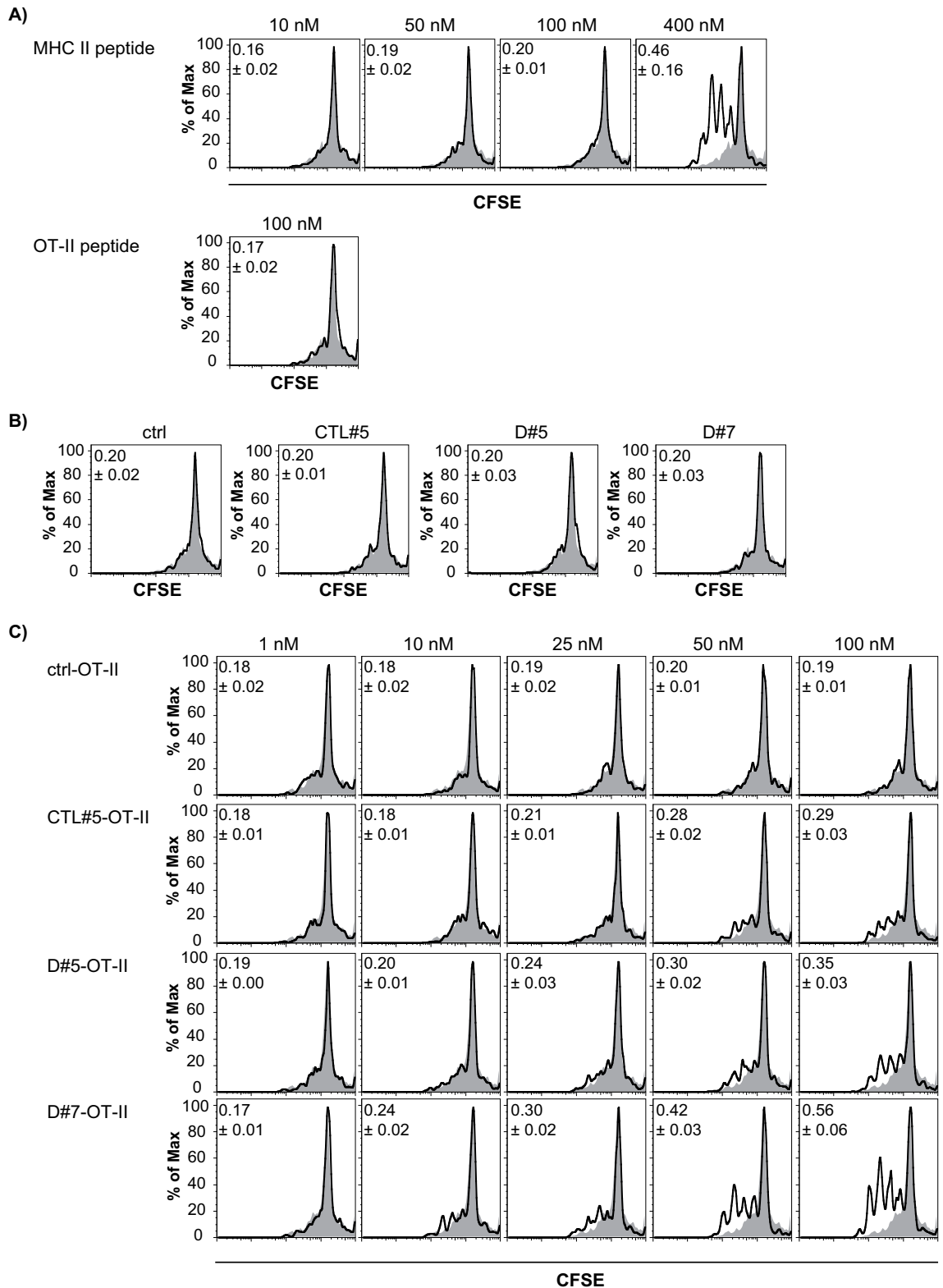**A)**
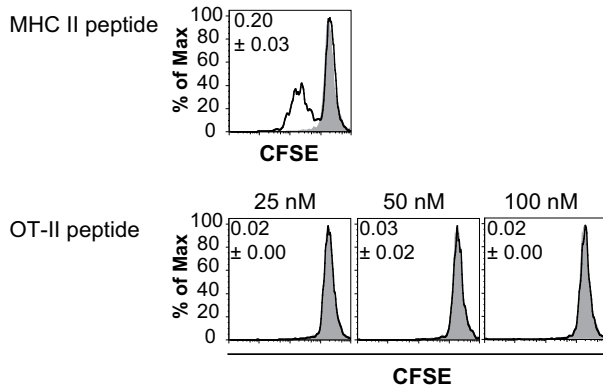
B)
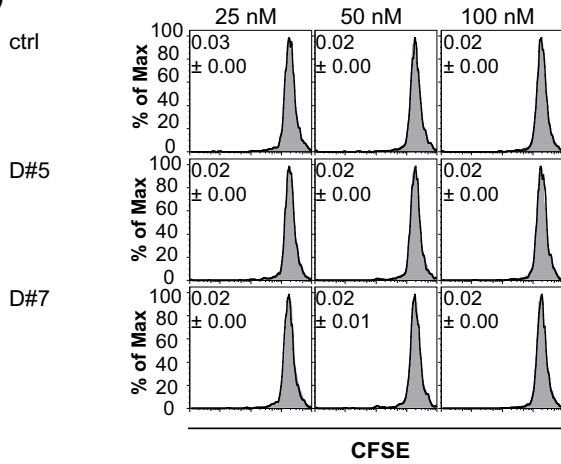
C)

Figure S 9.4.1: Activation of CD4 T cells
BM-DCs were treated with different concentrations of MHC II peptide or 100 nM OT-II peptide **(A)**, 100 nM of oligonucleotides **(B)** or increasing concentrations of aptamer-peptide conjugates **(C)**. Subsequently, BM-DCs were co-cultured for 72 h with CFSE-labeled OVA-dependent CD4 T cells and the proliferation profile indicated by changes of CFSE signals was measured by flow cytometry. FACS histograms with one representative profile out of triplicate measurement are depicted. Numbers gives the division index (mean ± SD). The non-proliferated population is shown in grey.
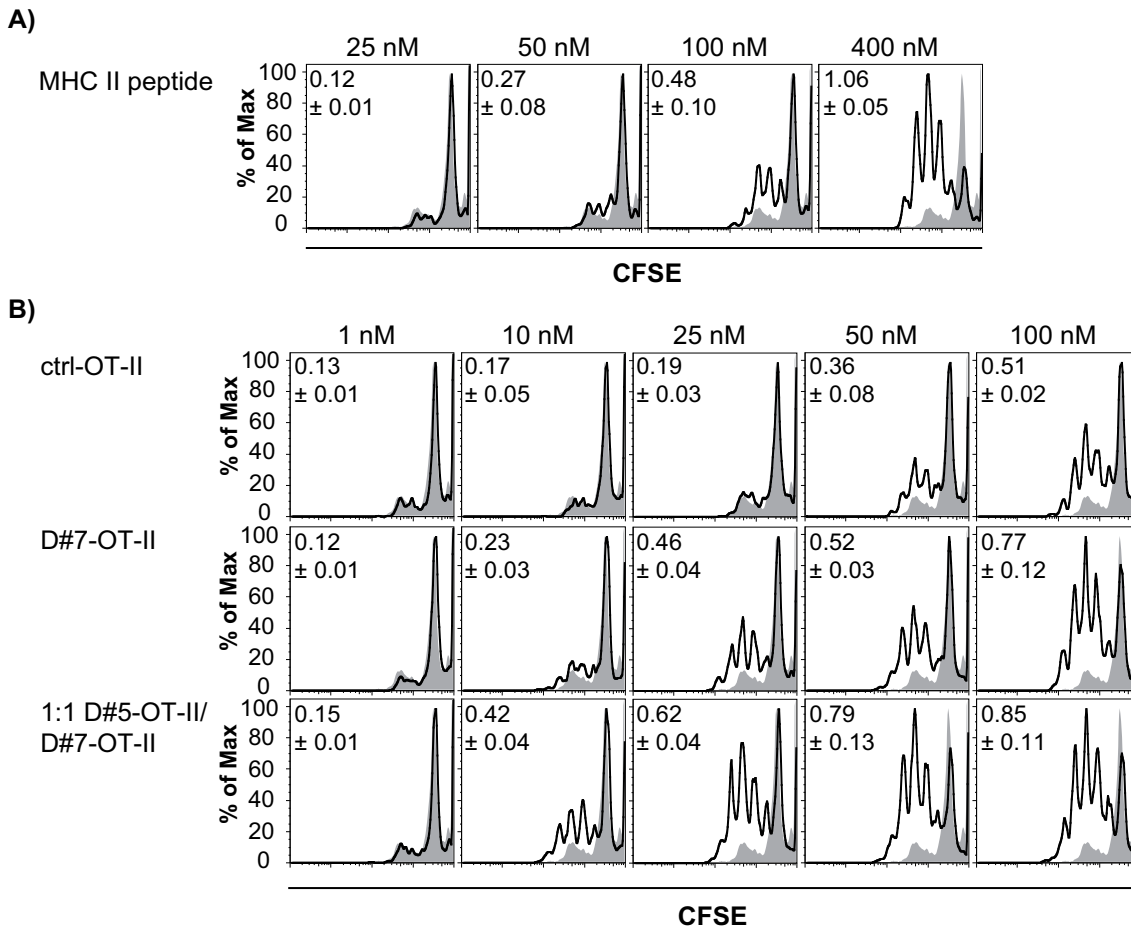
Figure S 9.4.2: Activation of CD4 T cells
BM-DCs were treated with different concentrations of MHC II peptide or 100 nM OT-II peptide **(A)**, 100 nM of oligonucleotides **(B)** or increasing concentrations of aptamer-peptide conjugates **(C)**. Afterwards, BM-DCs were co-cultured for 72 h with CFSE-labeled OVA-dependent CD4 T cells and the CFSE profile was measured by flow cytometry. FACS histograms with one representative profile out of triplicate measurement are depicted. Division index (mean ± SD) is depicted within the FACS histograms. The non-proliferated population is shown in grey.

A)

B)

Figure S 9.4.3: Activation of CD4 T cells
BM-DCs were treated with different concentrations of MHC II peptide or 100 nM OT-II peptide **(A)**, 100 nM of oligonucleotides **(B)** or increasing concentrations of aptamer-peptide conjugates **(C)**. Next, BM-DCs were co-cultured for 72 h with CFSE-labeled OVA-dependent CD4 T cells and the proliferation profile was measured by flow cytometry. FACS histograms with one representative profile out of triplicate measurement are depicted. Numbers gives the division index (mean ± SD). The non-proliferated population is shown in grey.

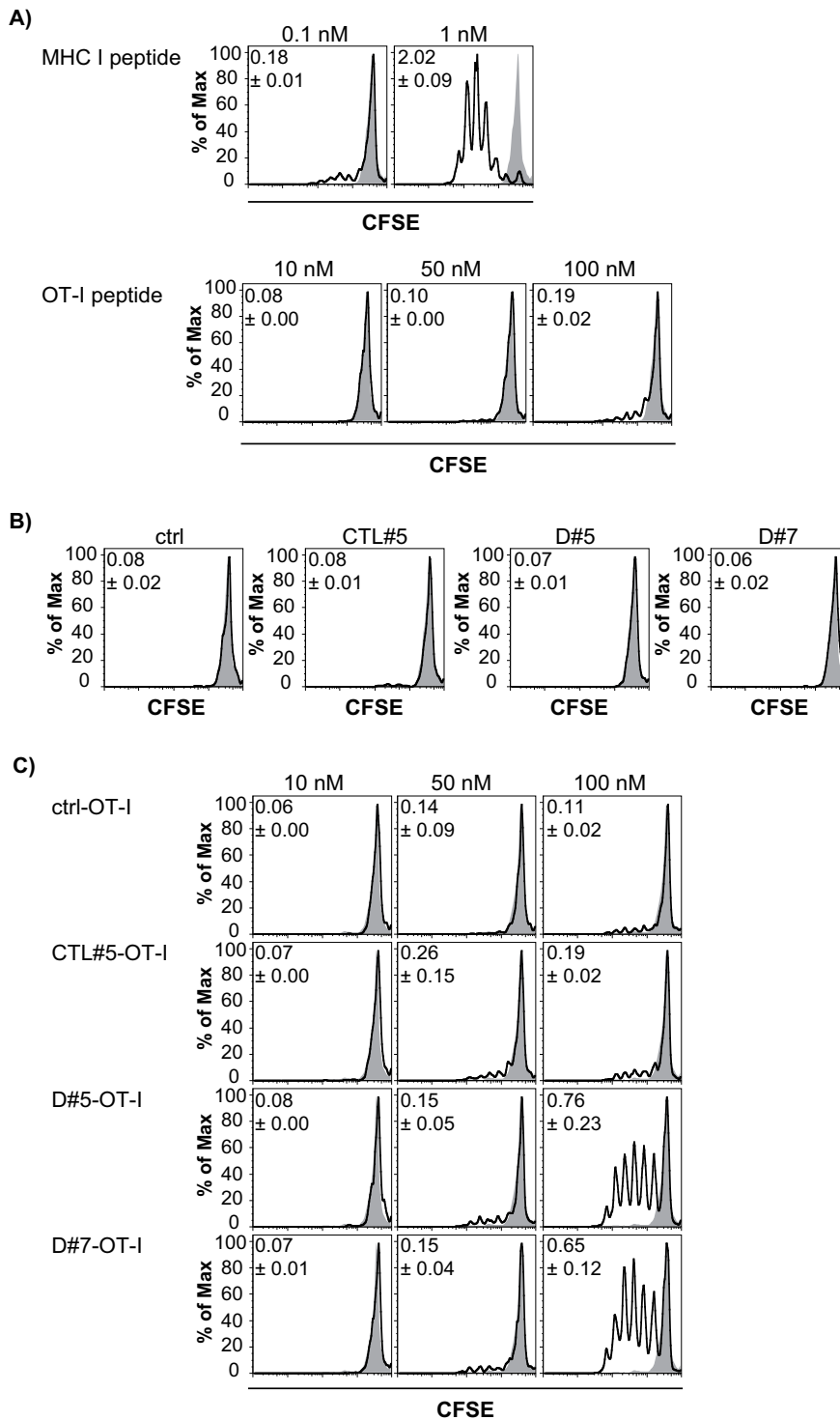## 9.5 Aptamer-targeted activation of CD8 T cells

Figure S 9.5.1: Activation of CD8 T cells
BM-DCs were treated with different concentrations of MHC I or OT-I peptide (A), 100 nM of oligonucleotides (B) or increasing concentrations of aptamer-peptide conjugates (C). Afterwards, BM-DCs were co-cultured for 72 h with CFSE-labeled OVA-dependent CD8 T cells and the proliferation profile indicated by changes of CFSE signals was measured by flow cytometry. FACS histograms with one representative profile out of triplicate measurement are depicted. Numbers gives the division index (mean ± SD). The non-proliferated population is shown in grey.
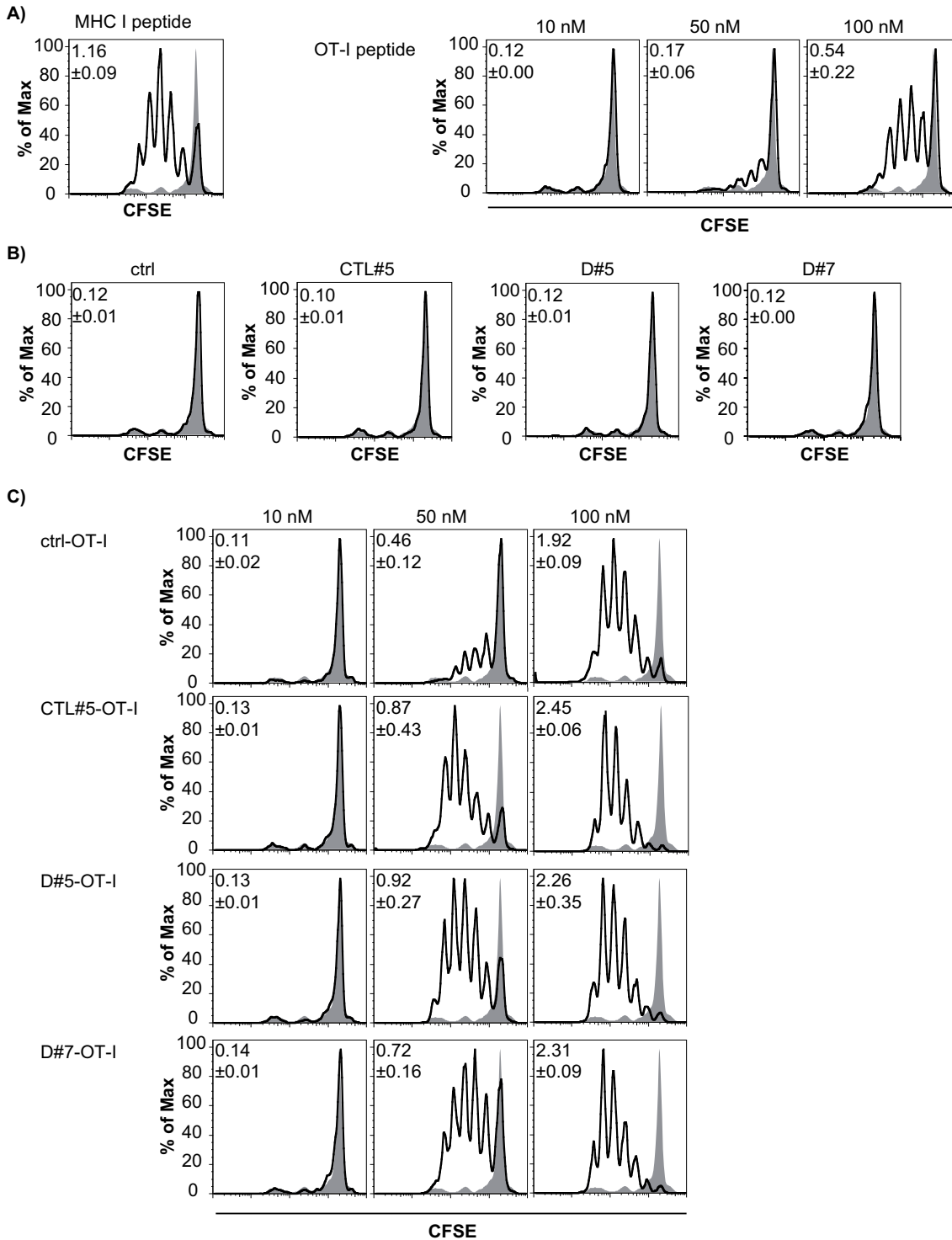
Figure S 9.5.2: Activation of CD8 T cells
BM-DCs were treated with 1 nM MHC I peptide or different concentrations of OT-I peptide **(A)**,
100 nM of oligonucleotides **(B)** or increasing concentrations of aptamer-peptide conjugates **(C)**.
Subsequently, BM-DCs were co-cultured for 72 h with CFSE-labeled OVA-dependent CD8 T
cells and the CFSE profile was measured by flow cytometry. FACS histograms with one
representative profile out of triplicate measurement are depicted. Division index (mean ± SD) is
depicted within the FACS histograms. The non-proliferated population is shown in grey.
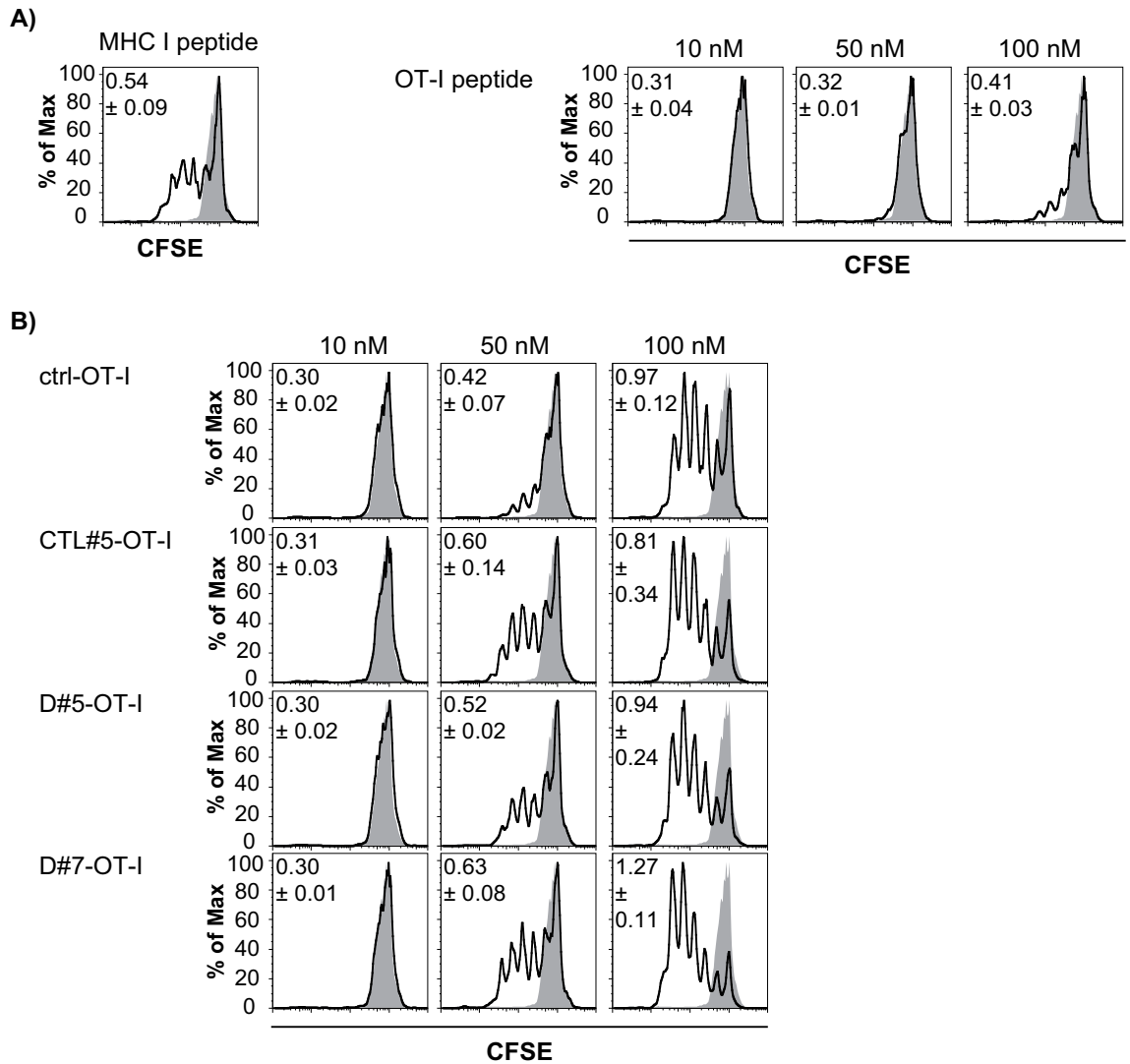
Figure S 9.5.3: Activation of CD8 T cells
BM-DCs were treated with 1 nM MHC I peptide, different concentrations of OT-I peptide **(A)** or increasing concentrations of aptamer-peptide conjugates **(B)**. Next, BM-DCs were co-cultured for 72 h with CFSE-labeled OVA-dependent CD8 T cells and the proliferation profile was measured by flow cytometry. FACS histograms with one representative profile out of triplicate measurement are depicted. Numbers gives the division index (mean ± SD). The non-proliferated population is shown in grey.
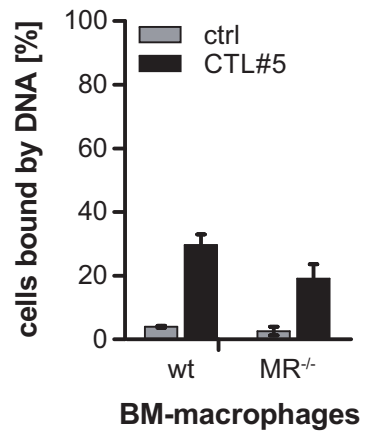
9.6 Binding of CTL#5 to BM-macrophages

Figure S 9.6.1: CTL#5 binds to wildtype and MR knockout murine bone marrow-derived macrophages

Murine bone marrow-derived macrophages were treated with 400 nM ATTO 647N-labeled CTL#5 and the amount of cells bound by CTL#5 was measured by flow cytometry and normalized to the control (ctrl) sequence. The experiment was done once in duplicates (mean ± SD).
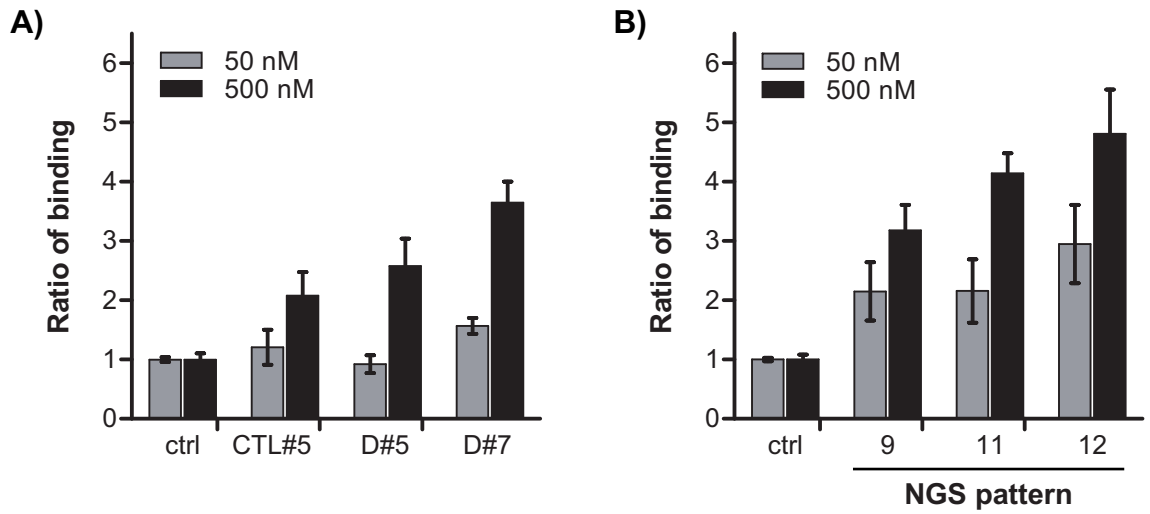
9.7 Binding of NGS patterns to BM-DCs

Figure S 9.7.1: Binding analysis of NGS patterns to DCs
NGS analysis of cell-SELEX revealed sequence patterns with increasing sequence frequencies from selection cycle 1 to 10. The consensus sequences of pattern 9-12 were chosen for flow cytometry binding analysis. BM-DCs were treated with 50 and 500 nM of ATTO 647N-labeled control sequence (ctrl), aptamers **(A)** or NGS pattern sequences **(B)** and analyzed by flow cytometry. Data were given as ratio of binding in comparison to the ctrl sequence (n=2, mean ± SD).

9.8 Binding of BM-DC aptamers to human blood cells

A)

blood monocytes

B)

baseline macrophages

C)

M1 (IFN-γ) macrophages

D)

M2 (IL-4) macrophages

E)

TPP macrophages

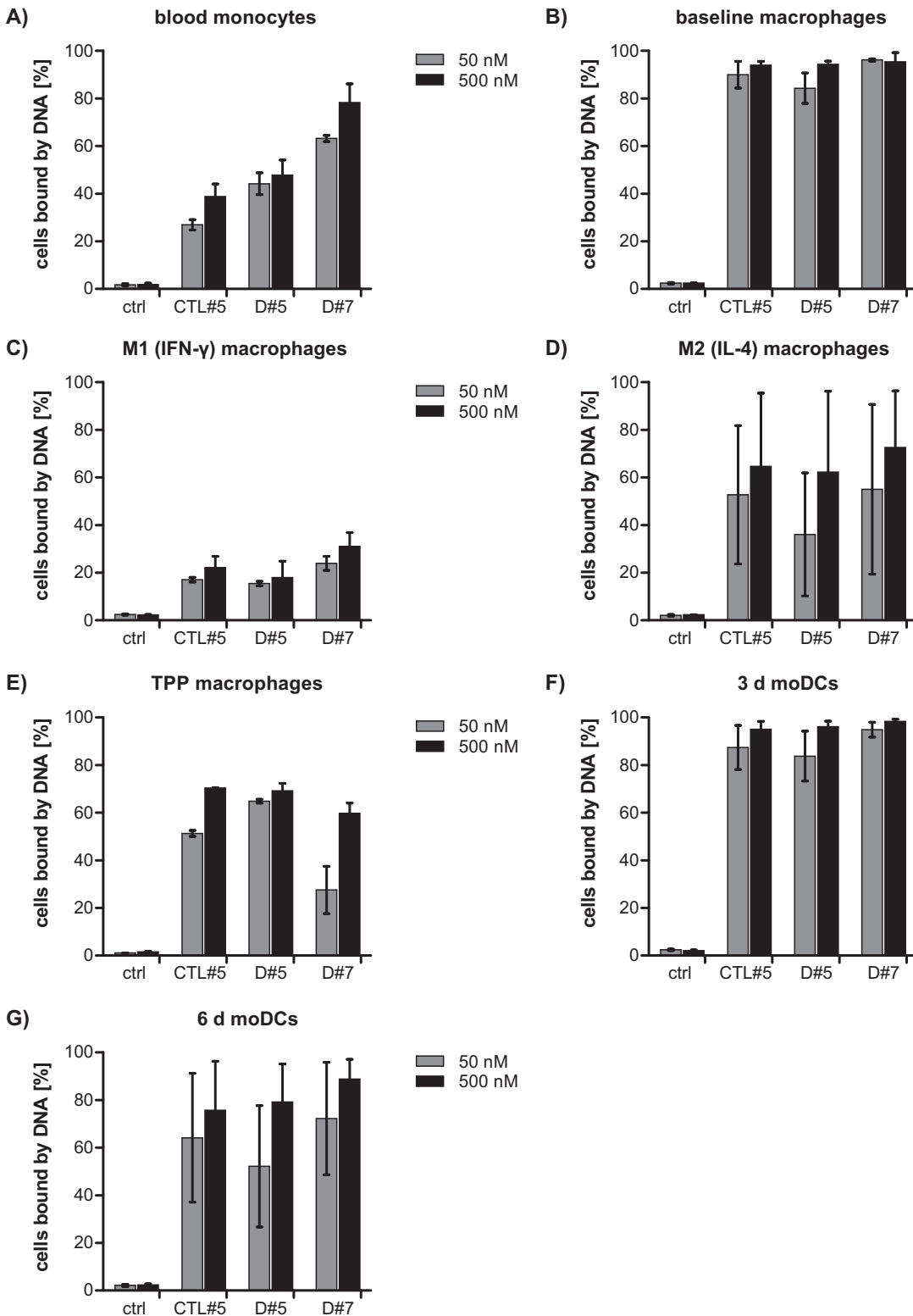**F)**

3 d moDCs

G)

6 d moDCs

Figure S 9.8.1: Binding analysis of human cells

The binding ability of BM-DC-targeting aptamers to human peripheral blood cells was analyzed by flow cytometry (mean ± SD). CD14+ blood monocytes of at least two different blood donors (exception E: n=1) were either used directly in FACS binding assay or further differentiated according to Xue et al.[184] and Nĩno-Castro et al.[194]. Cells were incubated with ATTO 647N-labeled aptamers and co-stained with cell surface marker CD14 **(A+B)**, CD86 **(C)**, CD23 **(D)**, CD25 **(E)**, CD209 **(F+G)**.

10　Abbreviations

APS	Ammoniumperoxodisulfate
BM-DC	Bone marrow-derived dendritic cell
BSA	Bovine serum albumin
CFSE	Carboxyfluoresceine succinimidyl ester
CLEC-1	C-type lectin receptor-1
CpG	Cytosine-phosphodiester-guanosine
CR	Cystein-rich
CTLA-4	Cytotoxic T-lymphocyte-associated protein 4
CTLD	C-type lectin-like domain
ctrl	Control DNA sequence
Cyt1 Sec7	Sec7 domain of Cytohesin 1
DAPI	4',6-diamidino-2-phenylindole
DC	Dendritic cell
DCIR	DC immunoreceptor
DC-SIGN	DC-specific ICAM-3 grabbing non-integrin
DEC-205	Dendritic and epithelial cells, 205 kDa
Dectin	DC-associated C-type lectin
DLEC	DC lectin
DNA	Deoxyribonucleic acid
DTT	1,4-Dithiothreitol
EDTA	Ethylendiamintetraacetic acid
EEA1	Early endosome antigen 1
ELISA	Enzyme-linked immunosorbent assay
ER	Endoplasmatic recticulum
ERAAP	Endoplasmatic recticulum aminopeptidase associated with antigen processing
Erk2	Extracellular signal-regulated kinase 2
FDA	Food and drug administration (USA)
FNII	Fibronectin type II
FRET	Fluorescence resonance energy transfer
GM-CSF	Granulocyte macrophage colony-stimulating factor
h	Human
HFIP	1,1,1,3,3,3-hexafluoro-2-propanol
HPLC	High-performance liquid chromatography
HTRF	Homogenous time-resolved fluorescence
IFN	Type I interferons
IL	Interleukin
LAMP-1	Lysosome-associated membrane glycoprotein 1
LC-MS	Liquid chromatography-mass spectrometry
LPS	Lipopolysaccharide
M-CSF	Macrophage colony-stimulating factor
MFI	Mean fluorescence intensity
MHC	Major histocompatibility complex
MR	Mannose receptor
MVB	multivesicular body
NGS	Next generation sequencing
ODN	Oligonucleotide
OVA	Ovalbumin
PAGE	Polyacrylamide gel electrophoresis
PAMP	Pathogen-associated molecular pattern
PBMC	Peripheral blood mononuclear cell

Abbreviations

PCC	Pearson's correlation coefficient
PCR	Polymerase chain reaction
PD-1	Programmed cell death 1
PEG	Polyethylene glycol
pIC	Polyinosinic:polycytidylic acid
PNK	Polynucleotide kinase
PRR	Pattern recognition receptor
PSMA	Prostate-specific membrane antigen
Rag2	Recombinant activating gene 2
RNA	Ribonucleic acid
SD	Standard deviation
SDS	Sodium dodecylsulfate
SELEX	Systematic evolution of ligands by exponential enrichment
TCR	T cell receptor
TEA	Triethylamine
TEAA	Triethylammonium acetat
TEMED	N,N,N',N'-tetramethylethylendiamide
Th	T helper cell
TLR	Toll-like receptor
TNF-α	Tumor necrosis factor α
WGA	Wheat germ agglutinin

11 Danksagung

Als erstes danke ich Prof. Günter Mayer für die Möglichkeit dieses spannende Thema zu bearbeiten und für seinen Enthusiasmus und seine Energie während der Betreuung des Projekts.

Des Weiteren danke ich Prof. Sven Burgdorf für die fruchtbare Kooperation und seine ständige Hilfsbereitschaft, sowie für die freundliche Übernahme des Zweitgutachtens.

Priv.-Doz. Gerhild van Echten-Deckert und Prof. Anton Bovier möchte ich dafür danken, dass sie mich beim letzten Schritt zur Promotion begleiten und sich als Mitglieder meiner Prüfungskommission zur Verfügung gestellt haben.

Alina Bartholomäus (intern), James Stunden (AK Latz) und den Mitgliedern der AK Schultze, insbesondere Dr. Susanne Schmidt und Heidi Theis, danke ich für die tatkräftige Unterstützung bei einigen experimentellen Teilen dieser Arbeit. Dr. Thomas Quast (AK Kolanus) danke ich für die freundliche Unterstützung am konfokalen Mikroskop.

Ich möchte mich bei allen Kollegen und Ex-Kollegen aus dem AK Mayer, dem AK Burgdorf und dem AK Famulok bedanken für die freundliche und lustige Arbeitsatmosphäre und die stete und große Hilfsbereitschaft. Besonders hervorheben möchte ich hier Dr. Verena Schütte und Dr. Laia Civit. Thanks for your inestimable support and friendship.

I am truly indebted and thankful to Dr. Verena Schütte, Dr. Laia Civit and Shannon Smith for their conscientious proofreading of my thesis, their helpful comments and suggestions.

Außerdem bedanke ich mich bei meinem Tantchen Claudia, meinem Schwesterherz Claudia, meinem Cousin Philip und meinen Schwiegereltern Helga und Kalle für ihre Liebe und ihre Unterstützung. Und dafür, dass sie stets versuchen zu verstehen was ich beruflich mache. ;-)

Meinen Schätzeleins Sarah, Stephan, Micha, Melli, Martina und David, sowie den Marburgern Anna, Michi, Cathi, Anne, Kathi, Johannes und Eve danke ich für das

Danksagung

Verständnis, die Ablenkungen und Freuden während der letzten Jahre. Ihr seid mein Rückhalt.

Abschließend möchte ich meinem Mann Dominique für seine Liebe, Geduld und Unterstützung danken. Du bist und bleibst mein Fels in der Brandung.